FEDERAL UNIVERSITY OF ESPIRITO SANTO
POSTGRADUATE PROGRAM IN ELECTRICAL ENGINEERING

Richard Junior Manuel Godinez Tello

A Novel Approach of Independent Brain-Computer Interface Based on SSVEP

Brazil

2016

Richard Junior Manuel Godinez Tello

A Novel Approach of Independent Brain-Computer Interface Based on SSVEP

Document presented to the Postgraduate Program in Electrical Engineering of the Federal University of Espirito Santo, as a partial requirement for the degree of Doctor in Electrical Engineering.

Supervisor: Dr. Teodiano Freire Bastos Filho

Co-supervisors: Dr. André Ferreira and Dr. Sandra Mara Torres Müller

Federal University of Espirito Santo – UFES

Postgraduate Program in Electrical Engineering

Brazil

2016

Richard Junior Manuel Godinez Tello

A Novel Approach of Independent Brain-Computer Interface Based on SSVEP

Document presented to the Postgraduate Program in Electrical Engineering of the Federal University of Espirito Santo, as a partial requirement for the degree of Doctor in Electrical Engineering.

Approved on September 1, 2016.

Dr. Teodiano Freire Bastos Filho
Supervisor
Federal University of Espirito Santo

Dr. André Ferreira
Co-supervisor
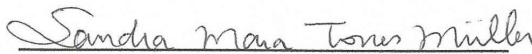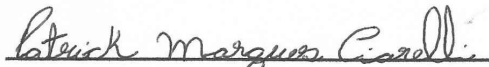Federal University of Espirito Santo

---

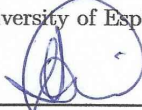**Dr. Sandra Mara Torres Müller**
Co-supervisor
Federal Institute of Espirito Santo

Dr. Patrick Marques Ciarelli
Federal University of Espirito Santo
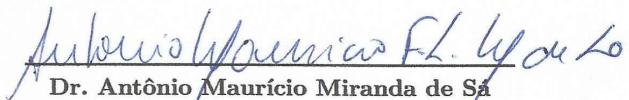
Dr. Eduardo Rocon de Lima
CAR/CSIC/Spain

Dr. Antônio Maurício Miranda de Sá
Federal University of Rio de Janeiro

This thesis is dedicated to my
loved ones:
my family

Acknowledgements

I am thankful to Prof. Dr. Teodiano who gave me the opportunity of showing and improving my knowledge. I appreciate his dedication and wise criticism that helped improve my scientific production. In the same way, I am grateful to my co-advisors, Prof. Sandra Müller and Prof. André Ferreira, who were kind enough to review my papers and express their constructive criticisms.

I am grateful to Prof. Dr. Sridhar Krishnan and colleagues of SAR Lab (Ryerson University - Canada) for the hours of conversations, advices and suggestions spent in Toronto. This thesis is also the effort of all of us. Also, I appreciate CAPES, FAPES and CNPq/Brazil for the financial support during my wonderful years as graduate student.

I want to thank all the friends that I met at LAI (Federal University of Espirito Santo - Brazil), who helped me directly or indirectly in my personal formation and professional since 2011.

Finally, I am grateful to my family who is the emotional support of my life and who is always with me, despite the distance, in the decisive moments of my life.

"The real voyage of discovery consists not in seeking new landscapes,
but in having new eyes"
(Marcel Proust)

Resumo

Durante os últimos dez anos, as Interfaces Cérebro Computador (ICC) baseadas em Potenciais Evocados Visuais de Regime Permanente (SSVEP) têm chamado a atenção de muitos pesquisadores devido aos resultados promissores e as altas taxas de precisão atingidas. Este tipo de ICC permite que pessoas com dificuldades motoras severas possam se comunicar com o mundo exterior através da modulação da atenção visual a luzes piscantes com frequência determinada. Esta Tese de Doutorado tem o intuito de desenvolver um novo enfoque dentro das chamadas ICC Independentes, nas quais os usuários não necessitam executar tarefas neuromusculares para seleção visual de objetivos específicos, característica que a distingue das tradicionais ICCs-SSVEP. Assim, pessoas com dificuldades motoras severas, como pessoas com Esclerose Lateral Amiotrófica (ELA), contam com uma nova alternativa de se comunicar através de sinais cerebrais. Diversas contribuições foram realizadas neste trabalho, como, por exemplo, melhoria do algoritmo extrator de características, denominado Índice de Sincronização Multivariável (ou MSI, do Inglês *Multivariate Synchronization Index*), para a detecção de potenciais evocados; desenvolvimento de um novo método de detecção de potenciais evocados através da correlação entre modelos multidimensionais (tensores); o desenvolvimento do primeiro estudo sobre a influência de estímulos coloridos na detecção de SSVEPs usando LEDs; a aplicação do conceito de Compressão (*Compressive Sensing*) na detecção de SSVEPs; e, finalmente, o desenvolvimento de uma nova ICC independente que utiliza o enfoque de Percepção Fundo-Figura (ou FGP, do Inglês *Figure Ground Perception*).

Palavras-chaves: Interface Cérebro Computador, ICC Independente, SSVEP, MSI, FGP.

Abstract

Over the past ten years, Brain Computer Interfaces (BCIs) based on Steady-State Visual Evoked Potentials (SSVEP) have attracted the attention of many researchers due to the promissory results and the high accuracy rates achieved. This type of BCI provides to people with severe neuromotor difficulties the possibility to communicate with the world around them using visual attention modulation to blinking lights at a given frequency. This thesis aiming at developing a new approach of Independent BCI, in which users are not required to perform neuromuscular tasks to select visual targets, a feature that distinguishes it from traditional SSVEP-BCIs. Thus, people with severe motor disabilities as Amyotrophic Lateral Sclerosis (ALS) have a new alternative channel to communicate with the world around them using brain signals. Several contributions were done in this thesis, such as: improvement of the feature extractor called Multivariate Synchronization Index (MSI) for detecting evoked potentials; development of a new method for detecting evoked potentials through correlating multidimensional models (tensors); a first study on the influence of colored stimuli in SSVEPs detection using LEDs; the development of the concept of Compressive sensing applied to SSVEPs; and, finally, the development of a novel independent BCI under an approach named Figure-Ground Perception (FGP).

Key-words: Brain Computer Interface, Independent SSVEP-BCI, SSVEP, MSI, FGP.

List of Figures

List of Tables

Nomenclature

ACC Accuracy

ALS Amyotrophiclateral Sclerosis

ANOVA Analysis of Variance

BCI Brain-Computer Interface

BSBL-BO Block-sparse Bayesian Learning Bound-optimization

CA Classification Accuracy

CANDECOMP Canonical Decomposition

CAR Common Average Reference

CCA Canonical Correlation Analysis

CMS Common-Mode Sensing

CR Compression Rate

CRT Cathode Ray Tube

CS Compressive Sensing

CTI Command Transfer Interval

DRL Driven Right Leg

DTA Dynamic Tensor Analysis

EEG electroencephalography

ERP Event-Related Potential

ErrP Error-Related Potentials

FA False Activation

FFT Fast Fourier Transform

FGP Figure Ground Perception

FGPA Field-Programmable Gate Array

FN False Negative

FP False Positive

GND Ground

HHT Hilbert-Huang Transform

ICA Independent Component Analysis

IMF Intrinsic Mode Function

ITR Information Transfer Rate

LASSO Least Absolute Shrinkage and Selection Operator

LCD Liquid Crystal Display

LED Light Emisor Diode

LIS Locked-In Syndrome

mcd Millicandelas

MEC Minimum Energy Combination

MP Macular Pigment

MSI Multivariate Synchronization Index

MWA Multi-Way Analysis

PARAFAC Parallel Factor Analysis

PC Personal Computer

PCA Principle Component Analysis

PPR Photoparoxysmal Response

PSD Power Spectral Density

PSDA Power Spectral Density Analysis

RLS Regularized least-squares

SCI Spinal Cord Injury

SD Standard Deviation

SNR Signal to Noise Ratio

SSVEP Steady-State Visually Evoked Potential

STF Spectral F-Test

SVM Support Vector Machine

TN True Negative

TP True Positive

VEP Visual Evoked Potential

WL Window Length

WLs Window Lengths

Table of Contents

1 Introduction

The current human communication channels are the result of a long evolution process, which distinguishes humans from other beings. Currently, mimes, gestures, writing and speech are the bases of an entire communication process that has been evolving over the years. In this communication evolution process intrinsically influenced by human ability, a new natural and spontaneous kind of communication appears as an option: the biosignals. This new manner of communication can improve the quality of life of people with any disability (for example, people unable to communicate through conventional ways) and even healthy people. Biosignals are physical quantities varying with time and used to control machines and systems (RECHY-RAMIREZ; HU, 2015). Figure 1 shows a block diagram of this kind of system.
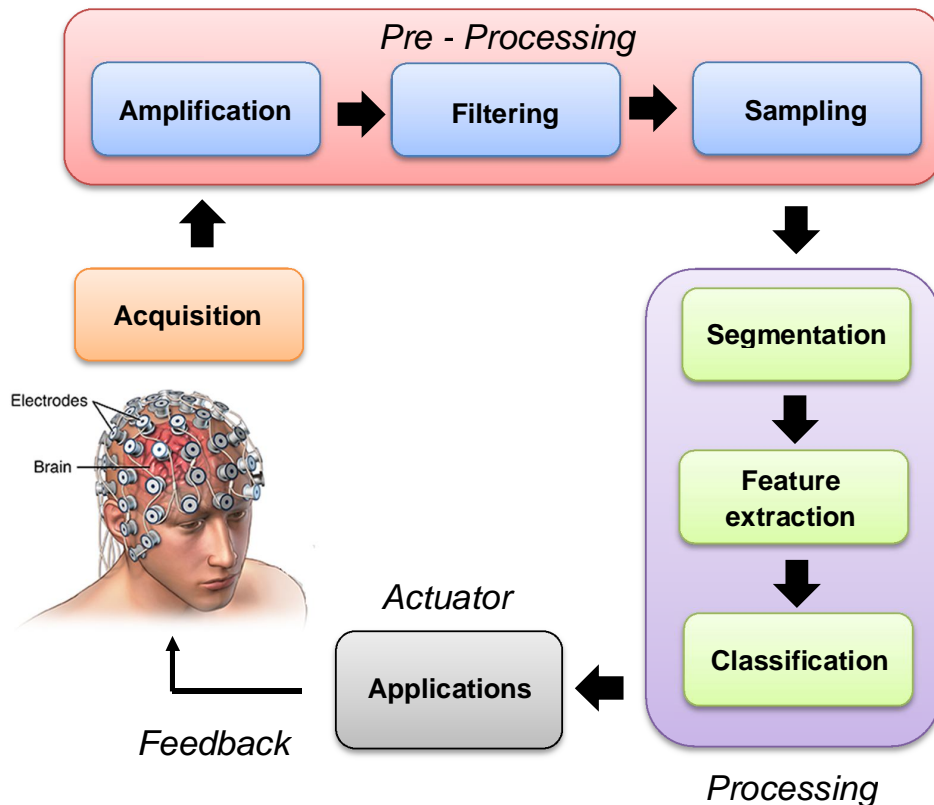
Figure 1: Biosignal acquisition and processing.

In the same way, Brain-computer interface (BCI) is a technology which provides human with a direct communication between the user's brain signals and a computer, generating an alternative communication channel that does not involve the traditional

way as muscles and nerves (WOLPAW et al., 2000). Among current BCIs, a noninvasive brain imaging method commonly employed is electroencephalography (EEG), which has the advantages of lower risk, be inexpensive and easily measurable, and can be applied and tested on large human population (CHEN et al., 2014; KELLY et al., 2005b). Furthermore, EEG provides electrical signals of high temporal resolution generated by neuronal dynamics from the scalp. Therefore, a BCI records brain signals and extracts EEG signal features, and these features are then translated into outputs or commands that act in a real world. BCI can be then used to control solution for people with severe motor disabilities (WOLPAW et al., 2000; KELLY et al., 2005b; GAO et al., 2003).

1.1   Problem Statement

Among the different kinds of BCIs, an approach called Steady-State Visually Evoked Potentials (SSVEPs) has attracted much attention of researchers. The main advantages of SSVEP compared to other BCI paradigms are its high signal-to-noise ratio (SNR), little user-training (or nothing), and high information transfer rate (ITR) (GAO et al., 2003; WANG; WANG; JUNG, 2010; BIN et al., 2009; CHEN et al., 2013). However, SSVEP is only capable of showing a good response if some setup parameters are previously adjusted (VIALATTE et al., 2010b). This factor makes that the research becomes complex due to the large quantity of conditions, such as: forms of stimulation, type of stimulation, color of the stimuli, problems of fatigue, feature extractors, classifiers, stimulus frequencies, electrode location, window length of processing, etc. Advances in the detection of visual evoked potentials have evolved from traditional ways as Fourier power spectrum or Power Spectral Density Analysis (PSD) (WANG et al., 2006), multidimensional signals (HUANG et al., 1998; TELLO et al., 2015a) and the use of simulated signals that act as "frequencies templates" (LIN et al., 2007; ZHANG et al., 2014a). A modified version of PSD called Spectral F-test (SA et al., 2006) was also developed, which has the goal of determining whether the spectrum at a certain frequency is statistically distinct from its neighbors, considering that the spectrum in this neighborhood is white. Huang et al. (1998) introduced the concept of Empirical Mode Decomposition (EMD) together with Hilbert transform, which was collectively called Hilbert-Huang Transform (HHT), used to extract time-frequency information from a nonlinear and non-stationary signal. It was regarded as an important progress since the Fast Fourier Transform (FFT). Since 2007, the use of simulated stimuli (templates) have drawn attention in the recognition of SSVEPs due to efficiency, lower computational cost, good performance and training-free compared to traditional ways of feature extraction and use of thresholds or decision trees for classification (TELLO et al., 2014b). Friman, Volosyak and Graser (2007) developed a technique called Minimum Energy Combination (MEC), which is based on finding combinations of strong electrode signals that remove noise and nuisance signals for EEG data. Lin et al.

(2007) introduced the use of canonical correlation analysis (CCA) for multi-channel detection SSVEP, which consists of formation of pairs of linear combinations, called canonical variables. The target is found by maximization of the correlation between the two sets (a multichannel EEG signal and a "Fourier series" of simulated stimuli). In 2014, Zhang et al. (2014a) developed a new method called Multivariate Synchronization Index (MSI). MSI is a technique that estimates the current synchronization between mixed signals and reference signals as a potential index for recognizing the stimulus frequency.

Figure 2 presents a concept-map of categorization of a Brain–computer interface. In a typical SSVEP-BCI several stimuli flickering at different frequencies are presented to the user. The subject overtly directs attention to one of the stimuli by changing his/her gaze attention (ZHANG et al., 2010). This kind of SSVEP-BCI is commonly called as "dependent", since muscle activities, such as gaze shifting, are necessary. However, patients with stroke trauma, poliomyelitis, amyotrophiclateral sclerosis (ALS), multiplesclerosis, and Guillain-Barré syndrome suffer from motor disabilities, which can disrupt their communication with the external environment, resulting in the so-called locked-in syndrome (LIS).

1.2 Motivation

One motivation for the realization of this thesis is the life history of the physicist Prof. Stephen Hawking, who used different interfaces to communicate. Prof. Hawking has a rare early-onset, slow-progressing form of amyotrophic lateral sclerosis (ALS), commonly known as motor neurone disease that has gradually paralysed him over the years. Currently, Prof. Hawking uses a channel of communication that consists of a single cheek muscle attached to a speech-generating device .

Examples such as the case of Prof. Hawking motivate the development of assistive technologies helping people who preserve the mental conditions and the reasoning of intact way.

1.3 Hypothesis

Based on the problem statement, "dependent" SSVEP-BCIs might not be applicable for patients with traumatic brain injuries. Nonetheless, an "independent" SSVEP-BCI can be an alternative solution, as it is controlled by subject's attentions without requiring head neuromuscular control or eye movements. But, can this independent SSVEP-BCI be comfortable, accurate, fast and on-line?
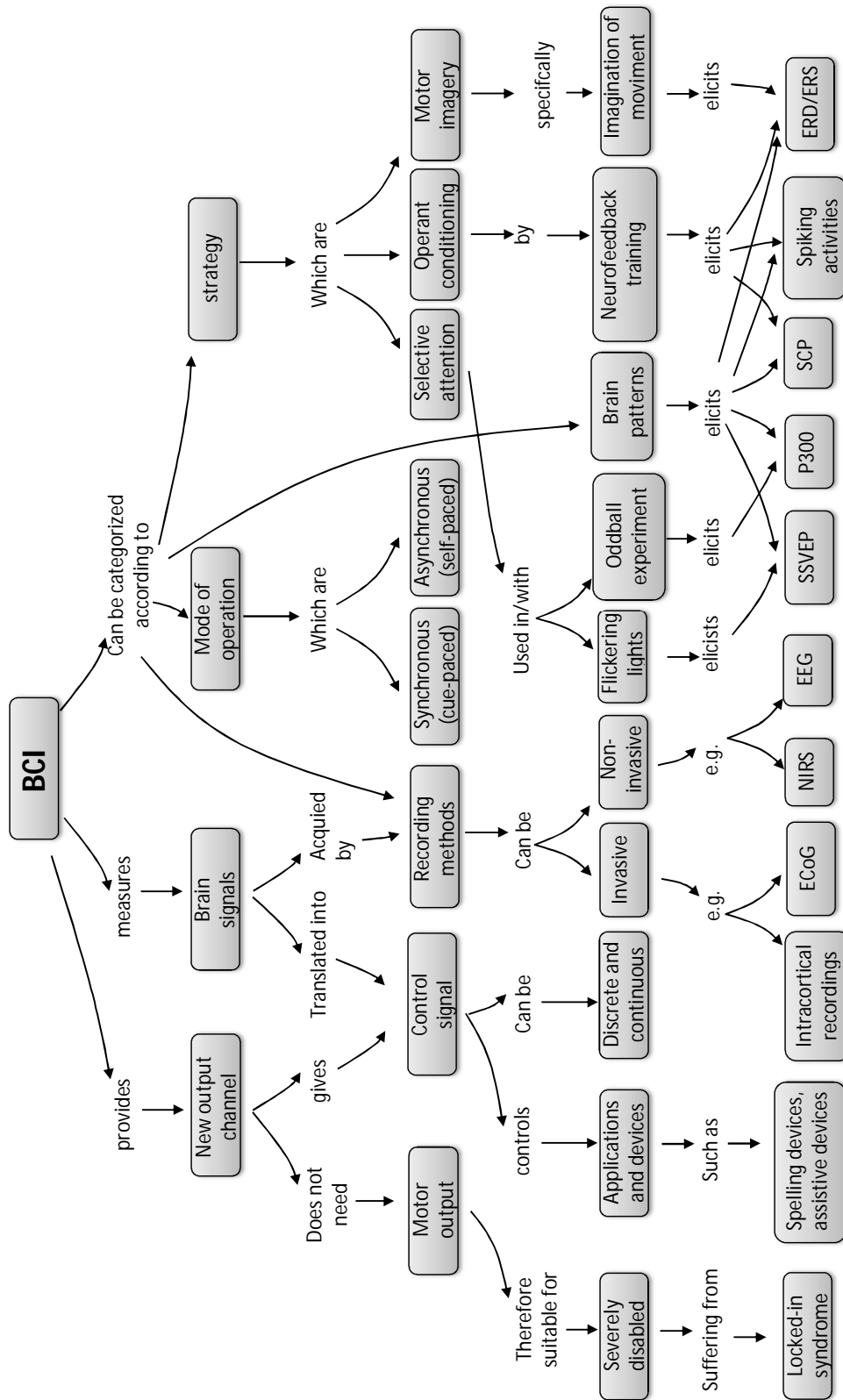
Figure 2: Brain–computer interface concept-map. Modified from (GRAIMANN; ALLI-SON; PFURTSCHELLER, 2010).

1.4　Thesis Objectives

The work presented in this thesis aimed at addressing directly the aforementioned existing problems. New approaches were investigated in order to develop a reliable, accurate and novel BCI that can offer to people with severe motor disabilities an alternative of communication using attentional modulation without requiring neuromuscular activities or eye movements. As a result, the following research goals were pursued in this work:

1. Study and evaluation, from the literature, of the performance of classifiers and feature extractors for SSVEPs detection.

2. Proposal of a new method for SSVEP detection.

3. Evaluation of the influence of colored stimuli on SSVEP detection.

4. Development of a novel approach applied to an Independent BCI-SSVEP.

1.5　Contributions of the thesis

The main contributions of this thesis are listed as follows:

1. Improvements of the Multivariate Synchronization Index (MSI).

2. A new method of SSVEPs detection based on tensor models (PARAFAC).

3. A first study about evaluation of the influence of colored stimuli using LEDs in SSVEPs.

4. Use of Compressive Sensive technique for an SSVEP-BCI.

5. Development of a new independent SSVEP-BCI using approach of Figure-Ground Perception (FGP).

1.6　Thesis Structure

In Chapter 2, a brief review of theoretical background was performed to describe concepts and differences between VEPs and SSVEPs. Topics related to trends in EEG acquisition and usability were addressed. Also, basic concepts about performance in BCIs were explained.

In Chapter 3, it was approached a section related to methodologies. Initially, it was defined our protocols of EEG acquisition that were used in the experiments. A state-of-the-art based on the last ten years about SSVEP-BCI research was also described,

allowing categorizing the studies according to its applications. A study about a comparison of techniques and technologies in SSVEP classification was also performed. The chapter ends with the proposal of a new method for SSVEPs detection through correlation analysis between tensor models.

In Chapter 4, it was introduced a novel study related to the influence of color in visual evoked potentials. It is worth to mention that none of the studies in the literature compared the performance of stimuli colors using LEDs.

In Chapter 5, a novel study of SSVEP detection was carried out for its application in compressive sensing (CS)-based brain-computer interface (BCI). Compressive Sensing (CS) is an emerging and promising technique for the development of low-power, small-chip, and robust BCI (PANT; KRISHNAN, 2014; ZHANG et al., 2013).

In Chapter 6, a new way of presenting SSVEP stimuli was evaluated, in which a portable stimulator based on two flickering stimuli representing the model face-vase was proposed. This novel concept of SSVEP-BCI is based on perception, where the well-known example of Rubin's face-vase illusion is here used in order to create a bridge of communication for subjects with severe motor disabilities.

In Chapter 7, a summary of contributions and future works that derived from this thesis is shown. Finally, the appendix details the publications derived of this thesis. The development of this thesis was performed in chronological order as shown in Figure 3. It were addressed all aforementioned objectives and during the studies were obtained contributions. In some cases, different studies were performed in parallel.
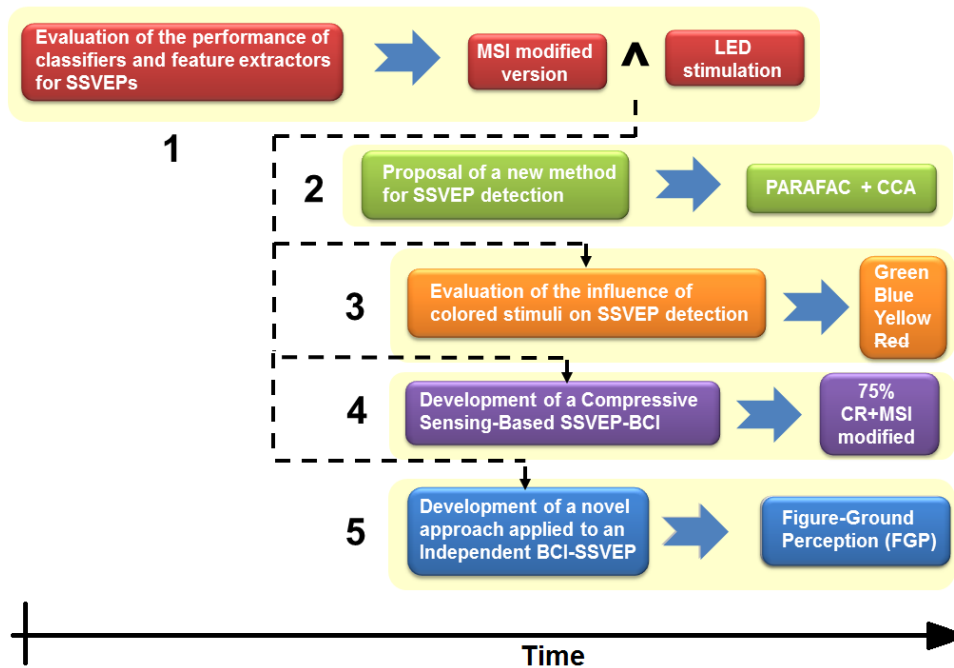
Figure 3: Chronological development of the thesis indicating objectives and achieved contributions.

2 Background

2.1 VEPs and SSVEPs

About 50 years ago, Regan (1966b) started experimenting with long stimulus trains, consisting of sinusoidally modulated monochromatic light. These stimuli produced a stable Visual Evoked Potencial (VEP) of small amplitude, which could be extracted by averaging over multiple trials (VIALATTE et al., 2010b). These electroencephalography (EEG) waves were termed as "steady-state" visually evoked potentials (SSVEPs) of the human visual system.

According to the original definition, steady-state potentials are to be distinguished from transient potentials, because their constituent discrete frequency components remain closely constant in amplitude and phase over a long time period (REGAN, 1989; VIALATTE et al., 2010b). Consequently, the amplitude distribution of the spectral content of SSVEP, with characteristic SSVEP peaks, remains stable over time. Because these characteristics are constant, many applications can be derived from SSVEP propagation properties.

Consequently, VEPs can be categorized into transient VEPs or SSVEPs according to waveform patterns (FAZEL-REZAI, 2011). Figure 4 illustrates the difference between transient VEPs and SSVEPs. While transient VEPs occur in reaction to visual stimuli which blink at a frequency of less than 3.5 Hz, SSVEPs occur in reaction to stimuli of higher blinking frequency (FAZEL-REZAI, 2011). A first difference between these two evoked responses is thus their range of application (FAZEL-REZAI, 2011). VEPs, for example, are used in the field of clinical medicine to examine the function of optic nerves and visual cortex (FAZEL-REZAI, 2011) and SSVEPs used for control of Brain Computer Interfaces.

While transient VEPs are typically only used for studying the visual system, the range of applications of SSVEPs is wider —from cognitive neuroscience and clinical neuroscience to neuro-engineering applications with Brain Computer Interfaces (BCIs). In addition, SSVEPs are less susceptible to artifacts produced by blink and eye movements (PERLSTEIN et al., 2003) and to electromyographic noise contamination (GRAY et al., 2003). The shape of the response in time domain is not usually sufficient to distinguish SSVEPs from transient VEPs. However, spectral response in the frequency domain is critical.
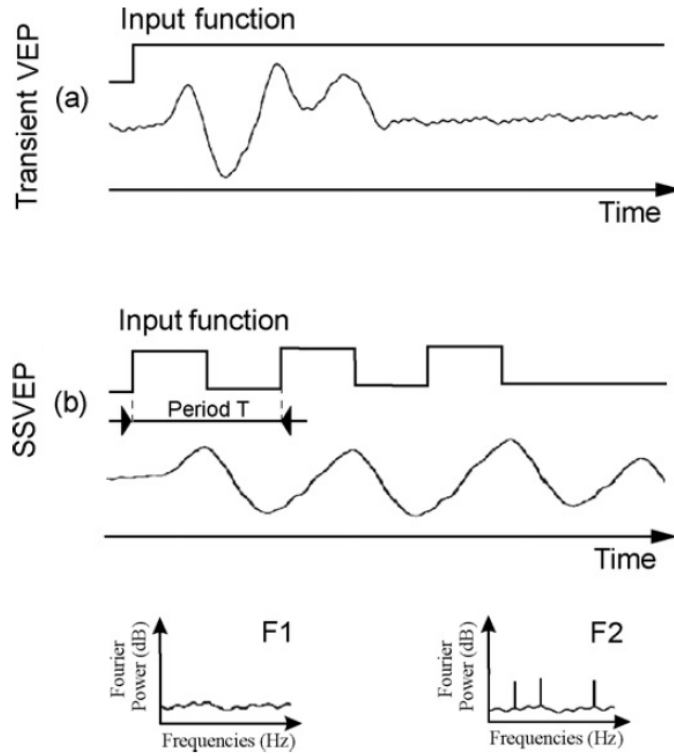
Figure 4: Transient VEP vs SSVEP — synthetic model. (a) The upper diagram represents the input function, with a square stimulation (transient), where the bottom trace is a transient VEP. (b) The upper diagram represents the input function, a periodic square wave (period T), where the bottom trace is a SSVEP. F1 and F2 indicate the frequencies for each type of evoked potential. Image from (VIALATTE et al., 2010b).

On the other hand, the amplitude and phase of the SSVEP are highly sensitive to stimulus parameters, such as color, contrast or modulation depth, and spatial frequency (REGAN, 1989; DING; SPERLING; SRINIVASAN, 2006). Many authors agree that the SSVEP is a response to the stimulus that has a complex amplitude and phase topography across the posterior scalp, with considerable inter-subject variability (WU et al., 2008; PASTOR et al., 2003; SRINIVASAN; BIBI; NUNEZ, 2006; AMIRI; FAZEL-REZAI; ASADPOUR, 2013).

Since the beginning of its conception, a Brain Computer Interface (BCI) was defined as a means of helping people with neuromotor complications. Nowadays, this concept is extended to applications that improve the life quality of any person. The study of SSVEPs and BCIs has led to success and great expansion of the called "SSVEP-BCI" and consequently to develop techniques of recognition of visual evoked potentials.

Over the last 20 years, several progress has been made on BCIs. The basic idea of using SSVEPs to drive a BCI dates back to 37 years ago, when the first ancestor of SSVEP-BCI was depicted in the publication of Regan (1979) (VIALATTE et al., 2010b). The BCI that was proposed in that study used closed-loop feedback to control the contrast of a

pattern stimulus directly from the SSVEP amplitude. SSVEP-BCIs have the advantage of having higher accuracy and higher Information Transfer Rate (ITR) than others BCIs (WU et al., 2011; ZHANG et al., 2012). In addition, short/no training time and few EEG channels are required (AMIRI; FAZEL-REZAI; ASADPOUR, 2013; VIALATTE et al., 2010b).

The more general idea of this technique is to encode user commands in flickering light stimuli that induce SSVEPs at different frequencies. In this technique, the user selects one of the commands by focusing on one of the flickering stimuli, and by analyzing the generated SSVEP, the BCI tries to infer which stimulus the user selected (see Figure 5).

2.2 Trends in EEG signal acquisition and usability

When the eye retina is excited by a stimulus at a certain frequency, the brain generates an electrical activity of the same frequency of the stimulus with its harmonics (HE, 2013). This stimulus produces a stable VEP of small amplitude termed as "Steady-State" Visually Evoked Potentials (SSVEPs) of the human visual system. SSVEPs and other VEPs depend on the user's gaze direction and thus require muscular control. In a typical SSVEP-BCI, several stimuli flickering at different frequencies are presented to the user. The subject overtly directs attention to one of the stimuli by changing his/her gaze attention (ZHANG et al., 2010). This kind of SSVEP-BCI is commonly called as "dependent" since muscle activities, such as gaze shifting, are necessary. According to Regan (WU et al., 2008; ZHU et al., 2010), a flickering stimulus of different frequency can evoke SSVEPs in low (5-12 Hz), medium (12–25 Hz) and high (>50 Hz) frequency bands. Each band presents a maximum amplitude in its range.

2.3 Evaluating the performance of a Brain-Computer Interface

A relevant issue in Brain-Computer Interfaces is the capability of efficiently converting user intentions into correct actions, and how to properly measure this efficiency, which can be through classification accuracy, Information Transfer Rate (ITR), letters or words per minute, kappa statistic, and others. The most traditional measured one is the ITR (VIALATTE et al., 2010b), the amount of information communicated per unit time. The ITR, first introduced by Shannon and Weaver (SHANNON; WEAVER, 1964) is expressed in bits per trial (bits per selection). If a single trial has N_c possible outcomes, if the probability p that this outcome is correct (accuracy of the BCI), and if finally each of the other outcomes has the same probability of selection (i.e., $(1-p)/(N_c-1)$), then
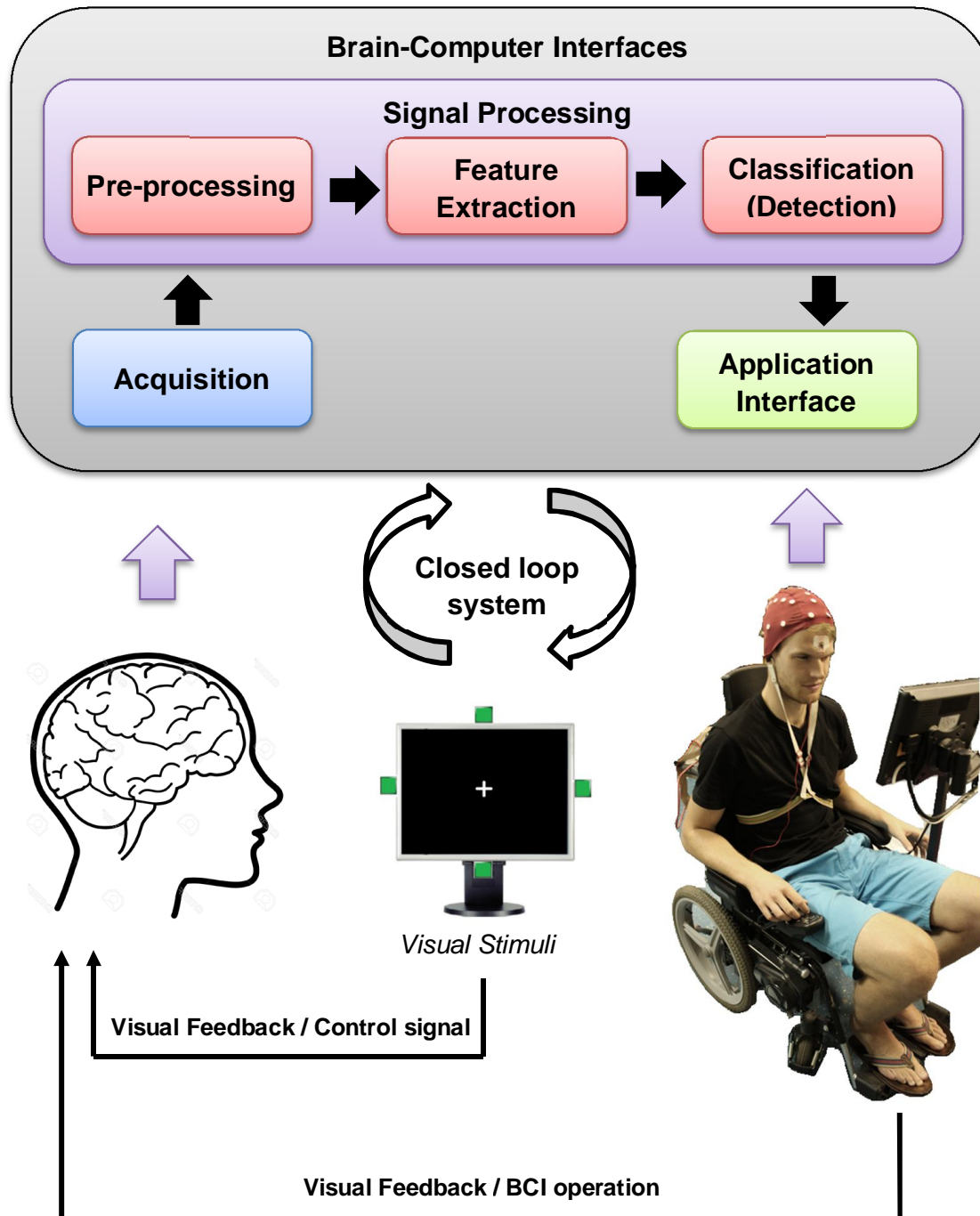
Figure 5: General scheme of a Brain-Computer Interface (BCI). Basic components of the BCI to control an application (wheelchair). The closed loop system indicated by black lines corresponds to an operant conditioning neurofeedback paradigm.

the information transfer rate in bits per trial (BpT) is (DORNHEGE et al., 2007):

$$BpT = \log_2{(N_c)} + p\log_2{(p)} + (1-p)\log_2{\left(\frac{1-p}{N_c-1}\right)}. \tag{2.1}$$

This formula makes the assumption that BCI errors and Error-Related Potentials (ErrP) detection errors are independent, which might not always be the case in particular situations like lack of concentration, longer lasting artifacts, or fatigue. ITR is the type of performance measurement for BCIs adopted in this thesis.

3 Methodology

3.1 Acquisition experiments

The acquisition of EEG signal can be conducted with different equipments. In this thesis, the experiments were performed using two different kinds of devices: BrainNet-36 and Emotiv Epoc Headset. BrainNet-36 is a wired medical device used for EEG signal recording manufactured by Lynx Tecnologia Ltd. With this experiment, twelve EEG channels were processed and recorded at 600 Hz, 1 to 100 pass-band filtered and with reference signal at the left ear lobe. The GND was placed on the forehead and the Ag/AgCl electrodes were placed according to the International 10–20 system (Figure 6). On the other hand, the Emotiv Epoc Headset includes 14 channels pre-assigned according to the International 10-20 system: AF3, AF4, F7, F3, F4, F8, FC5, FC6, T7, T8, P7, P8, O1, and O2 (Figure 7). The electrodes used for reference and common-mode sensing were fixed in parallel to locations that approximate the P3/P4 locations and the two mastoids. This device has 128 Hz of sampling rate and its electrodes need a saline solution to decrease the impedance between the scalp and electrodes. The signals acquired from the scalp are wireless transmitted to an USB receiver port of a PC.

3.2 The Visual Stimulator: Different types of stimulation devices for SSVEP-BCIs

In Table 1, a study of the most outstanding investigations related to SSVEP between 2007-2015 was conducted, which was categorized by stimulation technology (Light Emisor Diode - LED, Liquid Crystal Display - LCD monitor and Cathode Ray Tube - CRT monitor), color of the stimuli, frequencies used and applications. The table includes works from conferences, scientific journals and research groups consolidated in the area of Brain -Computer Interfaces. This table was prepared according to the most relevant researches found in Scopus, IEEE Xplore and ScienceDirect platforms.

According to Table 1, three groups can be distinguished where the technology of stimulation by LEDs showed a large number of studies in the last years, compared to LCD or CRT, remarking that the last work using CRT was in 2010. This can be due to the undoubtedly evolution of screens to LCD in terms of reduction of dimensions and great portability of these flat screens. On the other hand, the use of LEDs remains of high

Top view

Front panel

(a) Wired acquisition system

(b) Conductive gel and electrodes

(c) Lateral view of a volunteer using the EEG cap

Figure 6: BrainNet-36 acquisition system and its accessories.

Emotiv Epoc Headset

Electrodes and accessories

(a) Wireless acquisition system

(b) Saline solution

(c) Lateral view of a volunteer using Emotiv headset

Figure 7: Emotiv acquisition system and its accessories.

Table 1: Studies related to SSVEP-BCIs between the 2007-2015.

Technology	Reference	Color	Frequency [Hz]	Application
	(FRIMAN; VOLOSYAK; GRASER, 2007)	Red	(13,14,15,16,17)	Speller
	(LUTH et al., 2007)	Red	(13,14,15,16,17)	Semi-autonomous robot(rehabilitation)
	(MATERKA; BYCZUK; PORYZALA, 2007)	Green	(32,33,...,39,40)	Virtual Keypad
	(VALBUENA et al., 2007)	-	(13,14,15,16)	Semi-autonomous robot(rehabilitation)
	(MÜLLER-PUTZ et al., 2008)	Red	(6,7,8,13)	Research
	(GARCIA MOLINA, 2008)	-	(40,41,...,49, 50)	Research
	(PARINI et al., 2009)	Green	(6,7,...,16, 17)	Research
	(POURYAZDIAN; ERFANIAN, 2009)	-	(6-18) with step 0.25. Removed (9-11)	Research
	(WU; CHANG; LEE, 2009)	White	(30,31,32,33,34,35)	Communication System
	(BIAN et al., 2010)	White	(10,15,20,30)	Control a small ball on the computer screen
	(GOLLEE et al., 2010)	-	(13,14,15,16)	Respiratory assistance
	(LEE et al., 2010)	White	(31.25) x8 ea out of phase 45°	Research
	(MOLINA; ZHU; ABTAHI, 2010)	Green	(30,31,...,39,40)	Research
	(PFURTSCHELLER et al., 2010)	-	(8,13)	Hand orthosis control
	(VOLOSYAK et al., 2010)	Red	(12.5-20(step 0.5))	Research
	(WANG et al., 2010)	White	(7,8,9,10,11,12)	Research
	(WANG; LI; HUANG, 2010)	Blue	(9,11,13,15,17)	Electrical Car
	(ZHU et al., 2010)	Green	(30, 31,...,39, 40) ea with phases 0° e 120°	Research
LED	(BIAN et al., 2010)	White	(7,10,15,20)	Research
	(DIEZ et al., 2011)	Green	(37,38,39,40)	Control a small ball on the computer screen
	(MÜLLER et al., 2011)	Green	(37,38,39,40)	Research
	(ORTNER et al., 2011)	-	(8,13)	Hand Orthosis control
	(WU et al., 2011)	-	(30,31,32,33,34,35)	Control cursor movements
	(ZHU et al., 2011)	Green	(39 or 40) x4 ea with phases 0°,90°,180°,270°	Control cursor movements
	(ALLISON et al., 2012)	Red	(8,13)	Control a small ball on the computer screen
	(FALZON; CAMILLERI; MUSCAT, 2012)	Green	(7) x6 out of phase each 60°	Research
	(HWANG et al., 2012)	White	(5-9.9) with step 0.1	Speller
	(PUNSAWAD; WONGSAWAT, 2012)	White	(6,7,8,13)	Control of electrical device
	(XU et al., 2012)	-	(9,10,11,12)	Wheelchair
	(DIEZ et al., 2013)	Green	(37,38,39,40)	Wheelchair
	(SHYU et al., 2013b)	White	(21, 25) x8 ea with phases 0°,90°,180°,270°	Control Hospital Bed Nursing System
	(SHYU et al., 2013a)	White	(21–36) with different duty cycle	Research
	(YEH et al., 2013)	White	(20) x4 ea with phases 0°,90°,180°,270°	Research
	(CAO et al., 2014)	White	(7,8,9,11)	Wheelchair
	(KWAK; MULLER; LEE, 2014)	-	(9,11,13,15,17)	Exoskeleton Control
	(LIM et al., 2015)	White	(5.0-7.9 with a span of 0.1 Hz)	Speller
	(BIN et al., 2009)	Black/white	(6.7,7.5,8.6,10,12,15)	Research
	(CECOTTI, 2010)	Black/white	(6.66,7.5,8.571,7.059,8)	Speller
	(CHANG et al., 2010)	Black/white	(13,14,15)	Remote-Controlled Car
	(MÜLLER et al., 2010)	Black/white	(5.6,6.4,6.9,8)	Wheelchair
	(MÜLLER; BASTOS-FILHO; SARCINELLI-FILHO, 2010)	Black/white	(5.6,6.4,6.9,8)	Research
	(ZHANG; LI; DENG, 2010)	-	(8.57,10,12,15)	Research
	(WONG et al., 2010)	Black/white	(15) x4 ea with phases 0°,90°,180°,270°	Research
	(WONG et al., 2011)	Black/white	(6.67,8.57,12,13.33,17.14)	Research
	(VOLOSYAK, 2011)	Black/white	(6.67,7.50,8.57,10,12)	Speller
	(JIA et al., 2011)	-	(10,12,15)	Research
	(ANGEL; BOJORGES-VALDEZ; YANEZ-SUAREZ, 2011)	Black/white	(6-15)	DASHER writing system
	(CHUMERIN et al., 2011)	-	(10,8.57,7.5,6.67)	Control an avatar in a maze
	(ZHANG et al., 2011)	Black/white	(8.5,10,12,15)	Research
LCD	(BASTOS et al., 2011)	Black/white	(5.6, 6.4, 6.9,8)	Wheelchair
	(MÜLLER; BASTOS-FILHO; SARCINELLI-FILHO, 2011)	Black/white	(5.6,6.4,6.9,8)	Wheelchair
	(MÜLLER et al., 2011)	Black/white	(5.6,6.4,6.9,8)	Wheelchair
	(LI et al., 2011)	-	(10) x6 ea out of phase 60°	Research
	(LEE et al., 2012)	White/red	(13,14,15)	Remote-Controlled Car
	(ZHANG et al., 2012)	Black/red	(6.1,7.1,8.5,10.6)	Research
	(ZHANG et al., 2012)	Black/white	(7,11,13,17,19)	Remote-Controlled robot
	(HAN; HWANG; IM, 2013)	Black/white	(3, 3.33, 3.75, 4.285) for ten stimuli	Research
	(SINGLA; A., 2013)	-	(7, 9, 11,13)	Wheelchair
	(PUNSAWAD; WONGSAWAT, 2013)	Black/white	(6, 7,8)	Wheelchair
	(KIMURA et al., 2013)	Black/white	(8,9,11,12,13,15,17,20,24,30)	Research
	(PAN et al., 2013)	White/green	(5.45,6.0,6.67,7.5)	Research
	(ZHANG et al., 2014a)	Black/white	(7.5,8.6,10,12)	Control an avatar in a virtual stage
	(ZHANG et al., 2014b)	Black/Red	(6,8,9,10)	Research
	(YIN et al., 2015)	Black/white	(8.18,8.97,9.98,11.23,12.85,14.99)	Speller
CRT	(LIN et al., 2007)	-	(27-43) with step 2.0	Research
	(LOPEZ-GORDO; PELAYO; PRIETO, 2010)	Black/white	(15,15.48,15.71,17,17.86)	Control a small ball on the computer screen

usability due to obvious reasons of low cost, power, portability and flexibility. In contrast, the use of computer monitors (LCD or CRT) offers flexibility to easily modify parameters for stimuli in a BCI. BCIs using LEDs as stimulator usually require the development of dedicated hardware in addition to software. With this hardware, one can have a guarantee about the accuracy related to the signals and frequencies that are generated. LEDs are usually controlled by dedicated microcontrollers, unlike of programmed routines in computers and displayed in screens. In contrast of LEDs, problems with screens are evident with the accuracy of the frequencies generated due to the refresh rate of the screen or overload of threads in the computer.

Some studies related to comparison of technologies for stimulation were also reported in the literature. According to (WU et al., 2008), it was found that the SSVEP response elicited by an LED was largely compared to stimuli generated on computer screen. The selection of the kind of stimulator (LCDs, LEDs or CRTs) depends mainly on the complexity of the BCI; other parameters, such as frequency can also influence in this selection.

In Table 2, the studies from Table 1 were redistributed and grouped in different categories according to their applications: A (System communications), B (Home automation), C (Transport), D (Screen), E (Assistance and rehabilitation robotics) and F (Research).

Table 2: Categorization of studies based on SSVEP-BCI according to their applications

Label	Category	Description
A	System communications	Spellers, virtual keypads, etc
B	Home automation (Domotics)	control of fan, lights, television, radio, etc
C	Transport	Electrical car
D	Screen	Cursor, avatar, small ball, etc.
E	Assistance and rehabilitation robotics	Wheelchairs, exoskeleton, robotic walker, robotic hand, etc.
F	Research	Studies with general purpose.

In Figure 8 some applications from references cited below are shown: category A [in (FRIMAN; VOLOSYAK; GRASER, 2007; MATERKA; BYCZUK; PORYZALA, 2007; HWANG et al., 2012; YIN et al., 2015; LIM et al., 2015)], B [in (PUNSAWAD; WONGSAWAT, 2012)], C [in (CHANG et al., 2010; WANG; LI; HUANG, 2010)], D [in (BIAN et al., 2011; LEE et al., 2010; DIEZ et al., 2011; WU; CHANG; LEE, 2009; WU et al., 2011; ALLISON et al., 2012)], E [in (LUTH et al., 2007; DIEZ et al., 2013; SHYU et al., 2013b; CAO et al., 2014)] and F [in (MÜLLER-PUTZ et al., 2008; PARINI et al., 2009; MOLINA; ZHU; ABTAHI, 2010; VOLOSYAK et al., 2010; WANG et al., 2010; ZHU et al., 2010; MÜLLER et al., 2011; FALZON; CAMILLERI; MUSCAT, 2012; SHYU et al., 2013a; YEH et al., 2013)].

One of the contributions of this thesis was the development of a visual stimu-
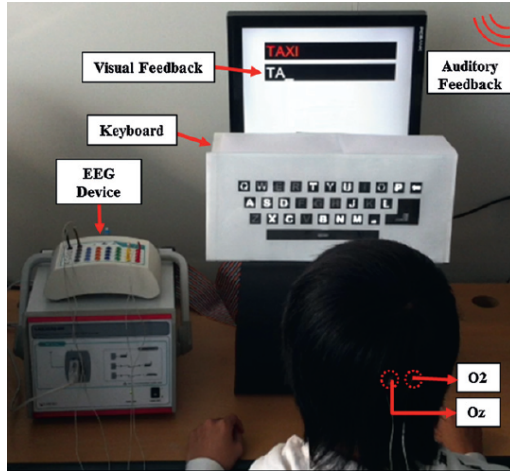
(a) Category A
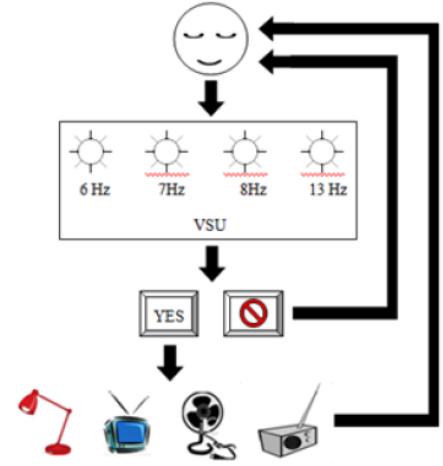
(b) Category B
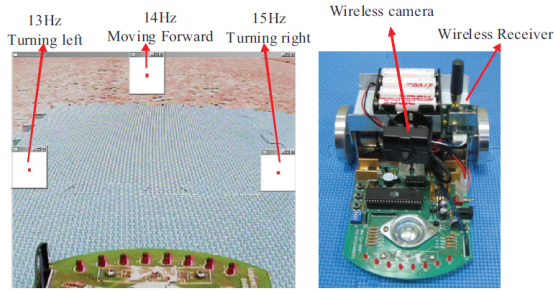
(c) Category C
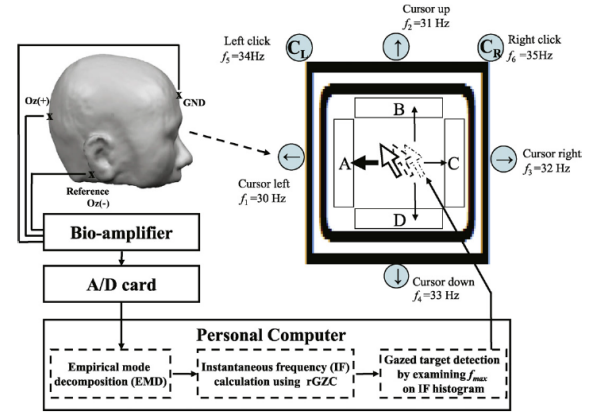
(d) Category D
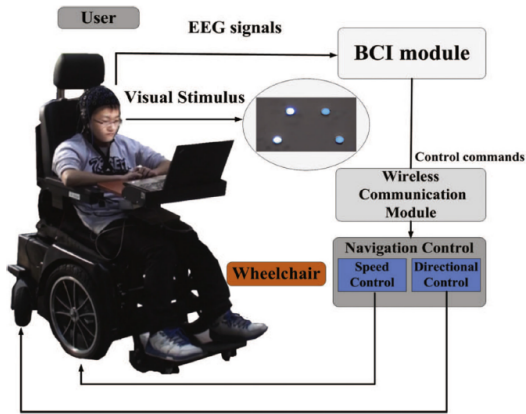
(e) Category E
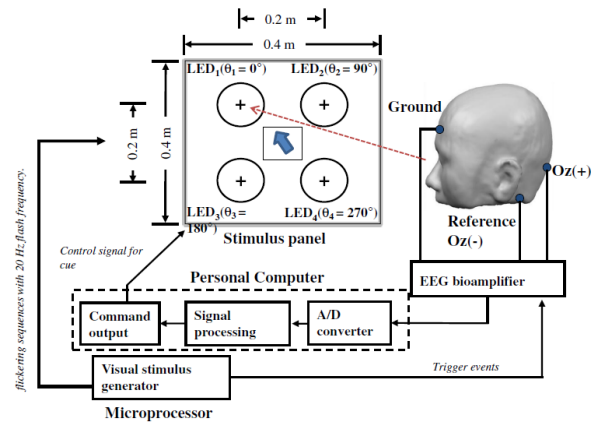
(f) Category F

Figure 8: SSVEP-BCI applications developed in the following references: (a) Hwang et al. (2012), (b) Punsawad and Wongsawat (2012), (c) Chang et al. (2010), (d) Wu et al. (2011), (e) Cao et al. (2014), (f) Yeh et al. (2013).

lator for SSVEPs using LEDs. The timing of LED flickers was controlled by a micro-controller (PIC18F4550, Microchip Technology Inc., USA), with 50/50% on-off duties. Previous simulations were performed to ensure its proper operation through Proteus Software (see Figure 9). The circuit was tested in a development board for microcontrollers, as shown in Figure 10a. On the other hand, a visual stimulator using LCD screen and Field-Programmable Gate Arrays (FPGA) Spartan®-3 was developed in order to perform comparisons between both kind of stimuli (See Figure 10b).
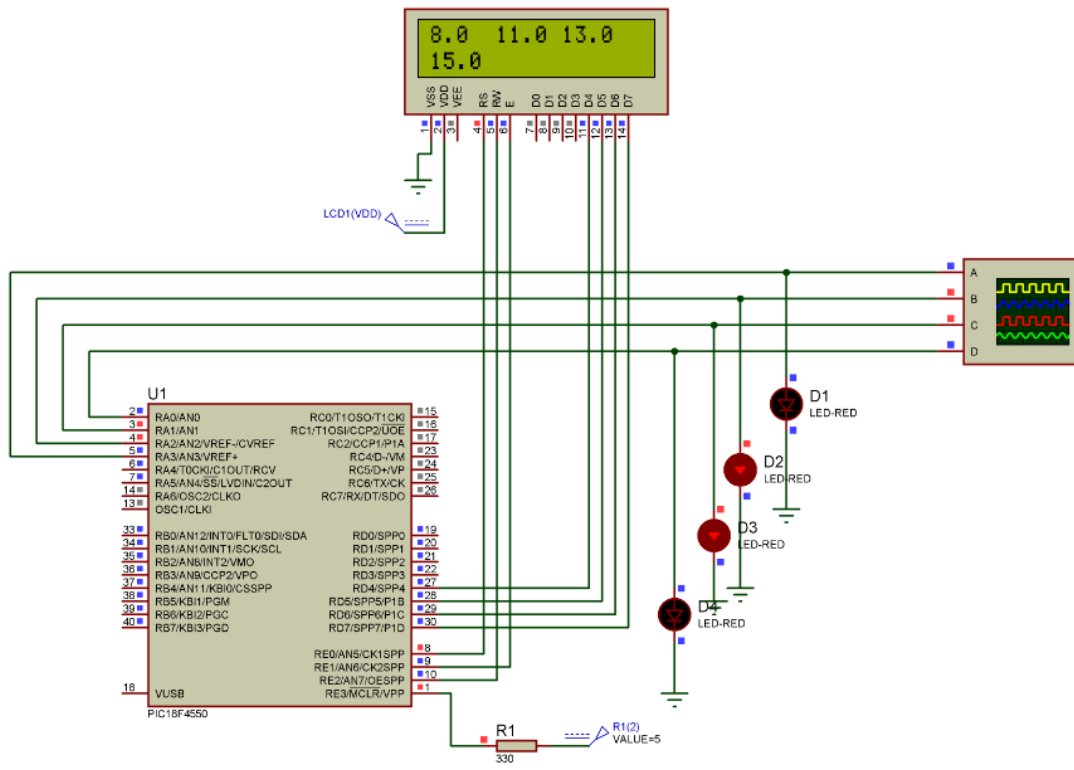
Figure 9: Simulations performed on Proteus software for operating the visual stimulator based on LEDs and PIC18F4550 microcontroller.

3.3   A Comparison of Techniques and Technologies for SSVEP Classification

In recent years, many researchers have made great efforts on the detection of steady-state visual evoked potentials for BCIs. However, more researches related to this area still lack due to SSVEP is dependent and affected by several parameters, such as: type of stimulation, color, shape, data window length, etc. Thus, we developed a set of experiments to evaluate three different aspects of SSVEP: (i) feature extraction; (ii) window lengths; and (iii) visual stimuli (LCD and LEDs).

(a)   (b)
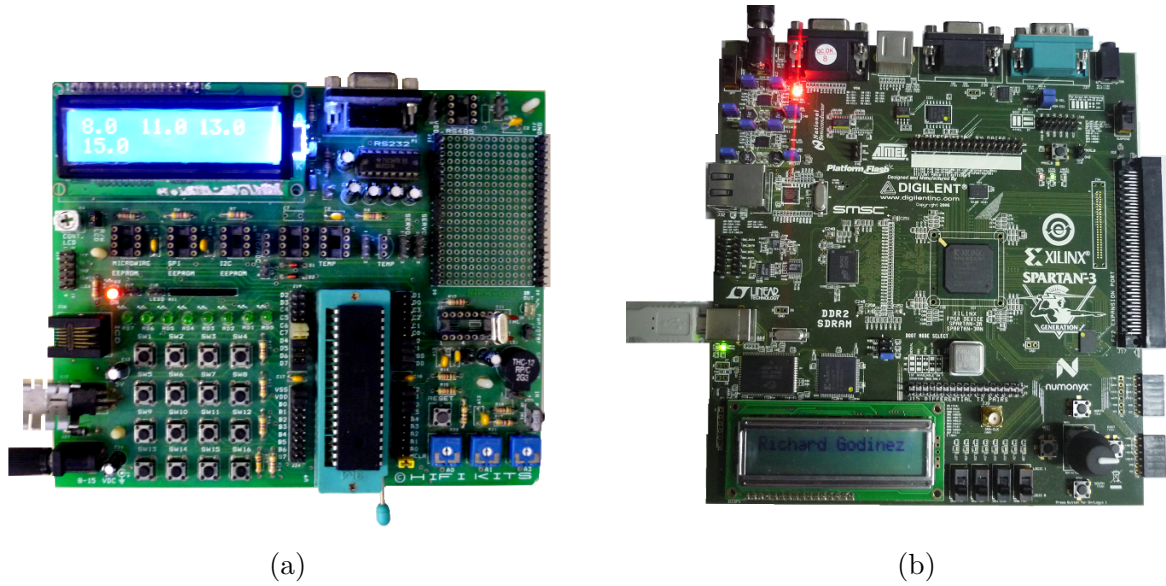
Figure 10: Stimuli generated by: (a) LEDs through a PIC microcontroller; (b) LCD through a FPGA.

3.3.1 Protocol

Seven subjects (five males and two females), aged from 26 to 32 years old (mean: 27.29 and standard deviation: $\pm$ 3.59), were recruited to participate in this study. The research was carried out in compliance with Helsinki declaration, and the experiments were performed according to the rules of the ethics committee of UFES/Brazil, under registration number CEP-048/08.

All measurements were noninvasive and the subjects were free to withdraw at any time without any penalty. Previously, a selection of volunteers was performed and topics related to precautions as visual problems, headaches, family history with epilepsy and problems related to brain damage were consulted.

For the development of this study, twelve channels of EEG signal with the reference electrode at the left ear lobe were recorded at 600 samples/s, with 1 to 100 Hz pass-band filter. The ground electrode was placed on the forehead. Using the extended international 10-20 system, the electrode positions chosen were P7, PO7, PO5, PO3, POz, PO4, PO6, PO8, P8, O1, O2 and Oz (Figure 11).

The equipment used for EEG signal recording in this study was the BrainNet-36. In order to conduct the experiments, the volunteers sat on a comfortable chair, in front of a 17 inches LCD display, 70 cm far from this. For the evaluation of the visual stimuli via LEDs, a coupling structure of small boxes (4cm x 4cm x 4cm) containing LEDs was mounted in the four sides of the LCD video display (Figure 12).

The participants were asked to watch the stimuli display, which were accurately generated by an FPGA-based subsystem (Xilinx Spartan3E). Such stimuli consisted of
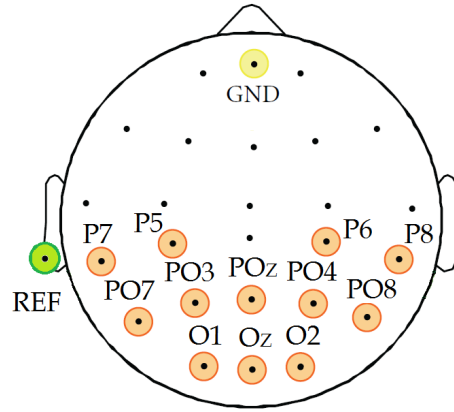
Figure 11: Electrode placement on the scalp during the experiments.
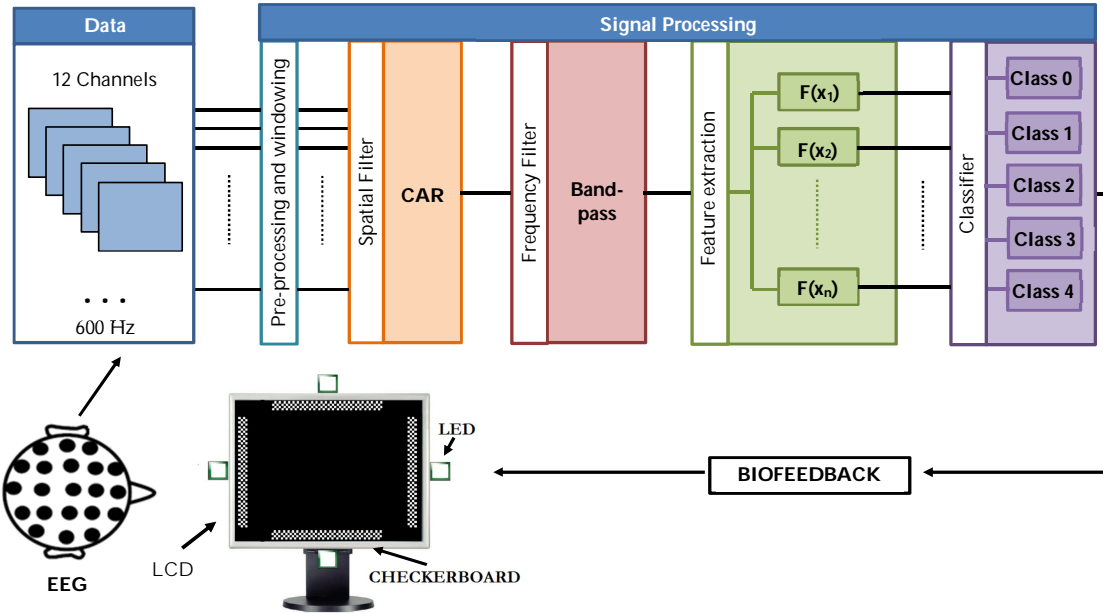
Figure 12: Block diagram of the system and setup for the visual stimuli with LCD and LEDs.

four stripes (checkerboard) presented simultaneously to the user (Figure 13). On the other hand, the timing of the four LEDs was precisely controlled by a microcontroller (PIC18F4550, Microchip Technology Inc., USA), with pulses 50/50% on-off duties.The LEDs have a luminous intensity from 8 to 10 millicandelas (mcd)), white color, covered with thin white papers diffusers.

For both types of stimuli (LCD and LEDs), the flickering frequencies were 8.0 Hz (top), 11.0 Hz (right), 13.0 Hz (bottom) and 15.0 Hz (left), see Figure 13.

3.3.2   Experimental Tasks

The experiments were performed offline, following the protocol shown in Figure 14. During the first five seconds, a cross on the display is shown to the volunteers. Then,
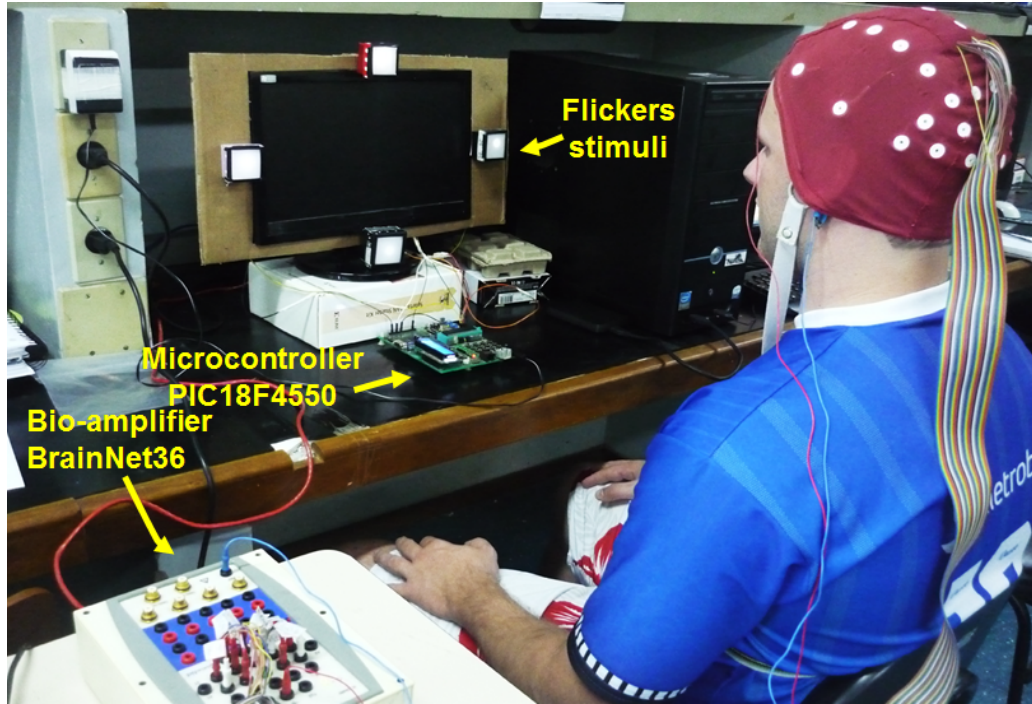
Figure 13: Volunteer sat in front of a LCD display rounded by four flickering stimuli provided by LEDs.

a beep is issued and the volunteer is instructed to fix his/her attention on the stimulus located on the top. After ten seconds for a break, in the next thirty seconds, the volunteer has to fix his/her attention to the right side. This protocol is repeated clockwise for the others stimuli, ending in a total time of 155 seconds.
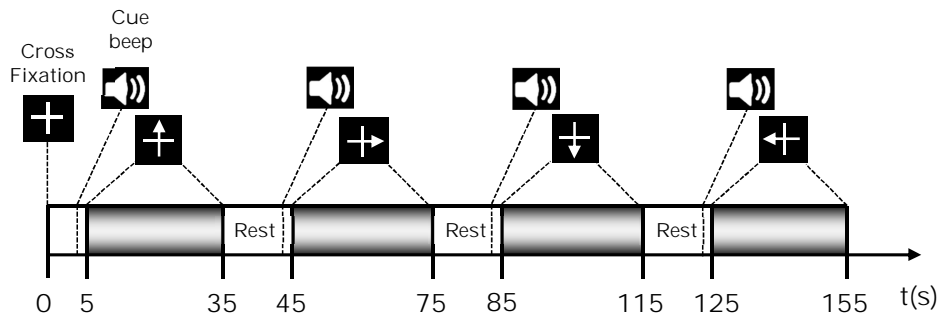
Figure 14: Sequence of events during EEG signal recording.

3.3.3 Data Analysis

The data from the twelve channels were segmented and windowed. Window lengths (WLs) used were 1, 2, 4, 5 and 10 s each one with an overlapping of 50%. Subsequently, a spatial filtering was applied using a Common Average Reference (CAR) filter, and a band-pass filter between 3-60 Hz was also applied for the twelve electrodes.

Although the twelve EEG channels were used during the spatial filtering process, just the three occipital channels located on the visual area (O1, O2 and Oz) were used in the evoked potential of the data analysis (feature extraction and classification). Figure 12 shows the block diagram of the system.

Researchers have developed various techniques of feature extraction and classification of SSVEPs, such as Power Spectral Density Analysis (PSDA) (WANG et al., 2006), Spectral F-Test (SFT) (SA et al., 2006; MÜLLER; BASTOS-FILHO; SARCINELLI-FILHO, 2010), Empirical Mode Decomposition (EMD) (HUANG et al., 1998), Minimum Energy Combination (MEC) (FRIMAN; VOLOSYAK; GRASER, 2007), Canonical Correlation Analysis (CCA) (LIN et al., 2007), Least Absolute Shrinkage and Selection Operator (LASSO) (ZHANG et al., 2012) and Multivariate Synchronization Index (MSI) (ZHANG et al., 2014a). All these methods are here compared, which are described in next sections.

3.3.3.1 Power Spectral Density Analysis - PSDA (SNR)

PSDA or Fourier Power Analysis (WANG et al., 2006) selects an optimal bipolar electrode with a high Signal to Noise Ratio $\text{SNR}(f_k)$, and assumes there are K targets with stimulus frequencies f_1, f_2, ..., f_k, respectively.

The Fourier power (Φ) is computed from the Fast Fourier Transform (FFT) over the whole signals, and the $\text{SNR}(f_k)$ of the SSVEP is afterwards computed using the ratio of Fourier power at a given frequency f_k to its n-adjacent frequencies power (VIALATTE et al., 2010a), such as:

$$\text{SNR}(f_k) = 10 . \log_{10} \left(\frac{n . \Phi\left(f_k\right)}{\sum\limits_{p=s}^{s.n/2} \Phi\left(f_k + p\right) + \Phi\left(f_k - p\right)} \right), \tag{3.1}$$

where s represents the frequency resolution, that in our study was $f_{res} = (\text{sample rate})/(\text{number of sampling points}) = F_s/\text{NFFT} = 600/4096 = 0.1465$ Hz, and n should be even (in this case 30 points were used). This SNR acts as a high-pass filter on the Fourier domain (letting only sharp Fourier peaks). The frequency with the largest $\text{SNR}(f_k)$ related to the SSVEP, can be recognized as follows:

$$O = \max_k \ \text{SNR}(f_k), \quad k = 1, 2, \dots, K. \tag{3.2}$$

It is necessary to emphasize that after the classification for each one of the three channels independently, there is a reclassification of the same by vote to select the best channel and finally determinate the winner class.

3.3.3.2 Spectral F-Test (SFT)

Spectral F-Test (SFT) is a technique based on PSDA (SA et al., 2006; MÜLLER; BASTOS-FILHO; SARCINELLI-FILHO, 2010), to evaluate synchronized spectral changes in the EEG signal recorded during visual stimuli, $x[k]$, at a given stimulus frequency, f_0. STF is applied as the ratio between the power in such frequency and the average power in L even neighboring frequencies, which is defined as

$$\hat{\phi}(f_0) = \frac{P_{xx}(f_0)}{\frac{1}{L}\sum\limits_{i=-L/2,i\neq0}^{i=L/2} P_{xx}(f_i)}, \tag{3.3}$$

where P_{xx} is the Power Spectral Density (PSD) of the signal $x[k]$ evaluated at the frequency f_0, and $P_{xx}(f_i)$ are the PSD values at the L neighboring frequencies closest to f_0.

This technique has the goal of determining whether the spectrum at the frequency f_0 is statistically distinct from its neighbors, considering that the spectrum in this neighborhood is white. Equation 3.3 is also used in (WANG; GAO; GAO, 2005) to evaluate the SNR of the SSVEP. Here, this expression is used to detect the evoked peaks that are rejected by the null hypothesis, H_0, which correspond to the absence of evoked response. The alternative hypothesis is that the null hypothesis is false, i. e., there is evoked response. Under the null hypothesis, $\hat{\phi}(f)$ is distributed as (SA et al., 2009)

$$\hat{\phi}(f_0) \mid_{H_0} \sim F_{2,2L}, \tag{3.4}$$

where $F_{2,2L}$ is the F distribution with 2 and $2L$ degrees of freedom. Consequently, H_0 is rejected (for $\alpha = 0.05$) using the critical value, given by

$$STF_{crit} = F_{(2,2L,\alpha)}. \tag{3.5}$$

In our study, $L = 32$ neighboring frequencies, which leads to a STF_{crit} of $F_{(2,64,0.05)}$ = 3.1404.

For the classification, a technique based on a tree decision classifier was used, which is shown in Figure 15.

3.3.3.3 Empirical Mode Decomposition (EMD)

Huang et al. (1998) introduced the concept of Empirical Mode Decomposition (EMD) together with Hilbert transform, which was collectively called Hilbert-Huang Transform (HHT), used to extract time-frequency information from a nonlinear and non-stationary signal. This method was regarded as an important progress since the FFT
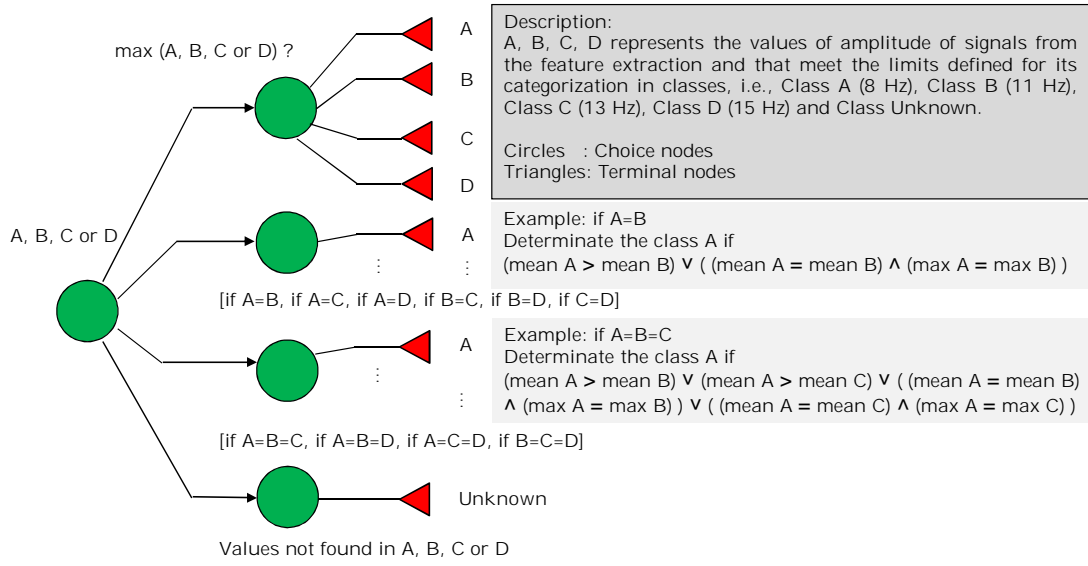
Figure 15: Structure of the rule-based classifier implemented.

(FELDMAN, 2011). The first step of the HHT method is the signal pre-processing. In this step, original data are transformed into n order Intrinsic Mode Function (IMF), satisfying the requirements of the Hilbert Transform through EMD (HUANG et al., 2008), in which the EMD approach attempts to sequentially decompose a signal into a finite number of intrinsic mode functions (IMFs) by iteratively conducting a shifting process (WU et al., 2011). An IMF is an analytical, self-constructed, well-defined, data-driven function, whose amplitudes and frequencies vary with time (HUANG et al., 1998). IMFs are denoted by $\sum_{j=1}^{J} \vec{c}_j(t)$ and into residue $r(t)$, such that (SOOMRO et al., 2013)

$$\vec{x}(t) = \sum_{j=1}^{J} \vec{c}_j(t) + \vec{r}(t), \tag{3.6}$$

where J represents the number of IMFs extracted, and $\vec{r}(t)$ is a residual function that represents a trend within the signal $\vec{x}(t)$.

In our study, the calculation of IMFs is made for the three occipital electrodes (O1, O2 and Oz). This algorithm is used as an input of a hybrid system. The IMFs can be then arranged in a $J \times D$ matrix, $\mathbf{C}$, where each row $\vec{c}_k$ represents the kth IMF:

$$\mathbf{C} = \begin{bmatrix} \vec{c}_1 \\ \vec{c}_2 \\ \vdots \\ \vec{c}_J \end{bmatrix}_{J \times D}, \tag{3.7}$$

where D is the number of selected data for each epoch.

Subsequently, the number of IMFs to be used is defined (all with the same number for the three channels). In our study, the best results were obtained for IMF of order 2 (IMF 2). Then, the PSD of these signals in decomposition was calculated. For this case, our classifier based on rules (Figure 15) finds the maximum values and performs a decision by majority vote for the selection of the class.

3.3.3.4   Minimum Energy Combination (MEC)

MEC is a technique of finding combinations of electrode signals that remove strong noise and nuisance signals for EEG data (FRIMAN; VOLOSYAK; GRASER, 2007). MEC is based on PCA (ZHANG et al., 2014a). For SSVEP data stimulated by a frequency f, the response can be modelated adding the noise (E), as follows:

$$\mathbf{X}^T = \mathbf{Y}^T\mathbf{A} + \mathbf{E} \tag{3.8}$$

where $\mathbf{X}$ is the EEG signal, and $\mathbf{Y}$ is the reference signal, as given in Equation 3.8. $\mathbf{A}$ is the amplitude matrix of size $2N_h \times N$ for all electrode signals, N_h is the number of harmonics and $\mathbf{E}$ is the noise matrix of size $M \times N$. The signals (from O1, O2 and Oz) are combined to extract the discriminative features, which can be achieved by linear transformation of $\mathbf{X}$.

The target at which the user gazes in the SSVEP-BCI is then determined through a criterion of maxima. More details can be viewed at (FRIMAN; VOLOSYAK; GRASER, 2007; ZHANG et al., 2014a).

3.3.3.5   Canonical Correlation Analysis (CCA)

Lin et al. (2007) first proposed the use of CCA for multichannel SSVEP detection, which is an array signal processing technique for EEG signals, that extracts CCA coefficients for all stimulus frequencies, and assumes the frequency with the largest coefficient as the SSVEP frequency (TANAKA; ZHANG; HIGASHI, 2012).

Describing it mathematically, this method assumes that $\mathbf{X}$ is a multichannel EEG signal, and $\mathbf{Y}$ consists of a "Fourier series" of stimulus signals (WEI; XIAO; LU, 2011), assuming that there are K targets with stimulus frequencies f_1, f_2,...,f_k, respectively. A pair of linear combinations $x = \mathbf{X}^T W_x$ and $y = \mathbf{Y}^T W_y$, called canonical variables, is found by using CCA between the two sets, such that the correlation is maximized. The reference

signals Y is set as

$$Y = \begin{bmatrix} \sin\left(2\pi f_k t\right) \\ \cos\left(2\pi f_k t\right) \\ \vdots \\ \sin\left(2\pi N_h f_k t\right) \\ \cos\left(2\pi N_h f_k t\right) \end{bmatrix}, \quad t = \frac{1}{F_s}, \frac{2}{F_s}, ..., \frac{T}{F_s}, \tag{3.9}$$

where f_k is the stimulus frequency, N_h is the number of harmonics, T is the number of sampling points (NFFT), and F_s is the sampling rate. In our study, we used $N_h = 3$ harmonics in the analysis.

It is worth to comment that the CCA method needs to find the weight vectors, W_x and W_y, that maximize the correlation between x and y, i. e., that constrains and limits conditions established by Equations 3.10 and 3.11.

$$E\left[xx^T\right] = E\left[x^T x\right] = E\left[W_x^T X X^T W_x\right] = 1 \tag{3.10}$$

$$E\left[yy^T\right] = E\left[y^T y\right] = E\left[W_y^T Y Y^T W_y\right] = 1 \tag{3.11}$$

Figure 16 shows the classification steps using CCA.
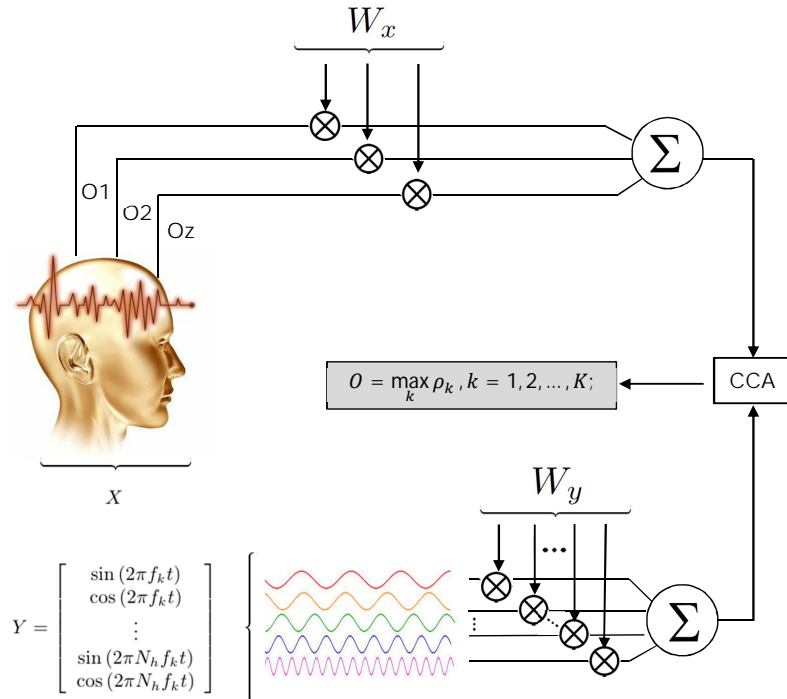
Figure 16: Block diagram for classification using CCA.

CCA measures the linear association between two sets of variables using its autocorrelation and crosscorrelation (BORGA; KNUTSSON, 2001), i.e., in mathematical terms, the total correlation is calculated as the ratio between the autocorrelation and crosscorrelation of the input and output vectors, as shown in Equation 3.12.

$$
\begin{aligned}
\rho_k = \underset{W_x, W_y}{\rho(x, y)} &= \frac{E[x^T y]}{\sqrt{E[x^T x] E[y^T y]}} \\
&= \frac{E[W_x^T X Y^T W_y]}{\sqrt{E[W_x^T X X^T W_x] E[W_y^T Y Y^T W_y]}}
\end{aligned}
, \tag{3.12}
$$

Finally, the process of correlation of these signals is executed, which determines the channel (from O1, O2 and Oz) and the class through a criterion of maxima, given by

$$
O = \max_k \rho_k, \quad k = 1, 2, ..., K. \tag{3.13}
$$

3.3.3.6 Least Absolute Shrinkage and Selection Operator (LASSO)

In this method, input signals are defined as $(\mathbf{x}^i, y_i), i = 1, 2, \ldots, N$; where $\mathbf{x}^i = (x_{i1}, \ldots, x_{ip})^T$ are predictor variables, and y_i are the responses (TIBSHIRANI, 1996). As in the usual regression set-up, we assume either that the observations are independent, or y_i is conditionally independent given x_{ij}. We assume that x_{ij} are standardized, so that $\sum_i x_{ij}/N = 0, \sum_i x_{ij}^2/N = 1$. Letting $\widehat{\beta} = (\widehat{\beta}_1, \ldots, \widehat{\beta}_p)^T$, LASSO estimate $(\widehat{\alpha}, \widehat{\beta})$ is defined as

$$
\left(\widehat{\alpha}, \widehat{\beta}\right) = arg_{min} \left\{ \sum_{i-1}^{N} \left(y_i - \alpha - \sum_j \beta_j x_{ij} \right)^2 \right\}. \tag{3.14}
$$

The solution of this equation is a quadratic programming problem with linear inequality constraints (TIBSHIRANI, 1996). LASSO estimate usually offers an analytical solution and a low variance estimate with high interpretability for a linear regression (ZHANG et al., 2012). The class is obtained through the criterion of maxima.

3.3.3.7 Multivariate Synchronization Index (MSI)

MSI is a method to estimate the synchronization between actual mixed signals and reference signals as a potential index for recognizing the stimulus frequency. Besides, in (ZHANG et al., 2014a) the use of a *S*-estimator as index is proposed. The *S*-estimator is based on the entropy of the normalized eigenvalues of the correlation matrix of four multivariate signals. Thus, MSI creates a reference signal from the stimulus frequencies used in an SSVEP-BCI, similarly to CCA.

EEG signals are denoted as matrix $\mathbf{X}$ of size $N \times M$, and reference signals are denoted as matrix $\mathbf{Y}$ of size $2N_h \times M$, where N is the number of channels, M is the number of samples, and N_h is the number of harmonics for sine and cosine components.

Reference signals $\mathbf{Y}$ are created in the same way as CCA (Equation 3.9). In our study, the input signals $\mathbf{X}$ are the signals from O1, O2 and Oz. Then, a correlation matrix is computed according to Equation 3.15. It is worth to comment that the autocorrelation matrices $\mathbf{C11}$ and $\mathbf{C22}$ for $\mathbf{X}$ and $\mathbf{Y}$, respectively, and the cross-correlation matrices $\mathbf{C12}$ and $\mathbf{C21}$, were changed in our study from the original version (ZHANG et al., 2014a) due to its inconsistency in the dimensions of each component for the formation of the correlation matrix $\mathbf{c}$. The efficiency of our algorithms has been demonstrated in several of our previous works (TELLO et al., 2014b; TELLO et al., 2015a; TELLO et al., 2014a; TELLO et al., 2014c; TELLO et al., 2015b; TELLO et al., 2015c; TELLO et al., 2015b). Thus, the following equations are proposed:

$$\mathbf{c} = \left[\begin{array}{cc} \mathbf{C11} & \mathbf{C12} \\ \mathbf{C21} & \mathbf{C22} \end{array} \right] \tag{3.15}$$

where,

$$\mathbf{C11} = \frac{1}{M}\mathbf{X}\mathbf{X}^T \tag{3.16}$$

$$\mathbf{C12} = \frac{1}{M}\mathbf{X}\mathbf{Y}^T \tag{3.17}$$

$$\mathbf{C21} = \frac{1}{M}\mathbf{Y}\mathbf{X}^T \tag{3.18}$$

$$\mathbf{C22} = \frac{1}{M}\mathbf{Y}\mathbf{Y}^T. \tag{3.19}$$

To reduce the influence in the synchronization measure of the autocorrelation and crosscorrelation of $\mathbf{X}$ and $\mathbf{Y}$, the following linear transformation is adopted:

$$\mathbf{U} = \left[\begin{array}{cc} \mathbf{C11}^{-(1/2)} & 0 \\ 0 & \mathbf{C22}^{-(1/2)} \end{array} \right]. \tag{3.20}$$

Then, the transformed correlation matrix is

$$\mathbf{R} = \mathbf{U}\mathbf{C}\mathbf{U}^T. \tag{3.21}$$

Let $\lambda_1, \lambda_2, \ldots, \lambda_p$ be the eigenvalues of matrix $\mathbf{R}$. Then, the normalized eigenvalues are calculated as follows:

$$\lambda\prime_i = \frac{\lambda_i}{\sum_{i=1}^{P} \lambda_i} = \frac{\lambda_i}{tr\left(\mathbf{R}\right)}, \tag{3.22}$$

where $P = N + 2N_h$. Then, the synchronization index between the two sets of signals can be calculated as

$$S = 1 + \frac{\sum_{i=1}^{P} \lambda_i log\left(\lambda_i\right)}{log\left(P\right)} \qquad (3.23)$$

Next, the synchronization index between the signals (from O1, O2 and Oz) and each reference signal $\mathbf{Y}$ is calculated, and the k indices $(S_1, S_2,...,S_k)$ are obtained. Finally, the class is computed through the criterion of maxima.

3.3.4 Experimental Results

All the aforementioned methods were evaluated in terms of accuracy to obtain the SSVEP frequencies. In addition, the Command Transfer Interval (CTI) is used to obtain the Information Transfer Rate (ITR), which is the most common measure to assess a BCI performance. CTI is defined as the total experimental time (Ttotal) divided by the number of total output digits or letters (Ntotal), i.e., Ttotal/Ntotal. On the other hand, ITR is defined by Equation 3.24 (WU et al., 2011).

$$\text{ITR} = \frac{\text{Bits}}{\text{Command}} \cdot \frac{60}{\text{CTI}}$$

$$\text{where,} \quad \frac{\text{Bits}}{\text{Command}} = \log_2 K + P \log_2 P + (1 - P) \log_2 \left(\frac{1-P}{K-1}\right), \qquad (3.24)$$

K is the total number of stimuli, and P is the accuracy.

Figure 17 shows the accuracy for each feature extractor evaluated using visual stimuli by LCD, showing also the ITR for each feature extractor and for each corresponding window length (WL) used. Similarly, Figure 18a and 18b show the results for visual stimuli via LEDs.

3.3.5 Discussion

According to the results obtained for the methods studied (Figures 17 and 18), MSI presented the highest accuracy in both cases (88% for LCD and 94% for LED), and this is even more noticeable when the window length (WL) is increased (Figures 17 and 18). Thus, it can be inferred that MSI has great potential applicability in SSVEP BCIs. It is also possible to notice that the maximum value of accuracy obtained for all participants was approximately 94%, using LEDs, and maximum ITR of 37 bits/min for LCD. It should be noted that Figures 17 and 18 show the different feature extractors chronologically ordered according to evolution of the state of art.
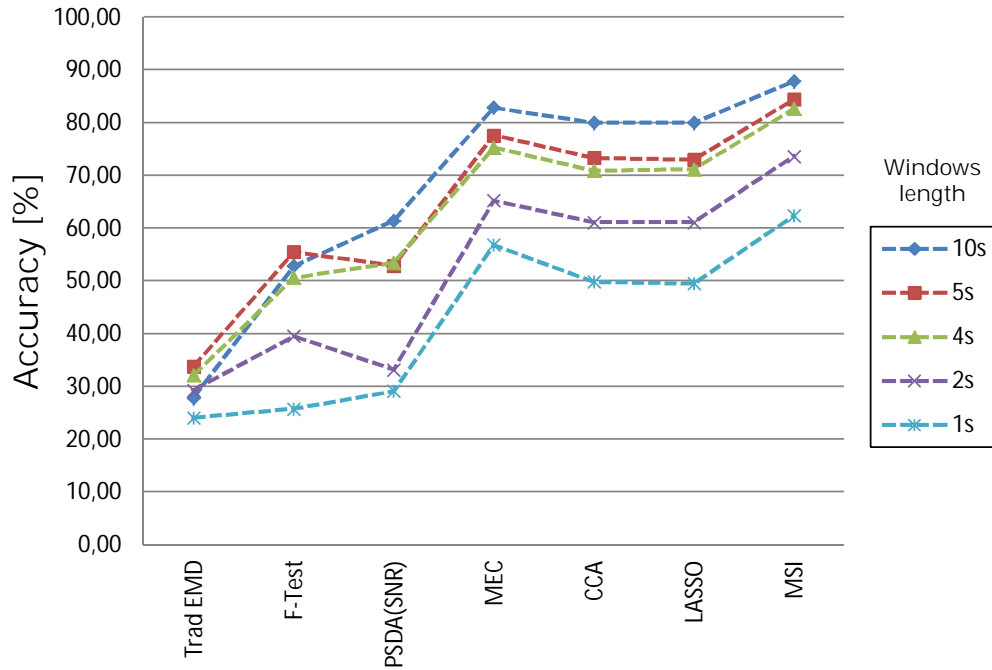
(a)
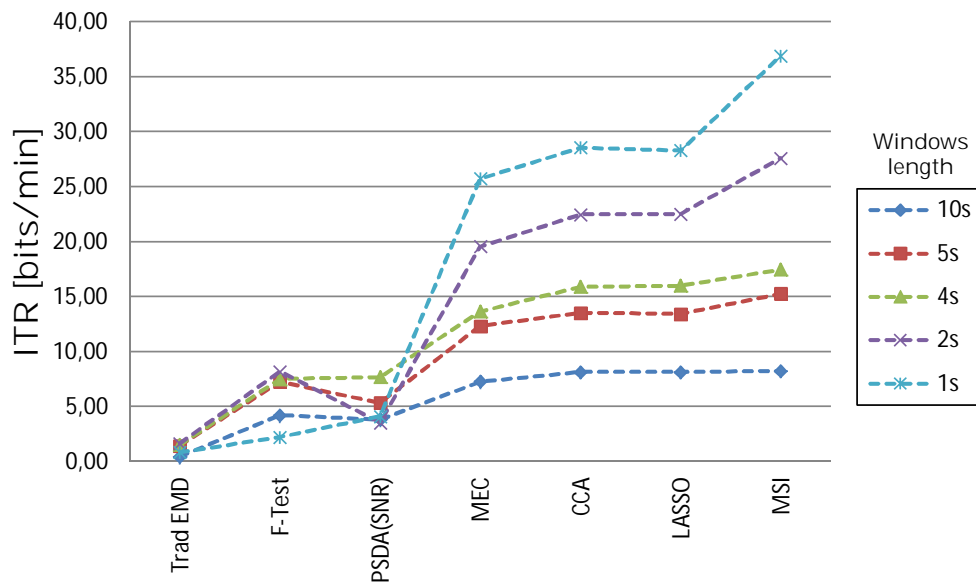
(b)

Figure 17: (a) Accuracy of each feature extractor evaluated using stimuli by LCD; (b) Corresponding ITR for stimuli by LCD.
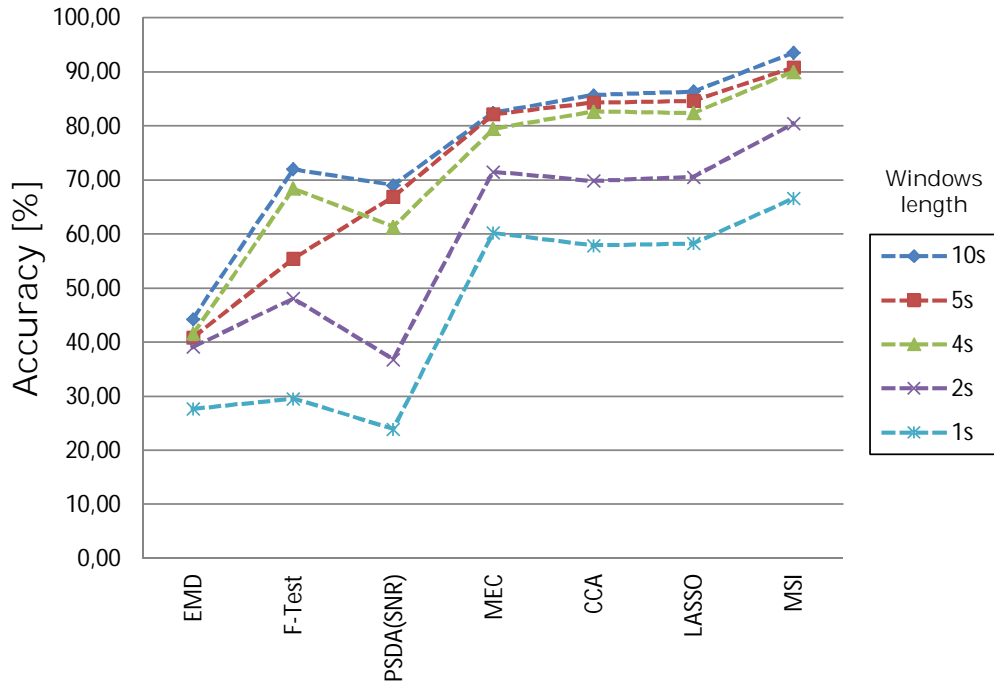
(a)
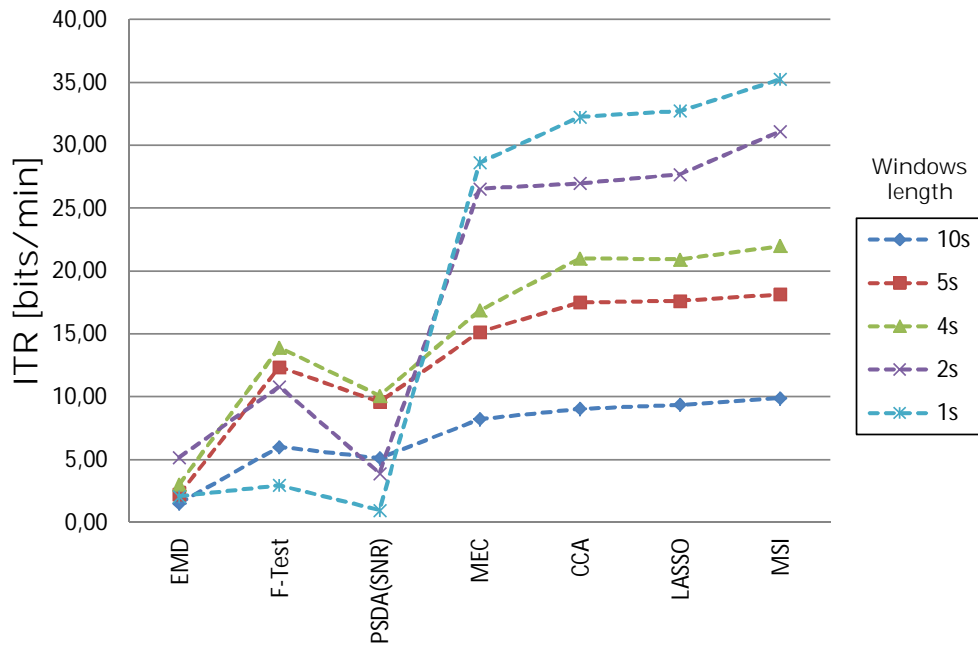
(b)

Figure 18: (a) Accuracy of each feature extractor evaluated using stimuli by LEDs; (b) Corresponding ITR for stimuli by LEDs.

Figure 19 summarizes the comparison for the different methods evaluated using Analysis of Variance (ANOVA), in which the accuracy is higher for MSI using visual stimuli by LEDs and WL of 4 s.
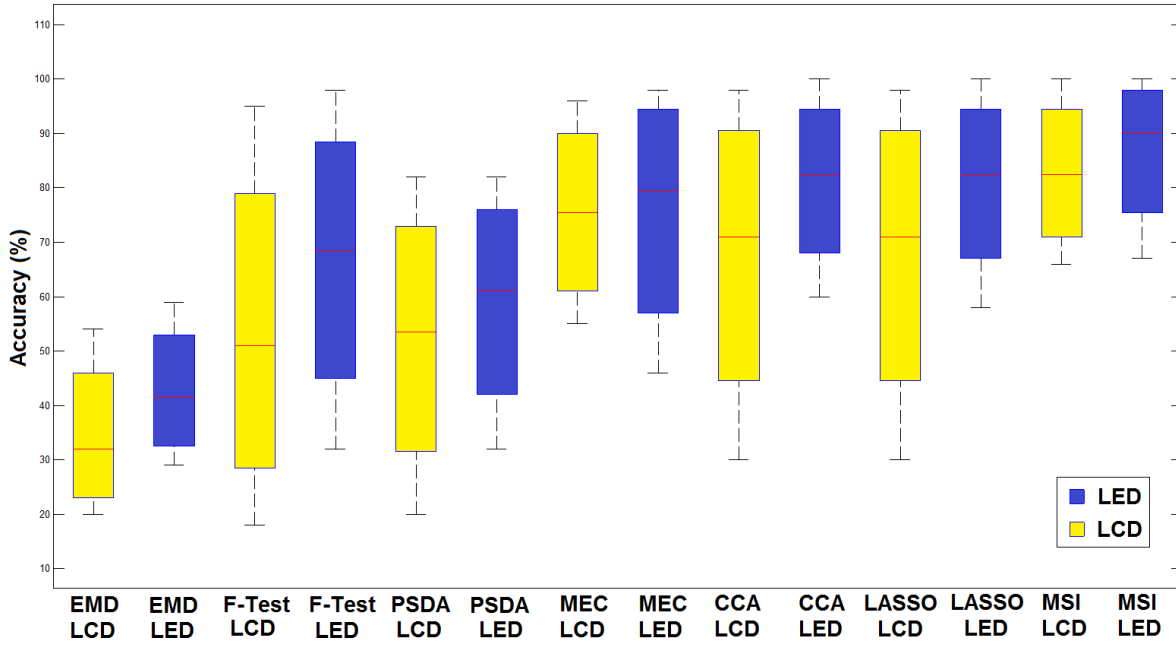
Figure 19: Analysis of Variance (ANOVA) in terms of accuracy for different methods and different visual stimuli (by LEDs and LCD), using WL of 4s.

3.4   A New Approach for SSVEP Detection Using PARAFAC and Canonical Correlation Analysis

The decomposition of Electroencephalogram (EEG) signals into interpretable building components has been of great interest along the years. However, traditionally two-way decomposition techniques, considering just two contextual dimensions or "signatures", e.g. time and frequency or time and spatial, have been used in the literature, which needs exploiting some additional constraints in the decomposition for the sake of uniqueness. Some examples of these techniques are: Principle Component Analysis (PCA), Independent Component Analysis (ICA) and Singular Value Decomposition (SVD). In order to obtain a more natural representations of an original multi-dimensional data structure, the use of tensor decomposition approaches is necessary, since additional dimensions or modes can be retained only in multi-linear models to produce structures that are unique and which admit interpretations that are neurophysiologically meaningful (CICHOCKI et al., 2009). Advances in developing high-spatial density array EEG have called to multidimensional signal processing techniques as multi-way analysis (MWA), Multi-Way Array (tensor) factorization/decomposition or Dynamic Tensor Analysis (DTA) (CICHOCKI et al., 2009).

Tensor-based methods are a more natural approach to handle signals that vary in more than two dimensions and seek to summarize the data into extracted factors, which are linear combination of the constituting variables. The well-known Parallel Factor Analysis (PARAFAC) decomposition is a powerful approach to decompose a tensor into building components (JANNEK et al., 2009). The PARAFAC model was independently proposed by Harshman (1970) and, subsequently, it was named Canonical Decomposition (CANDECOMP) by Carrol and Chang (1970) (MORUP et al., 2006; MIWAKEICHI et al., 2004). This model is a parsimonious extension of the factor analysis to higher orders (MORUP et al., 2006).

In the last years, several works have been performed in applying PARAFAC for EEG signal analysis, e.g., for estimating the sources of cognitive processing using a Wavelet decomposition (MIWAKEICHI et al., 2004), Event-Related Potential (ERP) analysis (MORUP et al., 2006), Wigner distribution for ERP (JANNEK et al., 2009), artifact removal (ACAR et al., 2007) and epileptic seizure localization (VOS et al., 2007). It was also used in BCIs based on Motor Imagery (CICHOCKI et al., 2009).

On the other hand, several approaches to recognize SSVEPs have been developed. However, these techniques are based on only two dimensions. Some studies ((LI; ZHANG; ZHAO, 2008) and (MANYAKOV et al., 2012)) related to classification of VEPs using PARAFAC were performed. In (LI; ZHANG; ZHAO, 2008), three classes of geometric figures were evaluated, flickering in 15 Hz, and a Support Vector Machine (SVM) classifier was used to discriminate classes from feature vectors, achieving a high classification accuracy (80%). Finally, in (MANYAKOV et al., 2012), two techniques ("maximum method" and "sharpness method") of recognition of SSVEPs were compared for all possible 2, 4 and 12 stimuli combinations applied to a BCI.

In this study, we propose a new way for detection of SSVEPs through correlation analysis between tensor models (using 3-way: channel×time×frequency) and simulated tensor model ("template"). The classification is obtained from comparison of each of the extracted signatures of the PARAFAC model with the corresponding simulated signatures of a target SSVEP signal. Here, we just consider the spectral and spatial signatures, considering that the SSVEP is present in the temporal signature. A maximum criterion decides which target is intended every 1 s, which makes it suitable for real time BCI applications.

3.4.1 The Parallel Factor (PARAFAC) model

PARAFAC can be employed for a space/frequency/time atomic decomposition of the EEG. This technique makes use of the fact that multichannel evolutionary spectra are multi-way arrays, indexed by electrode, frequency, and time.

This leads to the formulation of the parameter **S**, which is a three-way data array indicating channel, frequency, and time. The multichannel EEG evolutionary spectrum **S** is obtained from a channel by wavelet transform. In other words, the data matrix $\mathbf{S}_{(N_d \times N_f \times N_t)}$ is the 3-way time-varying EEG spectrum array obtained by using wavelet transformation, where N_d, N_f, and N_t are the number of channels, steps of frequency, and time samples, respectively. For wavelet transformation, a complex Morlet mother function was used. Thus, the energy $S(d, f, t)$ of the channel d at frequency f and time t is given by the squared norm of the convolution of a Morlet wavelet with the EEG signal $v(d, t)$.

The basic structural model for a PARAFAC decomposition of the data matrix $\mathbf{S}_{(N_d \times N_f \times N_t)}$ of elements S_{dft} is defined as:

$$\hat{S}_{dft} = \sum_{k=1}^{N_k} a_{dk} b_{fk} c_{tk}. \tag{3.25}$$

PARAFAC decomposes this array into the sum of "atoms". The kth atom is the tri-linear product of loading vectors representing spatial ($\mathbf{a}_k$), spectral ($\mathbf{b}_k$), and temporal ($\mathbf{c}_k$) "signatures". Under these conditions, PARAFAC can be summarized as finding the matrices $\mathbf{A} = \{\mathbf{a}_k\}$, $\mathbf{B} = \{\mathbf{b}_k\}$, and $\mathbf{C} = \{\mathbf{c}_k\}$, which explains **S** with minimal residual error (see details in Figure 20). N_k is the PARAFAC model order.
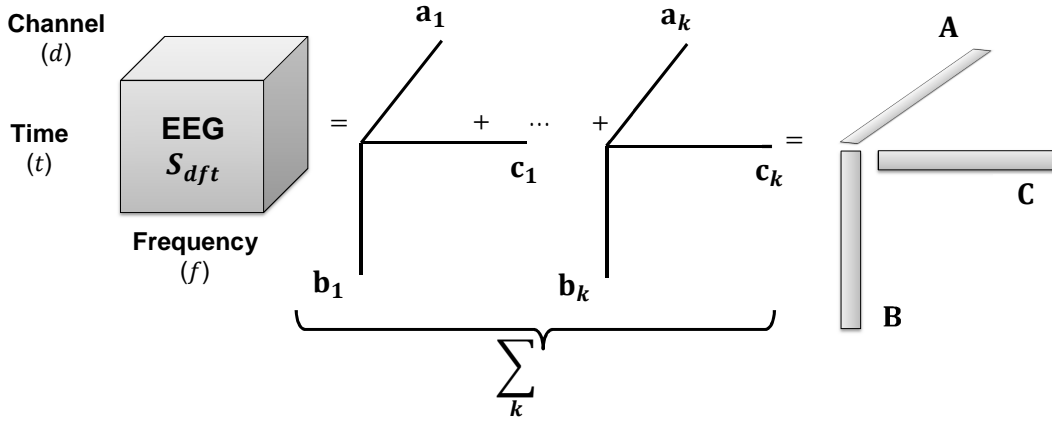
Figure 20: Graphical explanation of the PARAFAC model. Adapted from (MIWAKEICHI et al., 2004).

The uniqueness of the solution is guaranteed when rank($\mathbf{A}$)+rank($\mathbf{B}$)+rank($\mathbf{C}$) $\geq 2N_k + 2$. This is a less-stringent condition than either orthogonality or statistical independence (MIWAKEICHI et al., 2004). N_k needs to be determined priorly. There are several techniques for PARAFAC model order selection, e.g., CORCONDIA (BRO; KIERS, 2003), DIFFIT, CONVEX-HULL. Here, we use CORCONDIA for PARAFAC model order selection. The decomposition (shown in Equation 3.25) is achieved finding $\min_{a_{dk} b_{fk} c_{tk}} \|\hat{S}_{dft} - \sum_{k=1}^{N_k} a_{dk} b_{fk} c_{tk}\|$. Since the $\hat{S}_{dft}$ are spectra, this minimization must be carried out under the non-negativity constraint for the loading vectors. This particular

variant of PARAFAC has been developed by Bro (1998). PARAFAC produces the vectors $\mathbf{a}_{k(N_d \times 1)}$, which is the kth component loading vector that can be seen as topographical maps, $\mathbf{b}_{k(N_f \times 1)}$ is the spectrum for kth component, and $\mathbf{c}_{k(N_t \times 1)}$ is the temporal signature for component k.

The main advantage of this method is that it provides us with a unique decomposition of the time-varying EEG spectrum provided that the condition is satisfied corresponding to the best model in the least-squares sense (MIWAKEICHI et al., 2004).

In addition, the CCA technique measures the linear association between two sets of variables using its autocorrelation and cross-correlation, i.e., in mathematical terms, the total correlation is calculated as the ratio between the autocorrelation and cross-correlation of the input and output vectors. Finally, the process of correlation of these signals is executed and the classes are obtained through a criterion of maxima.

3.4.2   Subjects and EEG preparation

Five healthy male subjects (mean age: 26.2 years old; standard deviation: 2.3) were recruited to participate in this study. The research was carried out in compliance with Helsinki declaration, and the experiments were performed according to the rules of the ethics committee of UFES/Brazil, under registration number CEP-048/08. Previously, a selection of volunteers was performed and topics related to precautions as visual problems, headaches, family history with epilepsy and problems related to brain damage were consulted. The volunteers reported not presenting any of these problems.

The same setup of section 3.3.1 was used in this study, but with only two LEDs flickering at 8.0 Hz (top) and 13.0 Hz (bottom), see Figure 21. During the first five seconds a cross on the screen is shown to the volunteers. Then, a beep is issued and the volunteer is instructed to fix the attention on the stimulus located on the top. After fifteen seconds, the volunteer has a rest of five seconds. Finally, in the last fifteen seconds, the volunteer has to fix the attention to the bottom flicker.

Initially, two 3-way *channel* × *frequency* × *time* template tensors for two target SSVEP signals of 8 Hz and 13 Hz were generated (see Figure 22). The template SSVEP signal constituted of the summation of sine and cosine signals at the target SSVEP's frequency. Based on the hypothesis that the visual evoked potentials contain more energy in the occipital region, the spatial signature was considered just for O1, O2 and Oz channels, and zero elsewhere. Finally, assuming a 1s SSVEP signal, a WL of 1 second was considered for the temporal signature.

Let f_i denote the visual stimulus frequency in Hz. Thus, total H harmonic sine vectors $s_1^i, s_2^i, \ ... \ , s_H^i$ and cosine vectors $c_1^i, c_2^i, \ ... \ , c_H^i$ for frequency f_i, all of the length L,

Figure 21: (a) Electrodes location using 10-20 system; (b) LCD screen showing the cue of beginning with the two LEDs coupled.

can be constructed as

$$s_j^i = [s_{j,1} s_{j,2} ... s_{j,L}]^T \quad \text{and} \quad c_j^i = [c_{j,1} c_{j,2} ... c_{j,L}]^T, \tag{3.26}$$

for $j = 1, 2, ..., H$, where

$$s_{j,r} = \sin(2\pi r f_i / f_s) \quad \text{and} \quad c_{j,r} = \cos(2\pi r f_i / f_s), \tag{3.27}$$

for $r = 1, 2, ..., L$, where f_s is the sampling frequency used for the acquisition of EEG signals. The reference matrix $\mathbf{M}_i$ of size $2H \times L$ corresponding to the stimulus frequency f_i can be constructed as

$$\mathbf{M}_i = [s_1^i, c_1^i, s_2^i, c_2^i, ..., s_H^i, c_H^i]^T, \tag{3.28}$$

where i refers to the number of targets, commands or visual stimuli and we have considered only the fundamental frequency as the simulated frequency generator, i.e. $H = 1$, in channels O1, O2 and Oz and all other channels were filled with matrices of zero values. On the other hand, every 1-s of the 12-channel input EEG signals without overlapping was used to generate the EEG tensor. Then a 3-component PARAFAC model was fitted, where the model order was selected via CORCONDIA method. The output of each PARAFAC model (templates and EEG signal) has three atoms for each dimension or signature (spatial ($\mathbf{a}_k$), spectral ($\mathbf{b}_k$), and temporal ($\mathbf{c}_k$), where $k = 1, 2, 3$), such as aforementioned.

According to our approach, the estimation of correlations between the extracted signatures and the corresponding template signatures should be calculated. After decomposition, only the spectral and spatial signature are here used for calculating the correlations, and the temporal signature is ignored, as we assume that there is a SSVEP signal in the EEG segment under analysis. Therefore, just these components were analyzed with
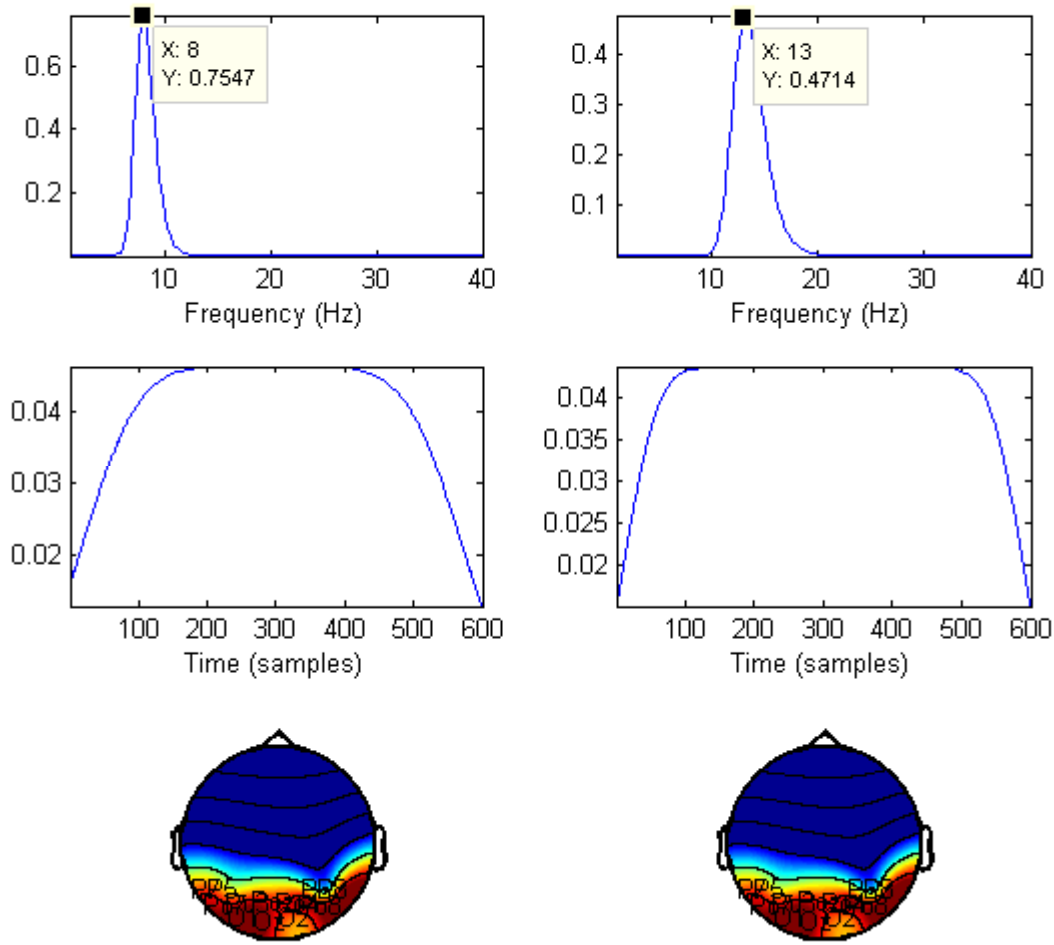
Figure 22: At the left side: template dimensions (*channel × frequency × time*) for 8 Hz; right side: 13 Hz, respectively.

the aim of ensuring the existence of evoked potentials in that region of the brain, and also locating its respective frequency component. Finally, the computation allows finding the highest correlation through a maximum criterion and thus, the class frequency and class channel are recognized. If the classes are the same, the frequency chosen is obtained, otherwise the result is not taken into account, being discarded. A graphical explanation of the process is illustrated in Figure 23.

3.4.3 Discussions

According to our results in the frequency dimension, Figure 24 shows the frequency spectrum of each frequency component (sub-components or atoms) for each data packet (every second) and for all subjects. It is possible to see the components highlighted in amplitude when the subjects were stimulated in 8 and 13 Hz. Our focus lies on the location of these frequency components and therefore it is possible to see that not always the same order indicates the stimulated frequency components. Results related to accuracy and ITR are shown in Table 3.
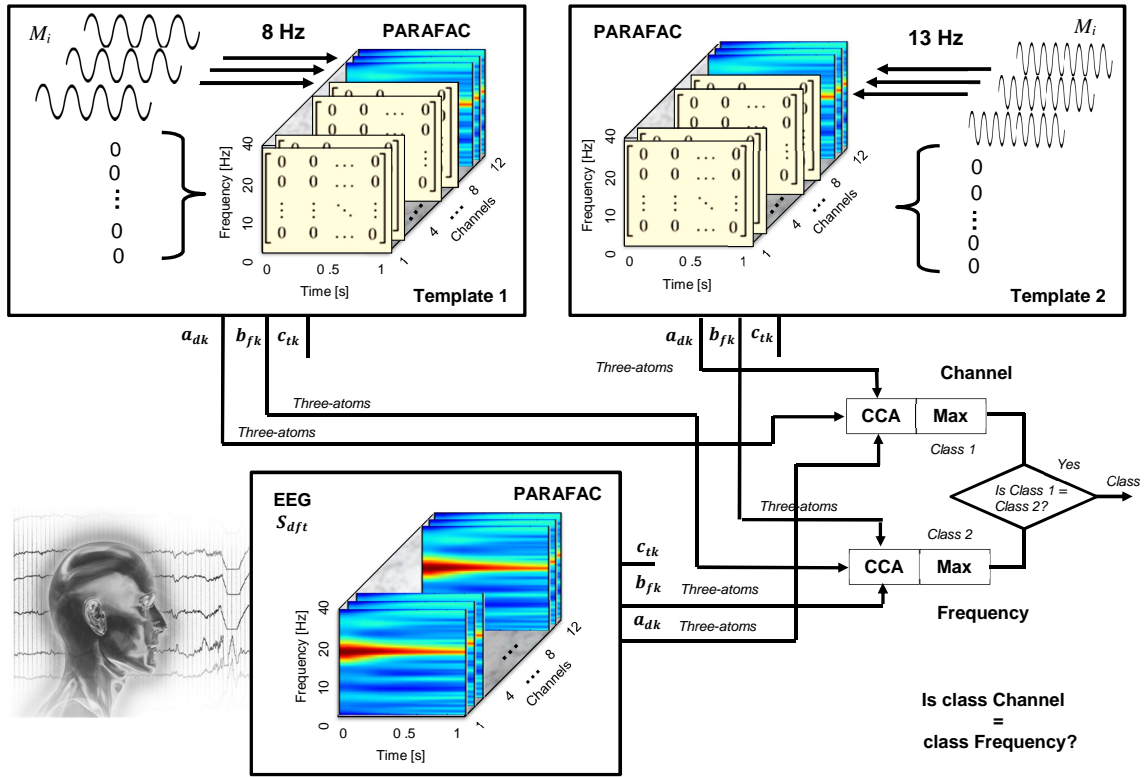
Figure 23: General schematic of our approach using PARAFAC.

| (a) | (b) |
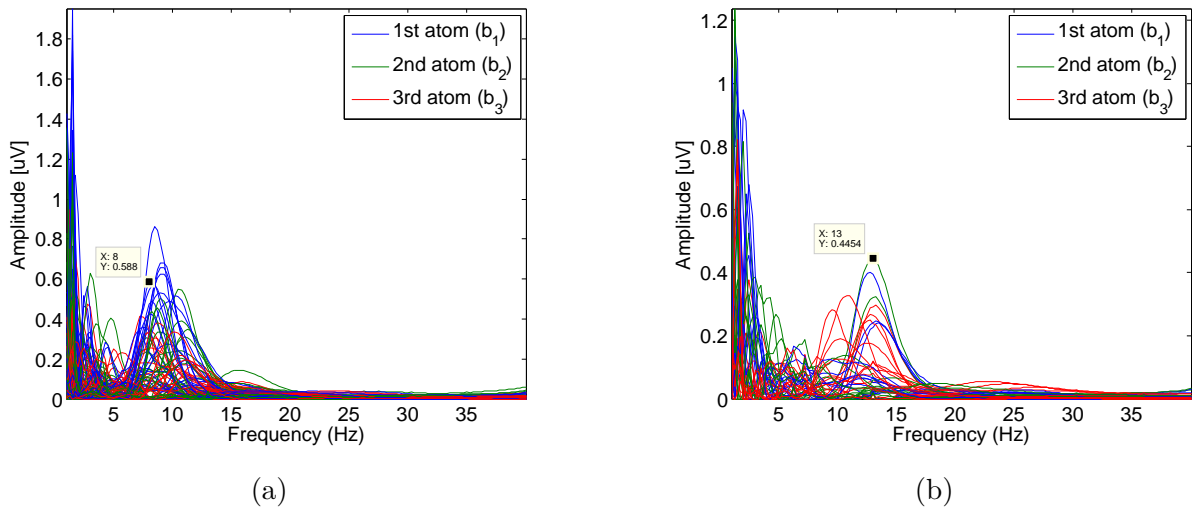
Figure 24: Spectrum from each frequency component ($\mathbf{b}_1$, $\mathbf{b}_2$ and $\mathbf{b}_3$ atoms) when subject 1 was stimulated with: (a) 8 Hz and (b) 13 Hz, respectively.

Table 3: Accuracy [%] and ITR using WL of 1 s.

	Frequency (class)		**Results**	
Subjects	8 Hz	13 Hz	Average	ITR [bits/min]
Subject 1	80.00%	60.00%	70.00%	7.13
Subject 2	73.33%	60.00%	66.67%	4.91
Subject 3	86.67%	80.00%	83.34%	21.01
Subject 4	73.33%	80.00%	76.67%	12.98
Subject 5	80.00%	86.67%	83.34%	21.01

This study has shown a new alternative for SSVEPs detection by using PARAFAC tensor models and canonical correlation analysis. The results are quite promising: the subjects 3 and 5 achieved the highest mean accuracy (83.34%) and ITR of 21.01 bits/min, considering a WL of 1 s. Indeed, increasing the WL would improve the results further as there is a trade-off between accuracy and speed.

Our experiments based on tensor models contribute to the studies related to analysis of natural representations of signals from multidimensional data structure. One of the main disadvantages of PARAFAC method is the significant computational cost estimated in the decomposition of tensors. Approximately, average time spent on decomposition was between 45 to 60 seconds. All computations were performed on a PC with Intel Core i7-4510U CPU @ 2.00GHz 2.60 GHz, 8.00 GB RAM and OS Windows 8.1 of 64-Bit.

4 Influence of stimuli color on SSVEPs

In the previous chapter, the basis for understanding the operation of a BCI-SSVEP, such as, performance, applications, stimulators and feature extractors were introduced. As mentioned, several parameters are intrinsically related to the performance of a BCI-SSVEP. Furthermore, there is still a deep study to be performed by academic community. In this section, a novel study related to the influence of color in visual evoked potentials was developed.

4.1 Visual Stimuli

The human eye has three color-sensitive cone-cell types (red, green and blue). According to studies performed by W. D. Wright (GREGORY, 1997), these three cone types have different responses for different stimulus wavelengths. Among the three cone types, the red-cone presents the best response followed closely by the green-cone, and with the blue one having the lowest response.

Experiments with visual stimuli have been performed about five decades ago (REGAN, 1966a; BIEGER; GARCIA-MOLINA, 2010), in order to verify their influence on amplitude and phase of SSVEPs, which are highly sensitive to stimulus parameters, such as color, luminance, repetition rate, contrast (modulation depth), and frequency. On the other hand, it is known that flickering stimuli can elicit epileptic responses to certain luminance or chromaticity, as higher luminance can induce higher risk of epilepsy (VIALATTE et al., 2010b), and chromaticity has strong impact on the human eye response in case of combination of colors (DREW et al., 2001). For example, red/blue and green/blue combinations have the strongest effect on pupil constriction, which can produce seizure attacks (DREW et al., 2001). Regarding frequency dependency, repetitive visual stimuli modulated at certain frequencies can also provoke epileptic seizures. According to Drew et al. (2001), lower frequency flickers generally produce more powerful constrictions, with color-dependence of flickers most visible between 3 and 6 Hz. In an other study, Fisher et al. (2005) show that flash and reversal pattern stimuli can provoke epileptic seizures especially in the 15-25 Hz range, but for some people, this upper limit of sensitivity can be as high as 65 Hz (FISHER et al., 2005).

There are some studies about the effects of colors on both SSVEP and ITR, plus a qualitative feedback of comfort provided by the volunteers (REGAN, 1966a; BIEGER; GARCIA-MOLINA; ZHU, 2010; CAO et al., 2012). In 1966, a study with red, yellow,

and blue stimuli was performed (REGAN, 1966a), however, these flashing lights were not from LEDs (Light Emitting Diodes) technology. According to that study, red elicited the strongest SSVEP response when modulated at approximately 11 Hz, and the response dropped dramatically at neighboring frequencies. Blue stimuli elicited a slightly weaker response, around 13 Hz, and yellow got the lowest SSVEP response.

Other study (BIEGER; GARCIA-MOLINA; ZHU, 2010) was performed in order to evaluate the refresh rate, environmental illumination, contrast, color, spatial frequency and size of visual stimuli. Single graphics stimuli (red, white, blue, green), color combination and reversal patterns (checkerboards) in LCD were also analyzed. In that study, white color got the highest value of ITR ($\approx$ 55 bits/min), although the lower level of comfort by users was considered. On the other hand, blue presented the highest level of comfort, with ITR of $\approx$ 32 bits/min. Red and green had similar level of comfort although lower ITR.

The work performed in (CAO et al., 2012) is similar to a part of the work developed in (BIEGER; GARCIA-MOLINA; ZHU, 2010), in which the stimuli were generated in a LCD display with a black background and single stimulus. The stimulus colors were red, white, blue, green and gray. That work also concluded that white achieved the highest ITR, followed by gray, red, green and blue colors. The average ITR was 32.3 bits/min.

Although the ITR can evaluate the effectiveness of each color, it is dependent on the signal processing technique used. However, to the knowledge of the author there is no study about the effect of stimulus color on the SSVEP amplitude using LEDs as visual stimulator. Thus, evaluating the SSVEP amplitude using LEDs is a must for now, since this technology of stimulation remains of high usability due to its low cost, low power, portability and flexibility. On the other hand, a comparative study of technologies for visual stimuli (LCD vs LED) was reported in (WU et al., 2008), which concludes that the SSVEP response elicited by LEDs is higher than that of a LCD display. However, that study did not present any kind of comparison about stimulus colors.

In our study, four flickering stimuli with different LED colors were used. The analyzed colors are red, green, blue and yellow. There are no color combination (for safety reasons), and four frequency values are used for the stimuli. Our study also evaluated the performance of such specific colors at different frequencies. A qualitative score of the degree of comfort is also here achieved. So far, for our knowledge, none of the studies in the literature did comparison of performance of stimuli colors using LEDs.

4.2   Protocol

Twenty subjects (seventeen males and three females), with ages from 21 to 36 years old, were recruited to participate in this study (average age: 27.9; Standard Deviation: 3.7).

The research was carried out in compliance with Helsinki declaration, and the experiments were performed according to the rules of the ethics committee of UFES/Brazil, under registration number CEP-048/08. The subjects were distributed into two experiments. The first group (Group 1) has ten volunteers: s1, s2, s3, s4, s5, s6, s7, s8, s9 and s10; and the second one (Group 2) has ten volunteers remaining: s11, s12, s13, s14, s15, s16, s17, s18, s19 and s20; both using different protocols, which will be discussed in subsequent lines. The subjects were free to withdraw at any time without any penalty. Previously, a selection of volunteers was performed and topics related to precautions as visual problems, headaches, family history with epilepsy and problems related to brain damage were consulted. The participants did not report any problems and no one had previous experience in using a BCI.

4.3 EEG Recording

The acquisition equipment (BrainNet-36) and electrodes were the same used in our previous studies. The data were processed on a personal computer with a 2.2 GHz Core 2 Duo processor. The EEG recordings in all subjects were executed by the same technician to minimize operation errors.

It is worth to comment that for both SSVEP response and classification studies, only O1, O2 and OZ electrodes were selected after the application of a Common Average Reference (CAR) spatial filter, which is based on studies that suggest that the highest values of energy for SSVEP detection are located on the occipital area of the cortex (RUSSO et al., 2007; KROLAK-SALMON et al., 2003; PASTOR et al., 2003; SAMMER et al., 2005; ZHANG et al., 2006). Thus, the twelve aforementioned electrodes were used at the initial stage only for application of the CAR spatial filter. According to our observations, the application of this spatial filter to the twelve electrodes actually improves the classification performance when selecting O1, O2 and Oz electrodes (TELLO et al., 2014b; TELLO et al., 2014a; TELLO et al., 2015c).

4.4 Stimulation Unit (SU)

A coupling structure of four small boxes ($4 \times 4 \times 4$cm) containing a LED in each one and covered with thin white paper diffusers was mounted. The diffused paper is also known as wax paper or paraffin paper and has the following properties: it is semi-transparent, completely smooth and moisture-proof. Figure 25(a) shows the block diagram of the acquisition and stimulation system.

The stimuli were generated by a microcontroller (PIC18F4550, Microchip Technology Inc., USA) with 50/50 % on-off duty cycles. LEDs of 5 mm of four different colors

(yellow, red, green, blue) and same luminous intensity (10,000 mcd) were used. Luminous intensity values of each LED were controlled by the microcontroller outputs (same port), guaranteeing, in this way, the same levels of luminous intensity. In addition, these values were measured through a light meter (ICEL MANAUS, model LD-590).

The flickering frequencies were 8.0 Hz, 11.0 Hz, 13.0 Hz and 15.0 Hz, which were used by the four colors of LEDs. These frequencies were chosen due to: 1) our previous studies (TELLO et al., 2014b; TELLO et al., 2014a; TELLO et al., 2014c) having shown that these generate strongest SSVEP responses; 2) safety recommendations specified in (FISHER et al., 2005); 3) studies conducted by Pastor et al. (2003) about the relationship between visual frequency stimuli and SSVEP amplitudes; 4) studies conducted by Herrmann (2001) showing peaks of SSVEPs at $\sim$ 15 Hz.

4.5   Experimental Procedure

The experiments were performed in offline mode. The participants were asked to observe the stimuli during 320 s. The stimuli consisted of sixteen sequences: four sequences for each color with four different frequencies. Each stimulus sequence lasted 15 s, followed by 5 s of break (rest), during whose time the EEG signals were recorded.

The two groups of volunteers (Group 1 and 2) followed different protocols in order to validate the results. Figure 25(a) shows the block diagram of the system, where a block called "synchronization signal" (which means a logical level from an algorithm developed in Matlab) generates a specific protocol for each group of participants. In that algorithm, volunteers of Group 1 underwent certain stimuli, which are graphically detailed in Figure 25(b); this protocol is called as "ordered", because colors and frequencies followed a determined order. On the other hand, the volunteers of Group 2 were stimulated in a randomic way in both frequency and color, calling this protocol as "randomic" (see Figure 25(c)).

A structure moved the boxes that contained the LEDs during each sequence of acquisition aiming at centralizing the flashing stimulus and keeping it completely still in front of the volunteer in order to standardize the protocol. The experiments were conducted in a quiet and dim room with illuminance of 300 lux measured through the light meter. Then, the volunteers sat on a comfortable chair, in front of the stimulator system, 60 cm far from this. The background plane was a black wall located very close and behind the stimuli.
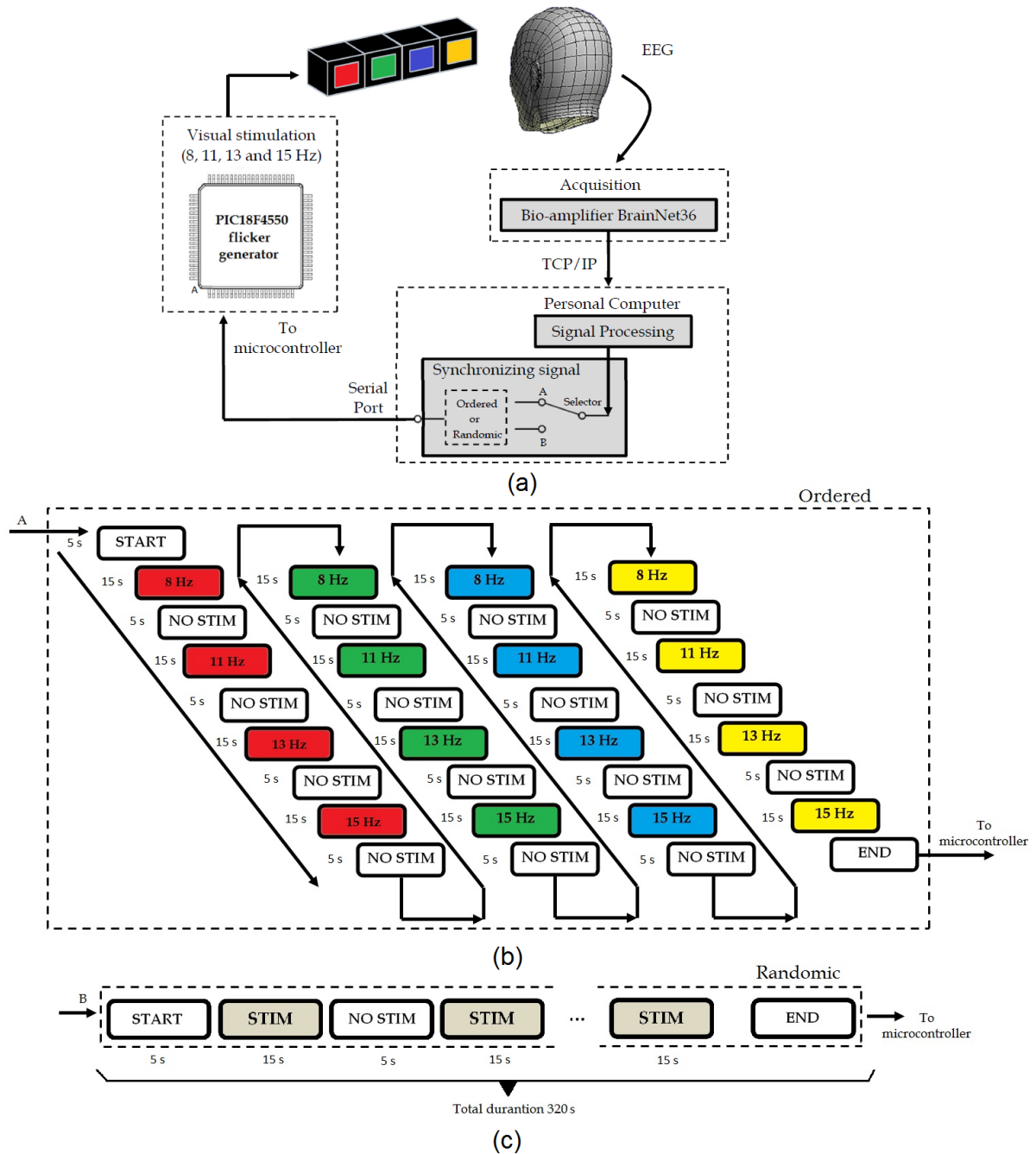
Figure 25: (a) Block diagram of the system; (b) Protocol used by volunteers of Group 1, called "ordered"; (c) Protocol used by volunteers of Group 2, called "randomic". Note that both protocols were performed with the same time duration of 320s.

4.6   EEG Pre-Processing and SSVEP Response Analysis

A Common Average Reference (CAR) spatial filter was applied to the EEG signals corresponding to each stimuli frequency and for each color, in order to reduce the correlation between channels originated by external noise. The CAR filter was computed according to Equation 4.1 (MCFARLAND et al., 1997):

$$V_i^{CAR} = V_i^{ER} - \frac{1}{n}\sum_{j=1}^{n} V_j^{ER}, \tag{4.1}$$

where V_i^{ER} is the potential between the ith electrode and the reference, and n is the number of electrodes used (in our case, twelve). After that, just the resultant signals from O1, O2 and Oz electrodes were selected, and a 5th-order elliptic band-pass filter between 3-60 Hz was applied. Since the elliptic filter has a transition band narrower than other filters and as harmonic components are very close, this type of filter was chosen as the more suitable. This filter has 1 dB of peak-to-peak pass-band ripple and 15 dB of stop-band attenuation down the pass-band value. The SSVEP amplitude response was obtained through PSDA (Power Spectral Density Analysis) or Fourier Power Analysis (WANG et al., 2006) with Hamming window. The SSVEPs response curves were calculated by the following formula:

$$P_{Norm}(f) = \frac{\bar{P}_f}{\max_f \bar{P}_f^{VS}}, \tag{4.2}$$

where $P_{Norm}(f)$ is a normalized amplitude value obtained by the relation between the average value ($\bar{P}_f$) among all subjects for each case (group and frequency), and $\max_f \bar{P}^{VS}$ denotes the maximum average amplitude value obtained from all cases of visual stimuli (VS) analyzed between the groups.

Such as aforementioned, the data from twelve EEG channels were segmented and windowed. The window lengths (WLs) used were 1, 2, 4 and 6 s; each one with an overlapping of 50 %. Signals from O1, O2 and Oz channels were selected after the process of CAR spatial filtering. After that, a 5th-order elliptic band-pass filter between 3-60 Hz was applied and the resultant signals were used in the feature extractor and classification steps.

4.7   Feature Extraction and Classification

Such as aforementioned in section 3.3.7, Multivariate Synchronization Index (MSI) is a novel method to estimate the synchronization between the actual mixed signals and the reference signals as a potential index for recognizing the stimulus frequency. Mathematically, this method assumes that $\mathbf{X}$ is a matrix of size $N \times M$ whose N represents

discrete-time EEG signal segments and M represents the channels from the occipital electrodes (O1, O2 and Oz). On the other hand, $\mathbf{Y}_i$ consists of a "Fourier series" of stimulus signals.

Let f_i denote the visual stimulus frequency in Hz, where $i = 1$ ($f_1 = 8$ Hz), 2 ($f_2 = 11$ Hz), 3 ($f_3 = 13$ Hz) and 4 ($f_4 = 15$ Hz) denote the target or class of our visual stimuli. Then, the total H harmonic sine vectors $s^i{}_1, s^i{}_2, \cdots, s^i{}_H$ and cosine vectors $c^i{}_1, c^i{}_2, \cdots, c^i{}_H$ for frequency f_i, all of length M, can be constructed as

$$s_j{}^i = [s_{j,1}, s_{j,2}, \cdots, s_{j,M}]^T, \tag{4.3}$$

$$c_j{}^i = [c_{j,1}, c_{j,2}, \cdots, c_{j,M}]^T, \tag{4.4}$$

for $j=1, 2, \cdots, H$, where

$$s_{j,r} = \sin(2\pi j r f_i / f_s), \tag{4.5}$$

$$c_{j,r} = \cos(2\pi j r f_i / f_s), \tag{4.6}$$

for r=$[0 : N - 1]$, where $f_s = 600$ Hz is the sampling frequency used for the acquisition of EEG signals. The reference matrix $\mathbf{Y}_i$, of size $2H \times M$, corresponds to the stimulus frequency f_i, which can be constructed as

$$\mathbf{Y}_i = \left[s^i{}_1 c^i{}_1 s^i{}_2 c^i{}_2 \cdots s^i{}_H c^i{}_H \right]^T. \tag{4.7}$$

In our case, we have considered the fundamental frequency (it is considered as the first harmonic) and two multiples (harmonics) as the simulated frequency generator, i. e. $H = 3$. Autocorrelation matrices $\mathbf{C}_{11}$ and $\mathbf{C}_{22}$ for $\mathbf{X}$ and $\mathbf{Y}_i$, respectively, and cross-correlation matrices $\mathbf{C}_{12}$ and $\mathbf{C}_{21}$ were changed from the original version (ZHANG et al., 2014a) due to its inconsistency in the dimensions of each component for the formation of the correlation matrix $\mathbf{C}^i$, such as explained in section 3.3.7. Recalling,

$$\mathbf{C}_{11} = (1/M).\mathbf{X}\mathbf{X}^T, \tag{4.8}$$

$$\mathbf{C}_{22} = (1/M).\mathbf{Y}_i\mathbf{Y}_i{}^T, \tag{4.9}$$

$$\mathbf{C}_{12} = (1/M).\mathbf{X}\mathbf{Y}_i{}^T, \tag{4.10}$$

$$\mathbf{C}_{21} = (1/M).\mathbf{Y}_i\mathbf{X}^T, \tag{4.11}$$

A correlation matrix $\mathbf{C}^i$ can be constructed as

$$\mathbf{C}^i = \begin{bmatrix} \mathbf{C}_{11} & \mathbf{C}_{12} \\ \mathbf{C}_{21} & \mathbf{C}_{22} \end{bmatrix} \tag{4.12}$$

The internal correlation structure of $\mathbf{X}$ and $\mathbf{Y}_i$ contained in the matrices $\mathbf{C}_{11}$ and $\mathbf{C}_{22}$, respectively, is irrelevant for the detection of the stimulus frequency (CARMELI et al., 2005). It can be removed by constructing a linear transformation matrix

$$\mathbf{U} = \begin{bmatrix} \mathbf{C}_{11}^{-1/2} & 0 \\ 0 & \mathbf{C}_{22}^{-1/2} \end{bmatrix}, \tag{4.13}$$

so that $\mathbf{C}_{11}^{1/2}\mathbf{C}_{11}^{1/2} = \mathbf{C}_{11},\mathbf{C}_{22}^{1/2}\mathbf{C}_{22}^{1/2} = \mathbf{C}_{22}$ and by applying the transformation $\mathbf{U}\mathbf{C}^i\mathbf{U}^T$, resulting in a transformed correlation matrix $\tilde{C}^i$

$$\tilde{C}^i = \mathbf{U}\mathbf{C}^i\mathbf{U}^T = \begin{bmatrix} I_{MxM} & \mathbf{C}_{11}^{-1/2}\mathbf{C}_{12}\mathbf{C}_{22}^{-1/2} \\ \mathbf{C}_{22}^{-1/2}\mathbf{C}_{21}\mathbf{C}_{22}^{-1/2} & I_{2Hx2H} \end{bmatrix} \tag{4.14}$$

of size $P \times P$, where $P=N + 2H$. The eigenvalues $\lambda^i{}_1, \lambda^i{}_2, \cdots, \lambda^i{}_P$ of $\tilde{C}^i$, normalized as $\tilde{\lambda}^i_m = \lambda^i{}_m / \sum_{m=1}^{P} \lambda^i{}_m$ for $m = 1, 2, \cdots, P$, can be used to evaluate the synchronization index S_i for matrix $\mathbf{Y}_i$ as in Zhang et al. (2014a):

$$S_i = 1 + \frac{\sum_{m=1}^{P} \tilde{\lambda}^i_m \log(\tilde{\lambda}^i_m)}{\log(P)}. \tag{4.15}$$

Then, i indices and their respective classes (S_1, S_2, S_3, S_4) were obtained. Finally, the class was obtained through a criterion of maxima.

$$S = \max_{1 \leq i \leq 4} S_i \tag{4.16}$$

Figure 26 shows the SSVEP response curves for each group of volunteers. From these responses curves, Table 4 shows the maximum peaks values for each group evaluated. The accuracy and ITR were computed for each case.

Table 5 presents scores provided by the volunteers. A statistical analysis was implemented using a nonparametric method of two-way analysis named Friedman's test with the purpose of finding out any effect for the level of comfort of the colors for each group of volunteers (Group 1 and Group 2). The results showed a statistic significance with p = 1.8949×10^{-5} using alpha = 0.05.
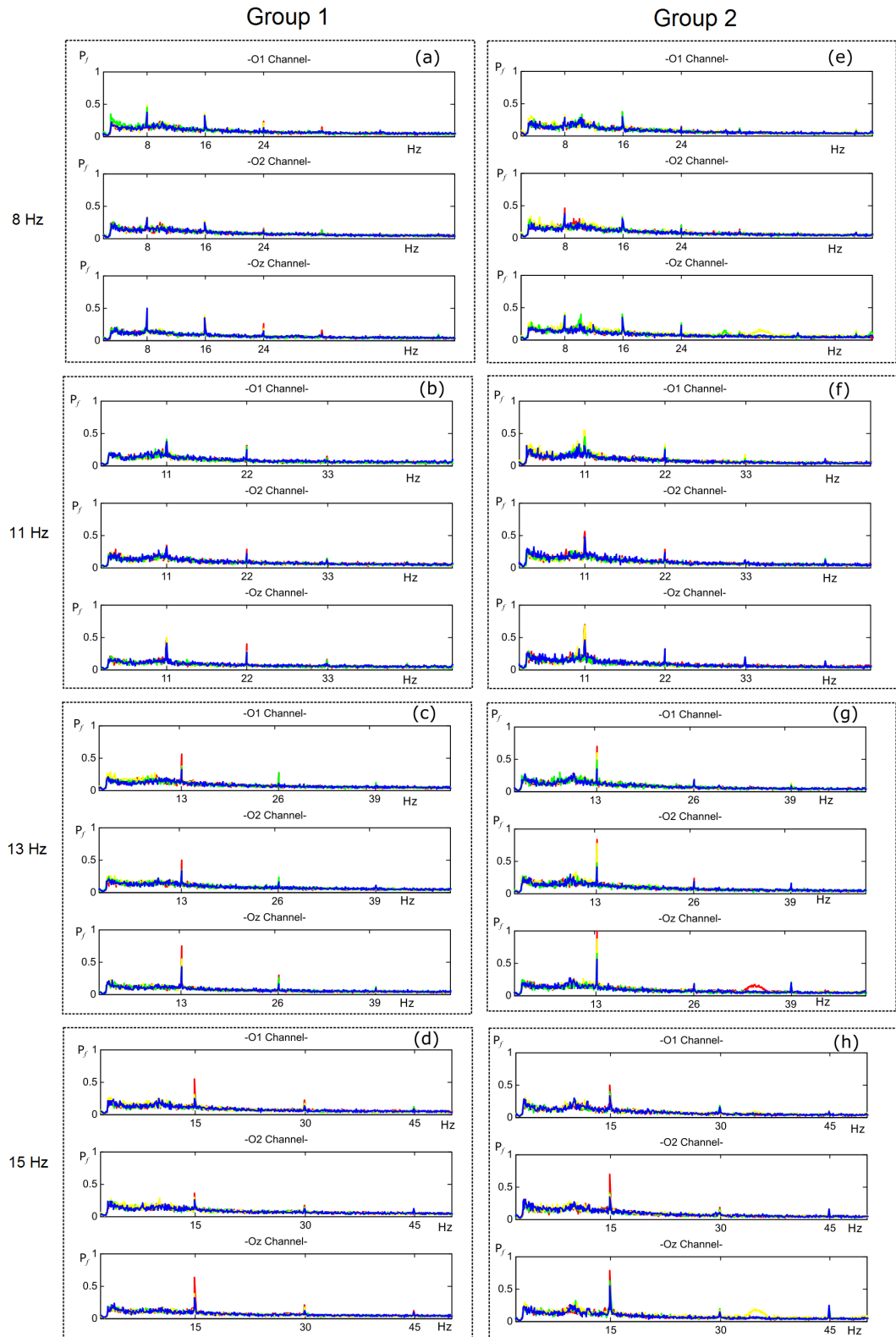
Figure 26: Normalized SSVEP response curves for channels O1, O2 and Oz from average results of volunteers of Group 1: ((a) 8 Hz, (b) 11 Hz, (c) 13 Hz and (d) 15 Hz); normalized SSVEP response curves for channels O1, O2 and Oz from volunteers of Group 2: ((e) 8 Hz, (f) 11 Hz, (g) 13 Hz and (h) 15 Hz).

Table 4: Maximum peaks values for each normalized amplitude response. The highlighted numbers indicate the highest values of amplitude based on comparison between different stimuli and channels for a specific frequency.

Freq.	Ch.	Group 1				Group 2			
		Red	Green	Blue	Yellow	Red	Green	Blue	Yellow
	O1	0.32	0.44	0.37	0.48	0.37	0.36	0.30	0.30
8 Hz	O2	0.32	0.27	0.32	0.33	0.46	0.36	0.37	0.34
	Oz	0.36	0.43	0.49	0.47	0.38	0.37	0.36	0.42
	O1	0.37	0.40	0.37	0.39	0.42	0.44	0.31	0.55
11 Hz	O2	0.34	0.25	0.32	0.29	0.56	0.34	0.47	0.46
	Oz	0.48	0.40	0.40	0.50	0.70	0.42	0.46	0.68
	O1	0.56	0.35	0.31	0.37	0.70	0.49	0.35	0.59
13 Hz	O2	0.49	0.34	0.33	0.32	0.83	0.47	0.40	0.77
	Oz	0.75	0.43	0.42	0.54	1.00	0.65	0.55	0.86
	O1	0.55	0.28	0.24	0.30	0.50	0.39	0.33	0.34
15 Hz	O2	0.36	0.25	0.26	0.29	0.70	0.41	0.34	0.38
	Oz	0.64	0.33	0.31	0.39	0.78	0.62	0.54	0.53

Table 5: Score provided by volunteers about the level of comfort regarding the stimuli color (7-point scale).

Group 1	Red	Green	Blue	Yellow	Group 2	Red	Green	Blue	Yellow
s1	4	5	3	4	s11	6	2	7	3
s2	2	5	6	3	s12	4	6	6	4
s3	4	6	3	5	s13	2	5	6	4
s4	3	6	4	3	s14	4	5	7	4
s5	4	6	5	4	s15	4	6	7	3
s6	3	5	4	4	s16	2	6	5	6
s7	4	6	3	5	s17	5	6	3	5
s8	2	5	5	3	s18	4	5	7	4
s9	3	5	4	6	s19	3	5	5	3
s10	4	7	3	4	s20	4	5	7	3
Average	3.30	5.60	4.00	4.10	Average	3.8	5.10	6.00	3.90
SD	0.82	0.70	1.05	0.99	SD	1.23	1.20	1.33	0.99

Figure 27 shows the average accuracy to detect the SSVEP for Group 1 and 2 derived from MSI method, respectively, with different Window Lengths (WL = 1, 2, 4 and 6 s).

Based on the results from Figure 27, it can be seen the accuracy is gradually enhanced with the increase of WL for all frequencies used and group of volunteers. The WL of 4 s was adopted as parameter of classification since the results were good and very similar to WL of 6 s in most of the cases analyzed.

Figure 28 shows the classification in a box plot representation corresponding to different frequencies stimuli (8, 11, 13 and 15 Hz) derived from the data of Group 1 and 2 with a WL of 4 s using MSI. A statistical analysis was also implemented using Friedman's test with the purpose of finding out any effect between colors and frequencies. Thus, the frequencies were distributed in pairs for their analysis both for the ordered and random stimulation: (i) 8 Hz and 11 Hz vs colors; (ii) 8 Hz and 13 Hz vs colors; (iii) 8 Hz and 15 Hz vs colors; (iv) 11 Hz and 13 Hz vs colors; (v) 11 Hz and 15 Hz vs colors; (vi) 13 Hz and 15 Hz vs colors. The statistical analysis results showed that, for Group: (i) $p = 0.0363$, (ii) $p = 0.1534$, (iii) $p = 2.0765 \times 10^{-4}$, (iv) $p = 0.0142$, (v) $p = 5.3185 \times 10^{-6}$ and (vi) $p = 1.2905 \times 10^{-4}$. The combinations (i), (iii), (iv), (v) and (vi) were statistically significant using alpha = 0.05. On the other hand, for Group 2: (i) $p = 0.5589$, (ii) $p = 0.9126$, (iii) $p = 0.62$, (iv) $p = 0.8457$, (v) $p = 0.6049$, (vi) $p = 0.1607$ were not statistically significant.

ITR was calculated from each value of accuracy and compared to comfort values of each stimulus color. Comparative graphics for ITR versus comfort are shown in Figure 29. In order to obtain a way to determine a good relationship between ITR and level comfort, we here proposed a method, which is based on a linear acting as a threshold. Thus, from the experiments, a diagonal line is automatically generated, which is determined by two points: a starting point (coordinates indicating minimum level of comfort and minimum ITR) and an end point (maximum level of comfort and maximum ITR, which is achieved when SSVEP is detected with 100% of accuracy). The values of the axis of ITR vary between a minimum and a maximum of 0 to 30 bits/min, respectively, and for each 5 bits/min, there is one level of comfort associated.

The decision for the best choice of color stimulus is taken according to the following rules:

- Each point of the graph represented a condition, involving data from ITR and level of comfort.

- The choice of the best color is determined by the following: the point that is closer to the coordinate of maximum ITR and maximum comfort (upper right) is taken as the first best option, while the following closer ones define the order of the others remaining.
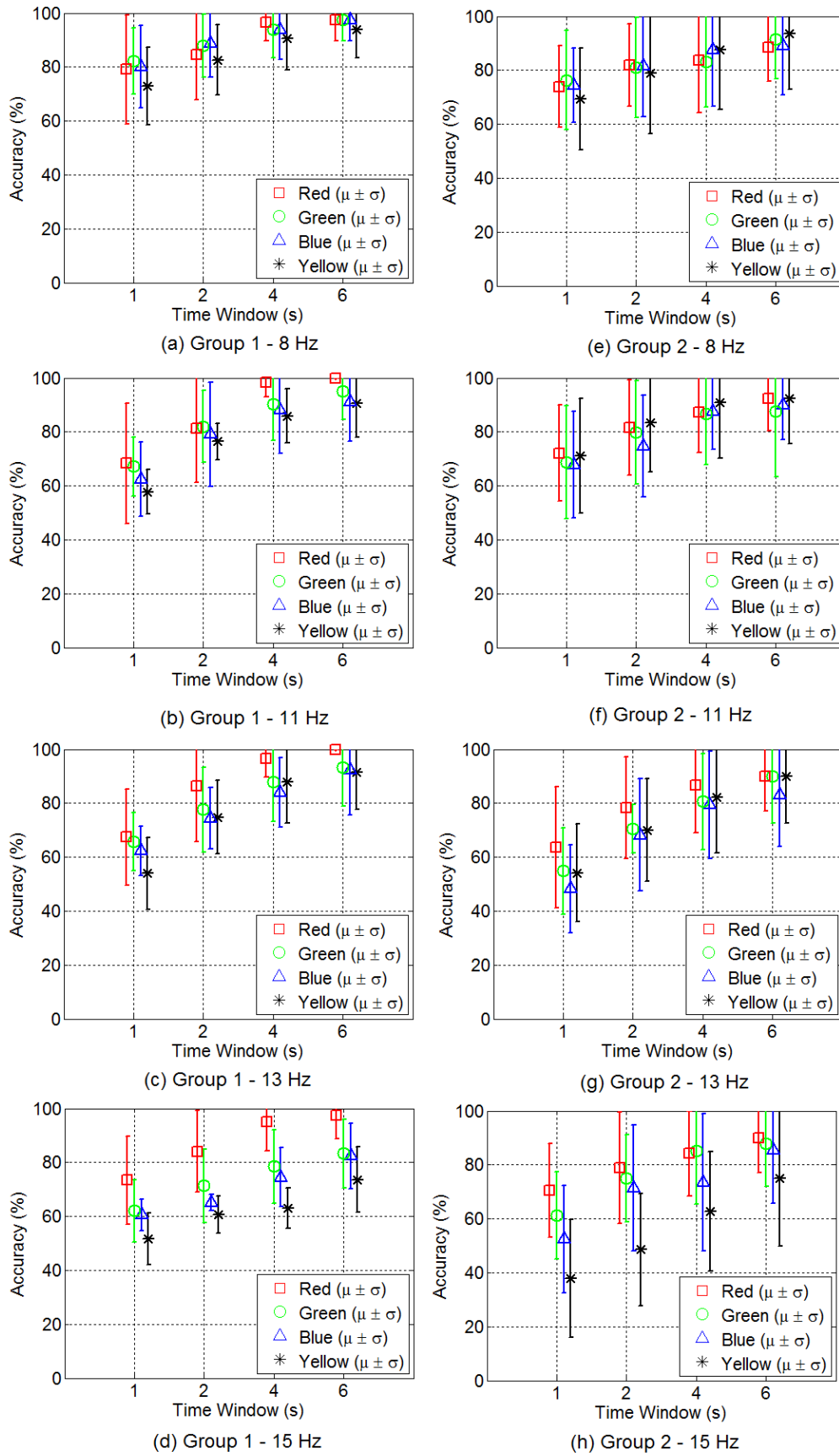
Figure 27: Average accuracy for SSVEP recognition for each color using MSI with different WLs and frequencies for Group 1 and 2: (a-e) 8 Hz, (b-f) 11 Hz, (c-g) 13 Hz, and (d-h) 15 Hz.
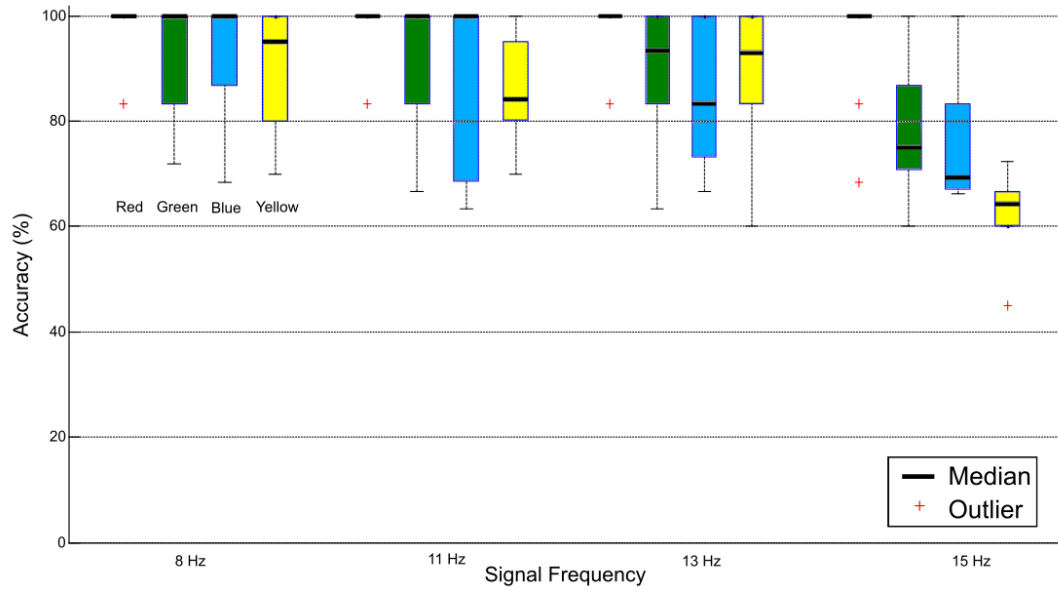
(a)
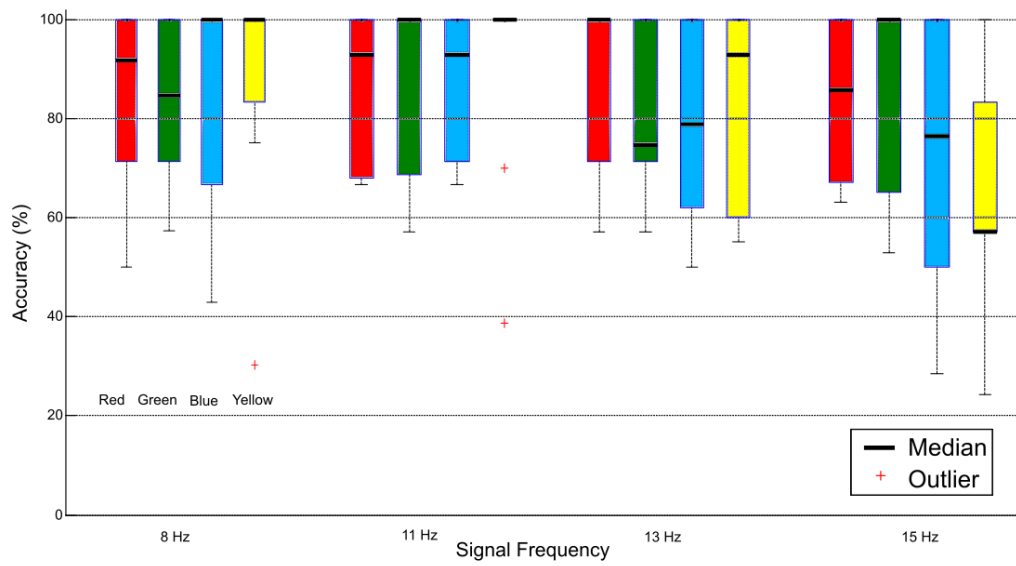
(b)

Figure 28: Median, quartiles and outliers of classification scores according to color with WL of 4 s corresponding to the different target frequencies (8, 11, 13 and 15 Hz), obtained through MSI for: (a) Group 1 and; (b) Group 2.

Figure 29 shows the comparison between the parameters of ITR versus comfort for WL of 4 s. The graphics were distributed in stimulus frequency for both groups of volunteers. Moreover, Table 6 shows a summary of the values obtained in ITR, and choice of the best colors based on Figure 29. Note that these choices are based on levels of comfort and are here called as "1", "2", "3" and "4".

Table 6: Average ITR (bits/min) for WL of 4 s and preferred colors by groups 1 and 2, according to color and frequency, respectively.

Groups	Frequency [Hz]	Red ITR [bits/min]	Green ITR [bits/min]	Blue ITR [bits/min]	Yellow ITR [bits/min]	Better choices (first choice/second choice)
Group 1	8	27.25	25.31	25.36	22.71	Green/Blue
	11	28.63	23.05	22.07	18.89	Green/Blue
	13	27.25	21.50	18.27	21.40	Green/Yellow
	15	26.52	15.11	12.55	7.17	Red/Green
Group 2	8	19.62	18.68	22.83	22.60	Blue/Green
	11	21.09	21.54	21.10	25.06	Blue/Green
	13	21.38	17.40	17.13	18.99	Blue/Green
	15	19.04	20.86	15.01	9.30	Green/Blue

In addition to results shown in Figure 29, the whole data were analyzed together. The data were grouped according to the color of indifferent way between groups or frequencies used. Thus, centroids were calculated since the coordinate values of each condition are known (see Figure 30), and a single cluster is assigned for each color. The centroid of the cluster is the center of the circle indicated with a mark "x".

4.8 Discussion

According to Figure 26, the amplitude of the SSVEP response is affected by both frequency and color of the stimuli, confirming the studies initially performed by Regan (1966a) and Drew et al. (2001).

In our study, the red color obtained the highest peaks of SSVEP amplitude in the majority of cases (Table 4). An interesting fact to highlight is that the fundamental frequency of each color reached the highest peak of amplitude, which is confirmed by the literature (HERRMANN, 2001). Also the frequencies of 13 and 15 Hz reached the highest peaks of amplitude response for both groups, which is confirmed by studies described in the curve of Wang et al. (2006), where the middle frequencies (13 and 15 Hz) exceeded in magnitude the low frequencies (8 and 11 Hz).

On the other hand, Figure 27 shows that the accuracy to detect SSVEP is gradually enhanced with the increase of WL for all frequencies and groups of volunteers. This is widely known since SSVEP signals in larger time-windows is increased (ZHANG et al., 2014a). According to the results of classification from Figure 27, a similar behavior from results between group 1 and 2 can be appreciable. However, from the results of
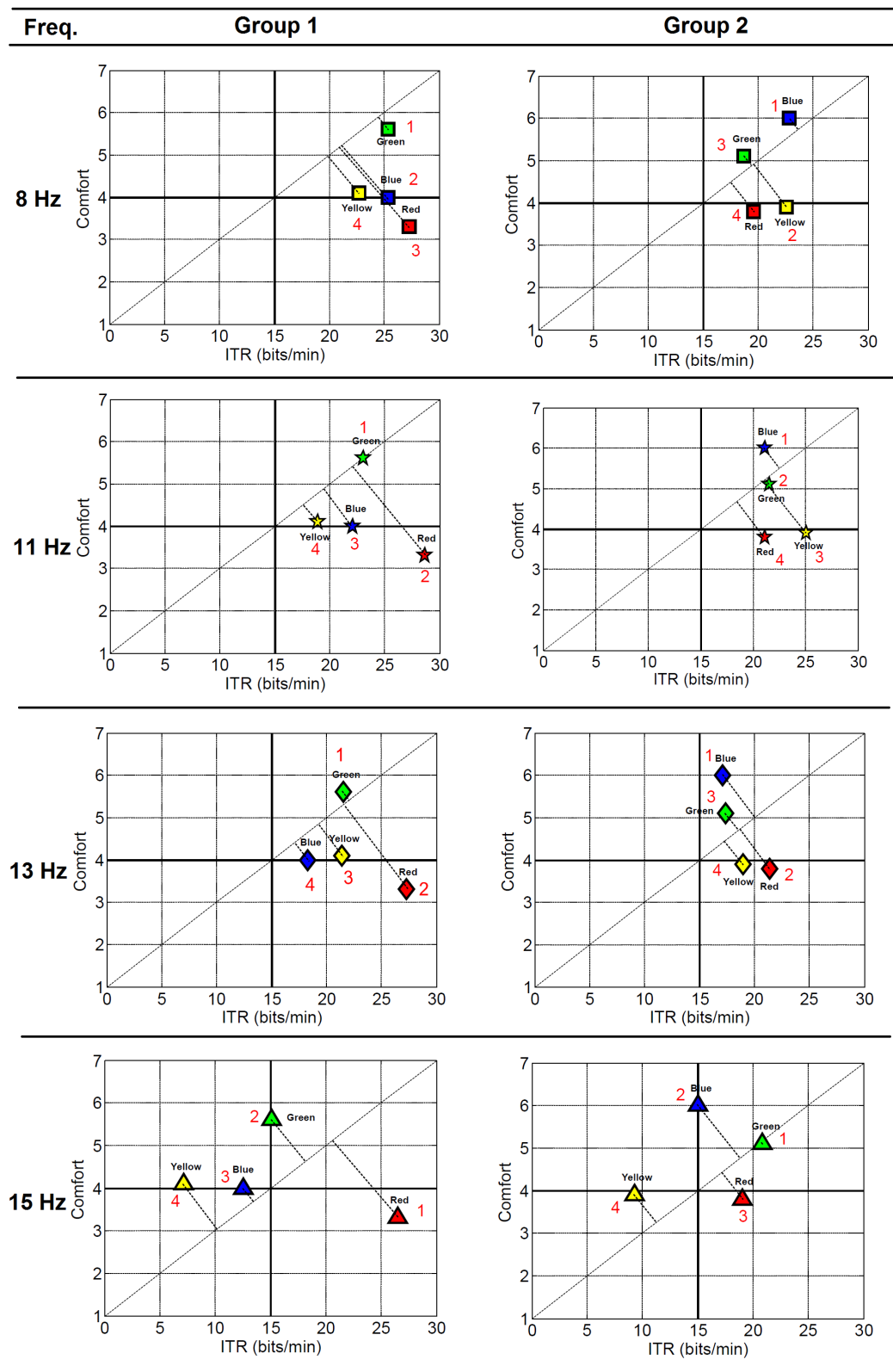
Figure 29: Plotting of average ITR versus average level of comfort for stimulus color and different frequencies for volunteers of Group 1 and Group 2. In addition, the order of choice of colors is also shown.
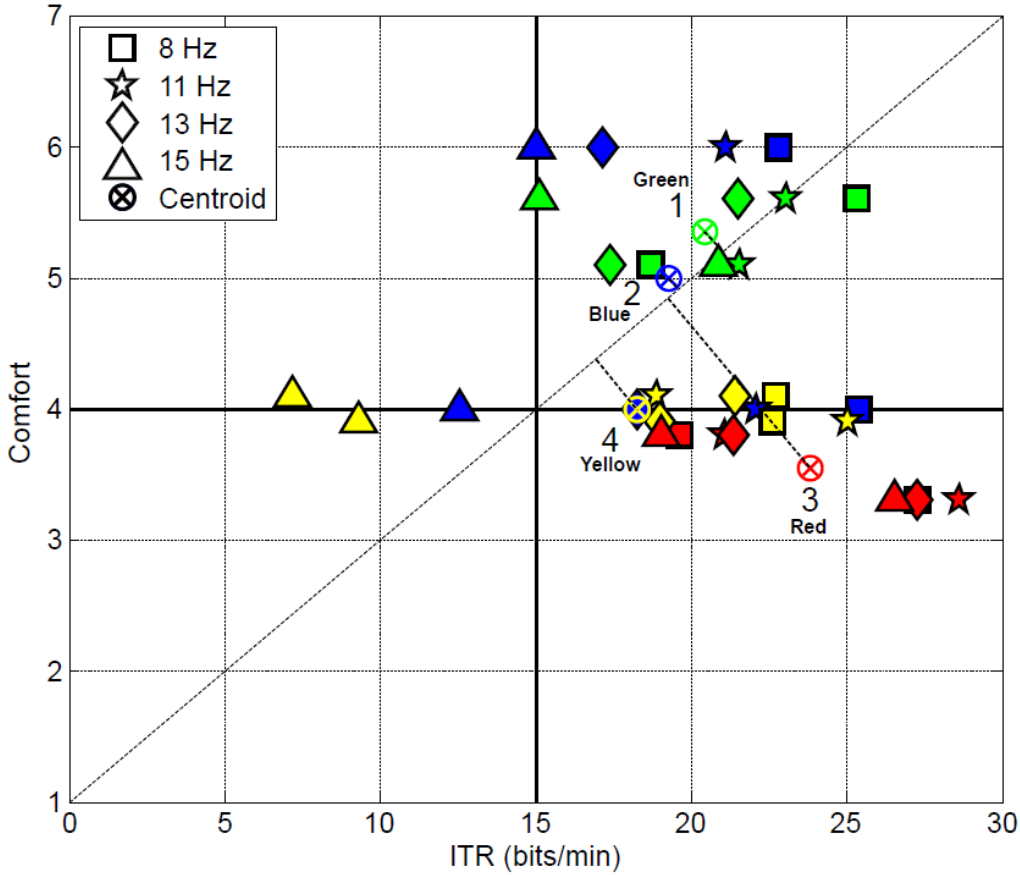
Figure 30: Scatter plot for all cases analyzed, clustered by color, using k-means method indicating its respective centroids.

group 2, a remarkable drop in the accuracy compared to its similar in group 1 can be observed. This fact may be related to visual accommodation when color stimuli of random way is presented, which is unlike of group 1, where the subjects previously knew the sequence of colors and frequencies. This aspect can be associated with the responses between color-sensitive cone pigments. Thus, that stabilization process could elicit delays in the modulation of attention. Modulation in attention is an important parameter for the increase of the precision in the recognition of visual evoked potentials (KIM et al., 2007). Despite of subjects having performed different protocols, in both groups the tendency in high accuracy terms is attributed to the frequency of 8 Hz, due to low dispersion of results (the points are not far apart and indicate a high precision) in Figure 29. These evidences could increase the development of accurate BCIs with frequencies very close to the beginning of alpha band, as in 8 Hz, and different colored stimuli.

In Figure 28, the accuracy values using a box plot for different analyzed frequencies using a WL of 4 s are shown. There, the median, quartiles and outliers were presented for better appreciation of the distribution of our results. The accuracy for 8 and 11 Hz achieved the highest results, which is contrary to the results of amplitude SSVEP presented in Figure 26, in which these frequencies have low amplitude. In addition, an

opposite situation occurs with the frequencies of 11 and 13 Hz. These results confirm some evidences about the fact that SSVEP amplitude is not decisive to detect it, for the frequency range analyzed, such as demonstrated in (KELLY et al., 2005a). In their studies, frequencies in alpha band allowed the detection SSVEPs in a more accurate way during the modulation attentional. Regarding to the colors, it is remarkable to observe that the red color achieved the highest median values followed by green, blue and yellow in most cases, for both group 1 and 2. In addition, a low accuracy was obtained for 15 Hz and yellow color, which implies this color is not a good choice for the development of a BCI.

According to Table 5, volunteers in group 1 and 2 agree that the red color turned out to be quite uncomfortable for them. Moreover, the green color was chosen on average by group 1, and blue by group 2, which were considered of best comfort for them. However, blue (and yellow) obtained an intermediate opinion from group 1, with a standard deviation of 1. According to results of ITR from Table 6, the red color got the highest values (25.52 - 28.63 bits/min) for group 1. It is worth to mention for group 2, red reached the highest ITR only at 13 Hz.

Based on the results, we observed that red provides, in most frequencies, both highest accuracy and ITR for detection of SSVEP. These results confirm studies of W. D. Wright (GREGORY, 1997) and Regan (1966a) about the response of the red color in the human eye. However, the red color, despite of the excellent results, showed to be the less comfortable to be used in a BCI. Moreover, the red color can be dangerous in combination with other colors (DREW et al., 2001) and, in low chromatic luminance, this color can induce epileptic responses (EBERSOLE; PEDLEY, 2002). This fact is confirmed by studies of Rubboli et al. (2004), showing red flicker could induce a Generalized Photoparoxysmal Response (PPR), which has a relation to epilepsy and visually induced seizures. For these reasons, its use requires some care.

From researches on color and selective attention in the literature, the red color has shown to receive an attentional advantage (ELLIOT; FAIRCHILD; FRANKLIN, 2014). In this aspect, researchers (LINDSAY et al., 2010; BUECHNER et al., 2014; POMER-LEAU et al., 2014; ELLIOT; FAIRCHILD; FRANKLIN, 2014; ELLIOT, 2015) agree that participants' visual search times were faster for desaturated red (relative to several other colored) targets. On the other hand, researches on color and alertness has shown that blue color increases subjective alertness and performance on attention-based tasks (CHELLAPPA et al., 2011). This aspect is quite related to the fact that the attention is a powerful means of increasing the visual components of SSVEP and therefore increases the accuracy in its detection (MORGAN; C.; HILLYARD, 1996).

As a summary, this study was performed by assessing twenty volunteers (none of them knew the protocol or had contact with a BCI), distributed into two different

protocols. In this study, an analysis of performance of colored stimuli for SSVEP response using different flickering frequencies was performed. This is the first study published related to effects on the amplitude of SSVEP and accuracy in its detection from visual stimuli of colored LEDs. In addition, subjective opinions from volunteers about aspects related to comfort were taken in account.

From our results, although red color is clearly special and has provided the majority of research attention, conceptually, blue and green seem reasonable candidates for use in an SSVEP-BCI, as both have positive links and have been shown to be associated with positive evaluation [blue, e.g., openness, peace (MEHTA; ZHU, 2009); green, e.g., calmness, success (MOLLER; ELLIOT; MAIER, 2009)]. This fact is confirmed in Table 6 and Figure 29, which agree with studies of (MEHTA; ZHU, 2009; MOLLER; ELLIOT; MAIER, 2009; ELLIOT, 2015), where green and blue got the highest nominations. The term "nomination" was attributed as number of times in which a kind of color is elected.

However, taking into account the large number of times nominated in our studies (5 out of 8, only as first choice), the green color is suggested in both groups as the first best choice for a comfortable, safe and accurate SSVEP-BCI. The red color was disregard of our nominations due to its low level of comfort and its trends to evoke epileptic responses. The results from Figure 30 confirm that green color is the most suitable option for visual stimuli, where the rule of selection of the best color was applied to each resulting centroid. Finally, the order of choice was the following: green, blue and yellow.

5 Development of a Compressive Sensing-Based SSVEP-BCI

SSVEP-BCIs are desired to be comfortable and portable (HAIRSTON et al., 2014), however traditional BCIs have numerous cables and wires. Thus, BCIs could be replaced by wireless ones, in order to be more comfortable for users. On the other hand, Compressive Sensing (CS) is an emerging and promising technique for the development of low-power, small-chip, and robust wireless BCIs (PANT; KRISHNAN, 2014; ZHANG et al., 2013). In addition, it is known that the use of sparse measurement matrix and reconstruction algorithm based on promoting temporal correlation can offer improved reconstruction performance for CS of certain physiological signals (PANT; KRISHNAN, 2013).

In a previous study (TELLO et al., 2015b), we applied CS on an EEG database obtained by using BrainNet-36 acquisition equipment, which acquires reliable EEG signals by using wired electrodes. It was found that 75% of Compression Rate (CR) of the EEG signals together a $\ell_p^{2d} - RLS$ algorithm offer a good accuracy rate in SSVEP detection. In that study, five subjects participated of the experiments and five compression rates were evaluated: 95, 90, 85, 80 and 75%. CS and MSI techniques were repeated 50 times by using a different measurement matrix $\mathbf{\Phi}$ each time. The error between the percentage of accurate estimation (PoAE) for the original EEG and for the reconstructed EEG signals was averaged over 50 repetitions, which is shown in Figure 31. Variance of PoAE for subject 3 is shown in Figure 32, where variance for the algorithm $\mathbf{\Phi}$ is less than or equal to 10 for $CR = 75\%$, 80%, 85%, and 90%. For these reasons, we chose CR of 75% as the most suitable, due to its stability and low error rate.

In this study, an analysis of the MEC (Minimum Energy Combination), CCA (Canonical Correlation Analysis), and MSI (Multivariate Synchronization Index) algorithms was carried out, which are popular for the detection of visual stimulus frequency in SSVEP-BCIs, in addition to $\ell_p^d - RLS$, $\ell_p^{2d} - RLS$, and $BSBL - BO$ algorithms (PANT; KRISHNAN, 2013), which are popular for reconstruction of physiological signals, for a CS-based SSVEP-BCI. Emotiv EPOC, a comfortable and portable wireless EEG acquisition device, was used in this study for EEG acquisition from the occipital region of the brain. The block diagram of this SSVEP-BCI is shown in Figure 33.
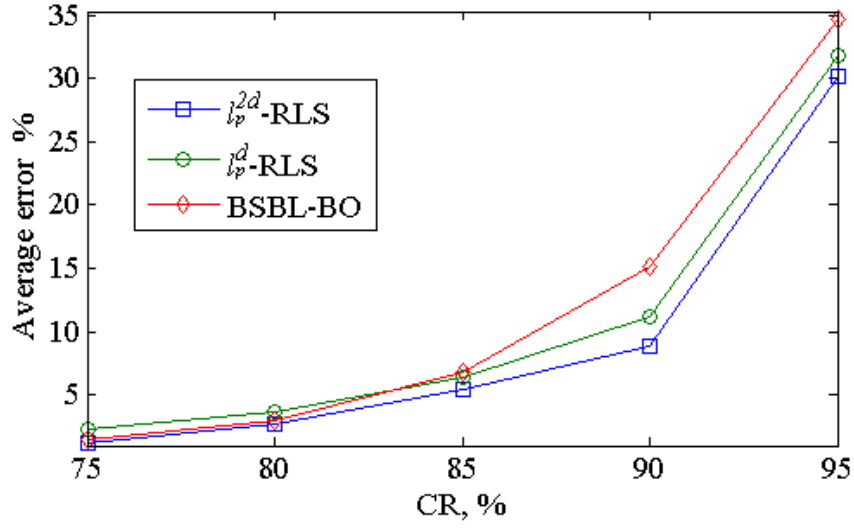
Figure 31: Average PoAE error for the $\ell_p^d - RLS$, $\ell_p^{2d} - RLS$ and $BSBL - BO$ algorithms.
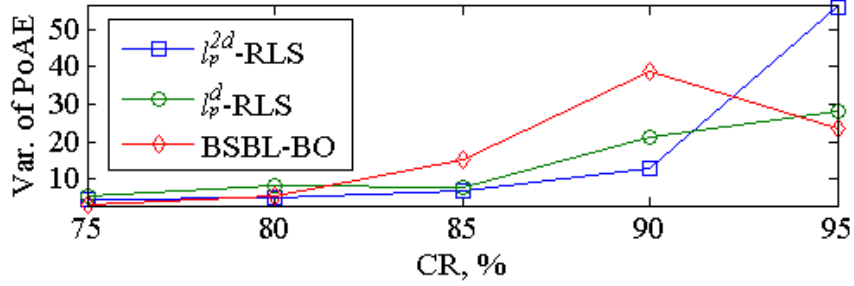
Figure 32: Variance of PoAE for subject 3 for the $\ell_p^d - RLS$, $\ell_p^{2d} - RLS$ and $BSBL - BO$ algorithms.
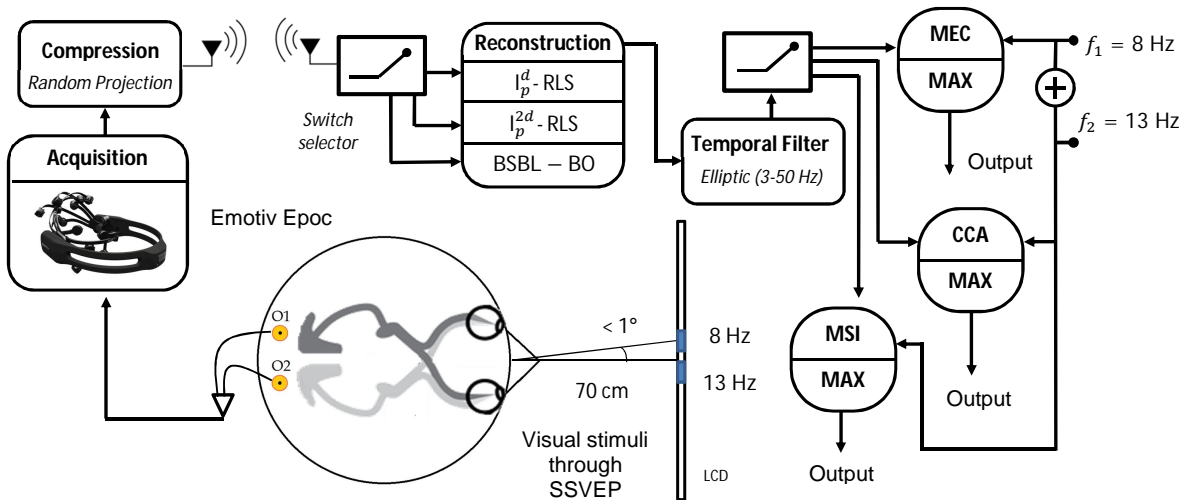
Figure 33: Block diagram of the proposed SSVEP-BCI system.

5.1   Block diagram of the SSVEP-BCI

The key blocks in Figure 33 are discussed below.

1. Acquisition

   Emotiv EPOC Headset is a wireless device used for acquiring signal. EEG signals from occipital O1 and O2 channels with 128 samples per second of sampling rate (f_s) were collected in this device. The sensors used for reference are: Common-Mode Sensing (CMS) and Driven Right Leg (DRL), which are fixed for default, and in parallel to P3/P4 channels (the two mastoids), respectively.

2. Compression

   CS is here used for signal compression, which involves segmenting EEG signals into non-overlapping segments $\{\boldsymbol{x}_i\}$, and applying the operation

$$\boldsymbol{y} = \boldsymbol{\Phi}\boldsymbol{x}, \tag{5.1}$$

   where vector $\boldsymbol{x}$ has length N representing a signal, and its measurement is vector $\boldsymbol{y}$ of length M. $\boldsymbol{\Phi}$ is a sparse matrix of size $M \times N$ with 5 numbers of unity valued nonzero components in each column, where $M \ll N$.

3. Reconstruction

   The signal reconstruction is carried out by using $\ell_p^d - RLS$, $\ell_p^{2d} - RLS$, and $BSBL - BO$ algorithms (PANT; KRISHNAN, 2014; PANT; KRISHNAN, 2013; ZHANG; RAO, 2013), where $\ell_p^d - RLS$ and $\ell_p^{2d} - RLS$ are based on solving the optimization problem

$$\underset{\boldsymbol{x}}{\text{minimize}} \frac{1}{2} \|\boldsymbol{\Phi}\boldsymbol{x} - \boldsymbol{y}\|_2^2 + \lambda f(\boldsymbol{x}), \text{with} \tag{5.2}$$

$$\text{the minimization of} \qquad \left\|\boldsymbol{x}^d\right\|_p = \left(\sum_{n=1}^{N-1} |x_n - x_{n+1}|^p\right)^{1/p} \text{and} \tag{5.3}$$

$$\left\|\boldsymbol{x}^{2d}\right\|_p = \left(|x_1 - x_2|^p + \sum_{n=1}^{N-1} |x_{n-1} - 2x_n + x_{n+1}|^p + |x_{n-1} - x_n|^p\right)^{1/p} \tag{5.4}$$

respectively, with $\lambda > 0$. On the other hand, $BSBL-BO$ algorithm divides signal $\boldsymbol{x}$ into signal blocks $\overrightarrow{\boldsymbol{x}_1}, \overrightarrow{\boldsymbol{x}_2}, \cdots, \overrightarrow{\boldsymbol{x}_s}$ as $\boldsymbol{x} = \left[\overrightarrow{\boldsymbol{x}_1}, \overrightarrow{\boldsymbol{x}_2}, \cdots, \overrightarrow{\boldsymbol{x}_s}\right]^T$, with signal $\boldsymbol{x}$ estimated as

$$\boldsymbol{x} = \sum\nolimits_0 \Phi^T (\lambda I + \Phi \sum\nolimits_0 \Phi^T)^{-1} \boldsymbol{y}, \tag{5.5}$$

where $\sum_0 = diag\{\gamma_1 \mathbf{B}_1, \gamma_2 \mathbf{B}_2, \cdots, \gamma_s \mathbf{B}_s\}$ and parameters γ_i and $\mathbf{B}_i$ control block-sparsity and correlation structure, respectively (PANT; KRISHNAN, 2014; ZHANG; RAO, 2013).

Once the EEG signals are reconstructed, MEC, CCA and MSI algorithms are applied to them for the detection of the visual stimulus frequency. These methods were explained in Chapter 3.

To conduct the experiment, each volunteer sat in a comfortable chair, in front of a 17-inch LCD monitor, and 70 cm away from it. Two stimuli based on checkerboards (4×4) were simultaneously presented in bilateral way. These stimuli were generated by a subsystem based on FPGA (Field-Programmable Gate Array) Xilinx Spartan 3E company. The stimuli were placed by side along a horizontal line separated by a small distance ($\approx$2cm) where the left and right target flickered at $f_1 = 8$ Hz (left) and $f_2 = 13$ Hz (right), respectively.

Three male subjects participated in the study (Mean: 29.7 and SD: 0.58). The research was carried out in compliance with Helsinki declaration, and the experiments were performed according to the rules of the ethics committee of UFES/Brazil, under registration number CEP-048/08. During the first five seconds, a fixed cross in the center of the screen was presented. After finalizing the first five seconds, a beep indicated to the volunteer to fix his/her attention on the left side of the stimulus for thirty seconds. At the end of this time, the volunteer had five seconds to take rest and another thirty seconds was asked to pay attention at the right side. The total duration of the experiment was 70 seconds. The eye movements were also monitored and volunteers were asked to keep a maximum visual angle of 1º for the stimulus selection to guarantee a minimum degree of eye movement.

5.2   Signal processing

Initially, EEG signals from O1 and O2 channels were extracted and transmitted. Once received, a compression stage of 75% of ratio was applied to the signals. During the compression, a signal-vector of length 42000 samples (70 seconds time f_s) was divided into total 42 non-overlapping segments each of length $Q = 1000$. A matrix w of size $Q \times 42$ was constructed by including the 42 segments as its columns. One value of the number of measurements was selected as $P = 250$, which corresponds to compression

ratio ($CR = 75\%$), where CR was computed as $(Q - P) \times 100/Q\%$. For reconstruction, $\ell_p^{2d} - RLS$, $\ell_p^d - RLS$, and $BSBL - BO$ algorithms were applied to the EEG signals from each of the 42 columns of Y_i. The $\ell_p^{2d} - RLS$ algorithm was applied with parameters $p = 1$, $T = 30$, $\lambda_1 = 1$, $\lambda_T = 10^{-2}$, $\epsilon_1 = 1$, $\epsilon_T = 10^{-2}$ and the $BSBL - BO$ algorithm was applied with parameters such as in (PANT; KRISHNAN, 2014) with the discrete-cosine transform basis. The EEG segments were reconstructed by applying the three algorithms, which were concatenated to construct three reconstructed versions of the signal $\boldsymbol{x}$. In the pre-processing stage, the data were segmented and windowed with window lengths (WLs) of 1 s and 4 s, each one, with overlap of 50%. Then, a temporal elliptic filter between 3-50 Hz was applied. MEC, CCA and MSI techniques were applied and the results were compared in terms of performance. The comparison of performance (mean and standard deviation) was tested in 50 repetitions of reconstructed EEG signals averaged for the three subjects in different WL, as shown in Figure 34. In addition, these results were also compared with the original EEG signal for each case. A summary of the results are shown in Table 7.
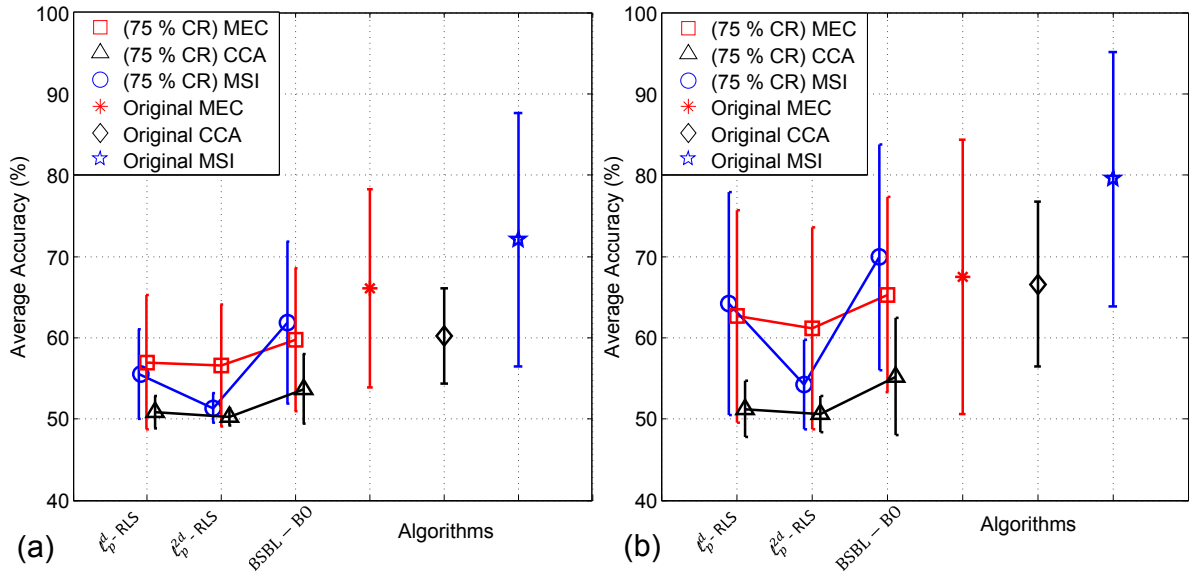
Figure 34: (a) Average of accuracy with WL of 1s and (b) 4s, respectively.

5.3 Conclusion and discussion

An analysis of MEC, CCA, and MSI algorithms for the detection of visual stimulus frequency in SSVEP-BCI systems was carried out. The analysis was done for the application in a CS-based wireless BCI. ℓ_p^d-RLS, ℓ_p^{2d}-RLS, and $BSBL - BO$ algorithms were applied for the reconstruction of the signals from the compressed data. MEC, CCA, and MSI algorithms were applied for the detection of visual stimulus frequency from the reconstructed EEG signals. According to the obtained results, MEC was found to offer the better trade-off between the highest mean value of CA offered by the MSI algorithm

and the lowest variance of the CA offered by the CCA algorithm. The $\ell_p^d - RLS$ algorithm was also found to balance the trade-off between the highest mean and lowest variance of CA offered by the $BSBL - BO$ algorithm and the lowest mean and highest variance of CA offered by the $\ell_p^{2d} - RLS$ algorithm. Also, the increase in the length of EEG signal was found to increase not only the mean value of CA but also the variance of CA.

Table 7: Summary of results related to Mean (μ) and Variance(σ) in [%].

WL	ℓ_p^d	ℓ_p^{2d}	BSBL-BO	WL	ℓ_p^d	ℓ_p^{2d}	BSBL-BO
1 s	**Mean** (μ)			4 s	**Mean** (μ)		
MEC	56.96	56.57	59.73	MEC	62.64	61.16	65.31
CCA	50.79	50.27	53.68	CCA	51.24	50.64	55.21
MSI	55.51	51.36	61.86	MSI	64.23	54.26	69.90
1 s	**Variance** (σ)			4 s	**Variance** (σ)		
MEC	8.28	7.48	8.77	MEC	13.09	12.43	11.97
CCA	1.99	1.08	4.27	CCA	3.46	2.22	7.20
MSI	5.52	1.86	9.95	MSI	13.68	5.47	13.89

6 Development of the Novel Independent SSVEP-BCI

6.1 Introduction

Such as aforementioned, in a typical SSVEP-BCI, several stimuli flickering at different frequencies are presented to users. The subject "overtly" directs his/her attention to one of the stimuli by changing his/her gaze (ZHANG et al., 2010). This kind of SSVEP-BCI is commonly called as "dependent", since muscle activities, such as gaze shifting, are necessary. However, patients with amyotrophiclateral sclerosis (ALS), multiplesclerosis and Guillain-Barré syndrome may suffer from severe motor disabilities, which can disrupt their communication with the external environment. Therefore, typical "dependent" SSVEP-BCIs might not be applicable for these subjects. Nonetheless, an "independent" can be an alternative solution, as this kind of BCI is controlled by subject's attentions without requiring head neuromuscular control or eye movements. It means that the attention is performed in a "covertly" form.

Several studies have shown that people can covertly shift attention to different spatial location tasks (MORGAN; C.; HILLYARD, 1996; KELLY et al., 2004b; ALLISON et al., 2008; ZHANG et al., 2009; LESENFANTS et al., 2014). Morgan, C. and Hillyard (1996) initially studied the effect of spatial attention on SSVEP, and Kelly et al. (2004b) emphatized that there is a reduction in 20 % of accuracy in detecting SSVEP when a volunteer does not perform eye movements compared to another who does it, which makes more complex the SSVEP detection. In that study, the terms "attended" or "unattended" implied an "overt" and "covert" attention, respectively. A similar procedure was performed using flickering letters in a CRT monitor by Kelly et al. (2005b), in which six out of eleven physically and neurologically healthy subjects demonstrated reliable control in binary decision-making, achieving at least 75 % of correct selections in five sessions, each with approximately 12 min duration. In (ALLISON et al., 2008), the hypothesis about whether overlapped stimuli can evoke changes in SSVEP was evaluated in a BCI. On the other hand, the modulation effects of SSVEP amplitude and phase response for covert shifts of attention were investigated by Zhang et al. (2009) for two distinct colors. Finally, LEDs were used as visual stimuli in an independent covert two-class SSVEP, which was evaluated with twenty-four healthy subjects and six LIS patients (LESENFANTS et al., 2014). The mean offline and online accuracies obtained for the healthy subjects were 85.00 ± 2 % and 74.00 ± 13 %, respectively, and subjects with LIS obtained 60.75 ± 8 % accuracy in

online tests.

According to literature, independent BCIs can be separated into two groups (see Figure 35): those that use bilateral flickers from checkerboards (MORGAN; C.; HILL-YARD, 1996; KELLY et al., 2004a; KELLY et al., 2005b), and those with an approach based on overlapped stimuli or mixed in a reduced space (ALLISON et al., 2008; ZHANG et al., 2009; LESENFANTS et al., 2014). Our independent BCI uses a different paradigm: "Figure Ground Perception (FGP)" based on LEDs, in which two images are simultaneously present to the subject (Binocular Rivalry).

(a)

(b)

(c)

(d)

(e)

(f)
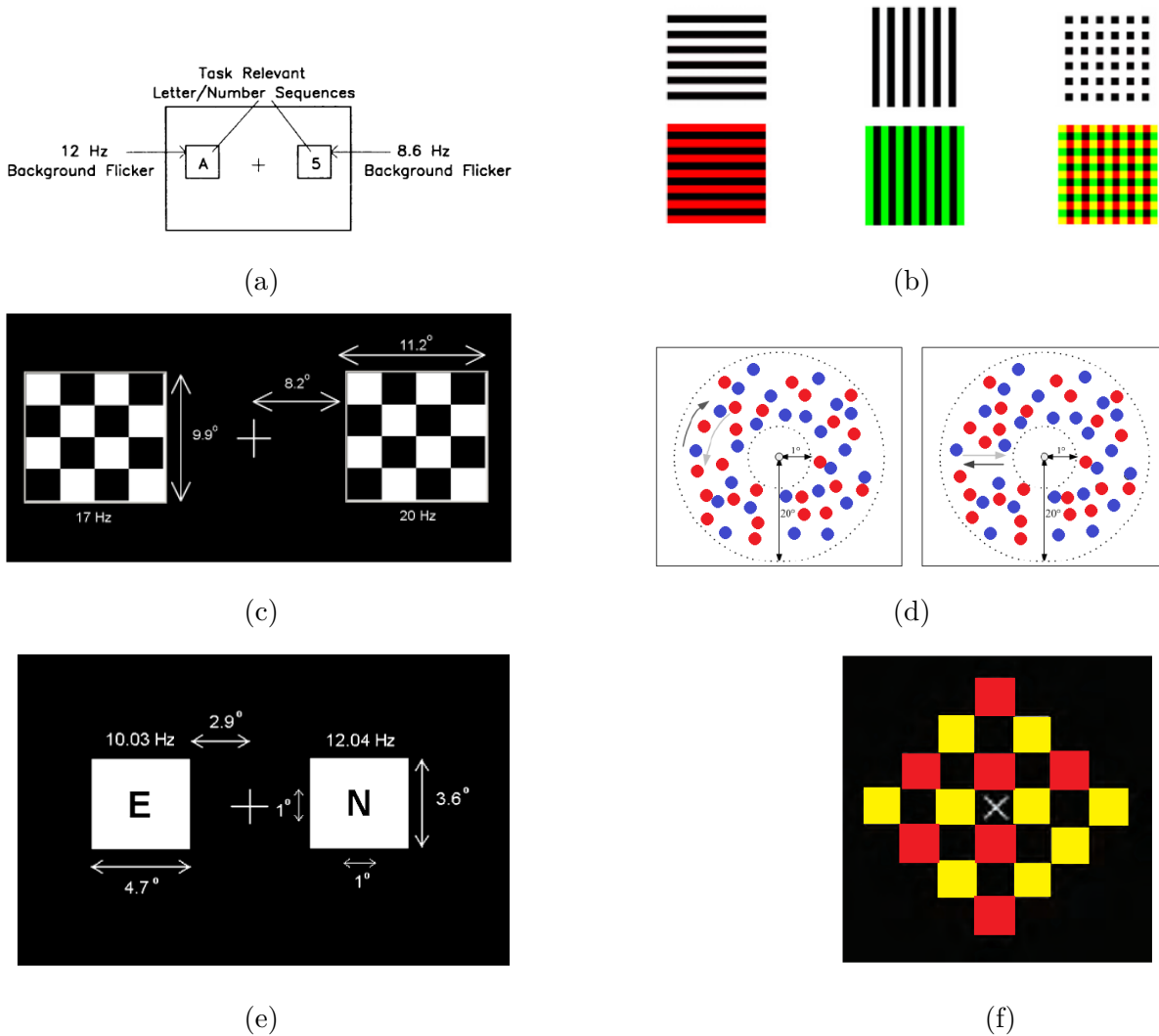
Figure 35: Stimuli used in an independent SSVEP-BCI and presented in the following references: (a) Morgan, C. and Hillyard (1996), (b) Allison et al. (2008), (c) Kelly et al. (2004a), (d) Zhang et al. (2009), (e) Kelly et al. (2005b), (f) Lesenfants et al. (2014).

6.2   Figure Ground Perception (FGP)

The classic Gestalt psychology demonstrates the existence of an early autonomous process of visual organization, which produces percepts that do not always conform to

previous knowledge or expectations about the stimulus, as small changes to the stimulus can induce extensive perceptual reorganization (WAGEMANS et al., 2012). Recordings of border-ownership signals in visual cortex demonstrate how a stimulus is interpreted and reorganized (QIU; HEYDT, 2007). Stephen E. et al. suggest that a slight modification of the conditions of the good continuation (which refers to the tendency for elements to be grouped to form smooth contours) may provide a spontaneous reorganization of shapes that might be observed in the area V2 of the visual cortex (WAGEMANS et al., 2012). On the other hand, according to (GRILL-SPECTOR, 2003), the lateral and ventral occipito-temporal areas are valuable for perceiving and recognizing objects and faces.

In 1999, Leopold and Logothetis suggested that the multistable perception is mostly non-sensory in its origin (PITTS; NERGER; DAVIS, 2007). Multistable perception is considered to be a powerful vehicle to recognize perceptual awareness from sensory processing that occurs in ambiguous figures such as the Necker cube (NECKER, 1832). In addition, the Rubin's face-vase illusion has mutually exclusive interpretation when is observed between dissimilar, and thus incompatible images, simultaneously presented to the two eyes (binocular rivalry) (STERZER; KLEINSCHMIDT; REES, 2009). In both cases, perceptual awareness of physically identical stimuli alternates stochastically between two (or more) interpretations. For ambiguous figures, a single stimulus is presented to both eyes, and perception switches ("reverses") between each possible interpretation for every few seconds (BRITZ; PITTS, 2011). According to the theory of multistable perception, the perceptual reversals are the necessary consequences of a generalized high-level "exploratory" mechanism that directs spatial and selective attention in a way that forces lower level perceptual systems to periodically refresh (STERZER; KLEINSCHMIDT; REES, 2009).

Regarding attention, the role of this in perceptual (re)organization is essential to be considered. Gestalt psychologists have pointed out that when attention is drawn to figures, the background regions of figures often go unnoticed (WAGEMANS et al., 2012). The way how the unattended objects are processed is difficult to be derived from phenomenal reports by participants of these experiments, who cannot avoid paying attention to the stimuli that they are supposed to judge. In contrast, neuronal recordings show the processing of all stimuli, whether attended or not. Neuro-physiological studies investigating whether perceptual organization processes are preattentive, influenced by attention, or take place only under attention, producing mixed results. In some situations, attention initiates a process of organization that reflects the intrinsic connectivity of the cortex. But in other situations, the organization emerges independently of attention, creating a structure for selective attention (WAGEMANS et al., 2012).

Generally, the visual attention is most controlled through eye movements, and the objects of interest are usually unambiguous. However, in multistable perception experi-

ments, covert attention (without voluntary eye movements) may be altered by this central exploratory mechanism (PITTS; NERGER; DAVIS, 2007).

In addition to changes in the figure in the field of multistable perception, a subconcept emerges, where the figure appears nearer than the background part, involving depth perception, and the background appears to be occluded by the figure. This perceptual experience is named "figure-ground perception" (PETERSON; SALVAGIO, 2009). Using this last concept, our work is presented here as a novel approach in SSVEP-BCIs (see Figure 36).

A portable stimulator based on LEDs designing the model face-vase is also proposed here (Figure 37). This kind of approach has the objective of being used for patients with severe motor disabilities where movements ocular are not required, with the information about the targets coming from visual lateral inhibition. Lateral inhibition is a term that describes the mutual interaction among the neural processing units of the same processing level of bio vision (HOOD; JERNIGAN, 1994; CHEN; HONGWEI, 2010). Characterized by the inhibition of behavior among the adjacent processing units. This interaction has positive effect on some of the early visual processing, such as edge enhancement and contrast enhancement, creating a contrast in stimulation that allows increased sensory perception. Lateral inhibition was first found and confirmed by Hartline et al., who conducted electrophysiological experiments of the Limulus visual (HARTLINE; WAGNER H. G.AND RATLIFF, 1956). Looking upon every ommatidia in the compound eye of the Limulus as a photo receptor, they found that a receptor could be inhibited by some other receptors in its proximity (CHEN; HONGWEI, 2010).

Therefore, visual lateral inhibition is the process in which photoreceptor cells aid the brain in perceiving contrast within an image. Experiments are typically conducted with achromatic stimuli, but a similar effect would hold for colored stimuli (CHEN; HONGWEI, 2010). The contrast effect would be related to the distribution of Macular Pigment (MP) in humans, which is a yellow pigment that is found in the inner layers of the central retina (HAMMOND, 2012). Humans have duplex vision: rods, which operate in dim light and are mostly not screened by MP, and cones, which operate at higher light levels and are screened by MP (HAMMOND, 2012). In dim light levels, the pigment migrates to the periphery, and in high light levels the pigment concentrates toward the center of the distal retina (DOUGLAS; MARSHALL, 1999). Details of this response can be seen in Figure 38.

Based on the principles of Figure 38, we decided to use blue and white colors for the photo-stimulation setup in order to create this contrast effect. Additionally, our previous research related to study of the effects of colored stimuli on SSVEP suggests that blue color in 11 Hz provides results of high accuracy and, at the same time, high level of user comfort in relation to other colored stimuli (TELLO et al., 2015a). Furthermore,
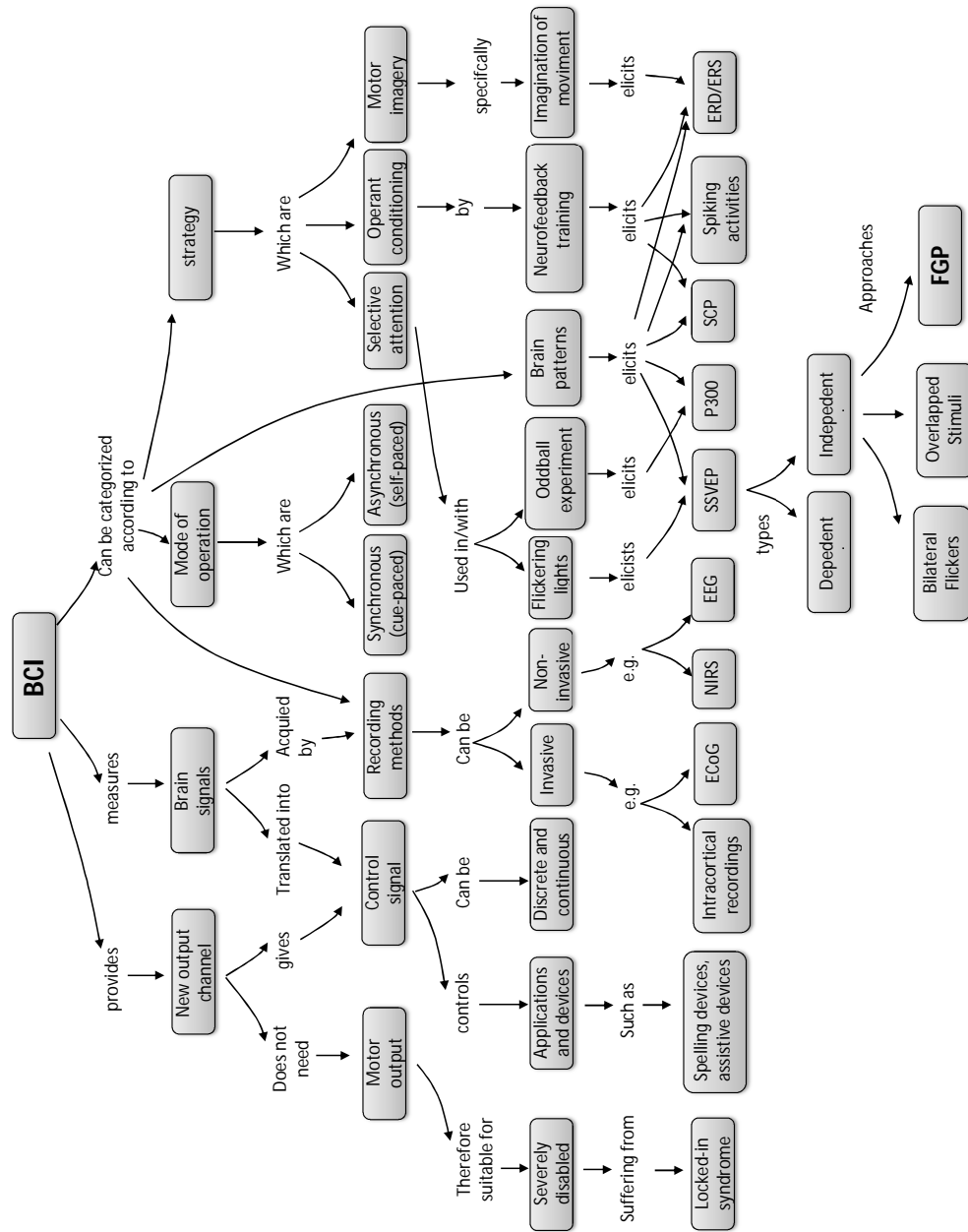
Figure 36: From Brain–computer interface concept-map, a novel approach in SSVEP-BCIs is presented in this study: Figure Ground Perceptionin (FGP). Modified from (GRAIMANN; ALLISON; PFURTSCHELLER, 2010).
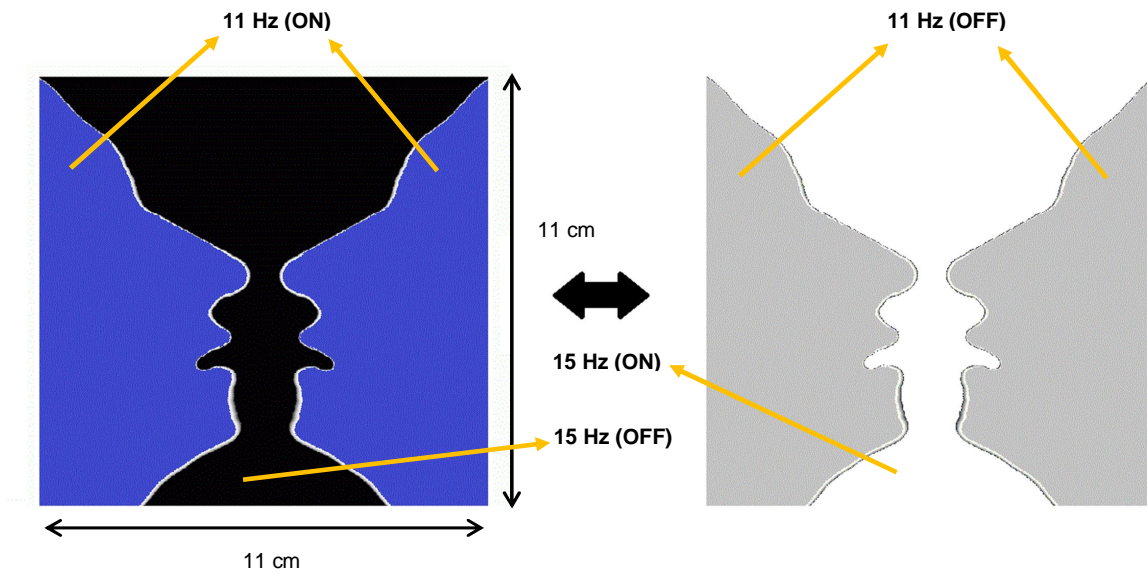
Figure 37: Dimensions and characteristics of the stimulator (faces-vase) and their respective frequencies (faces: 11 Hz; vase: 15 Hz).
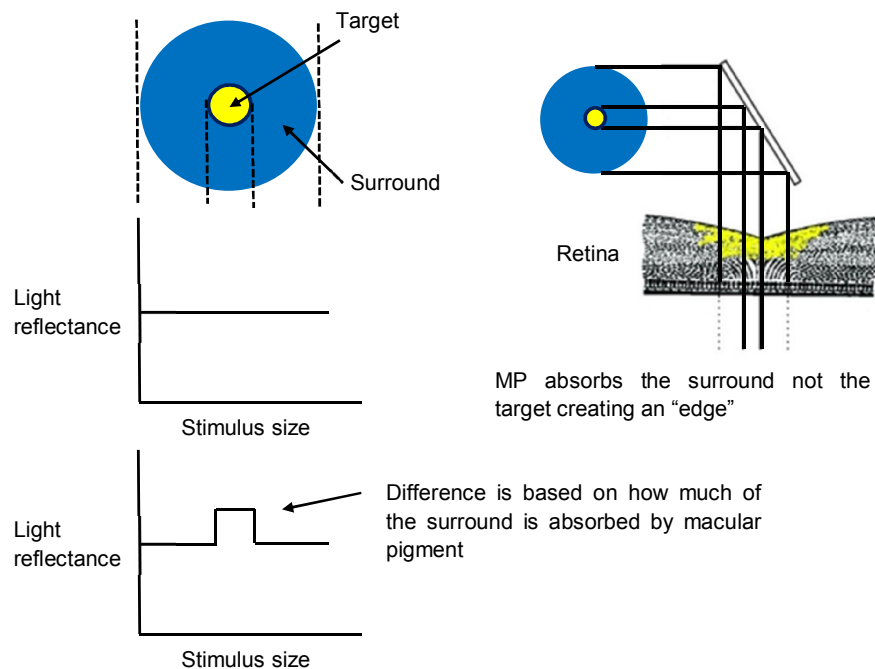
Figure 38: A blue surround with a yellow stimulus of equal luminance. Note that whatdefines the edge is based only on the wavelength or color difference. The luminance difference itself, however, will be exaggerated by differential absorption by macularpigment. Adapted from (HAMMOND, 2012).

according to our studies, white also offers quite promising results (TELLO et al., 2014b; TELLO et al., 2014a). The flickering frequencies used in this novel BCI are 15.0 Hz (vase) and 11.0 Hz (faces). More details can be seen in Figure 37.

6.3 Subjects

Ten subjects (all males), with ages from 27 to 36 years old, were recruited to participate in this study (average age: 29.0; SD: 4.06). The research was carried out in compliance with Helsinki declaration, and the experiments were performed according to the rules of the ethics committee of UFES/Brazil, under registration number CEP-048/08. The volunteers were labeled as: s1, s2, s3, s4, s5, s6, s7, s8, s9 and s10.

The subjects were free to withdraw at any time without any penalty. Previously, a selection of volunteers was performed and topics related to precautions as visual problems, headaches, family history with epilepsy and problems related to brain damage were consulted. The participants did not report any problems. In addition, no one had previous experience in using a BCI.

6.4 Equipment and setup of stimulation unit

For the development of our BCI, 12 channels of EEG with reference at the left ear lobe were recorded at 600 samples/s, with 1–100 Hz pass-band filter. The ground electrode was placed on the forehead. The EEG electrode placements were based on the International 10-20 System. The electrodes used were: P7, PO7, PO5, PO3, POz, PO4, PO6, PO8, P8, O1, O2 and Oz. The equipment used for EEG signal recording was BrainNet-36. The volunteers sat on a comfortable chair, in front of the stimulator, 70 cm from it. Figure 39 shows a volunteer with the acquisition system and the corresponding stimulator system designed.

At the beginning of the experiments, the participants were asked to watch the photo-stimulator, which is controlled by a microcontroller (PIC18F4550), with 50/50 % on-off duties. The block diagram and the experimental setup are shown in Figure 40.

The flickers stimuli are based on LEDs with two colors (blue for the faces and white for the vase) covered with thin white papers diffusers. The figure represents the vase, which is 3.5 cm depth with the faces, helping to create an effect of figure ground perception (FGP), as shown in Figure 40.

The experiments were performed off-line. During the first 5 s the volunteer stayed in a state of relaxation. Before finishing these 5 s, a beep was issued and the volunteer had to fix his/her attention on the stimulus located at the vase (15.0 Hz) for 30 s. A rest of 5 s and a new beep indicated to the volunteer fixing his/her attention to the faces (11.0
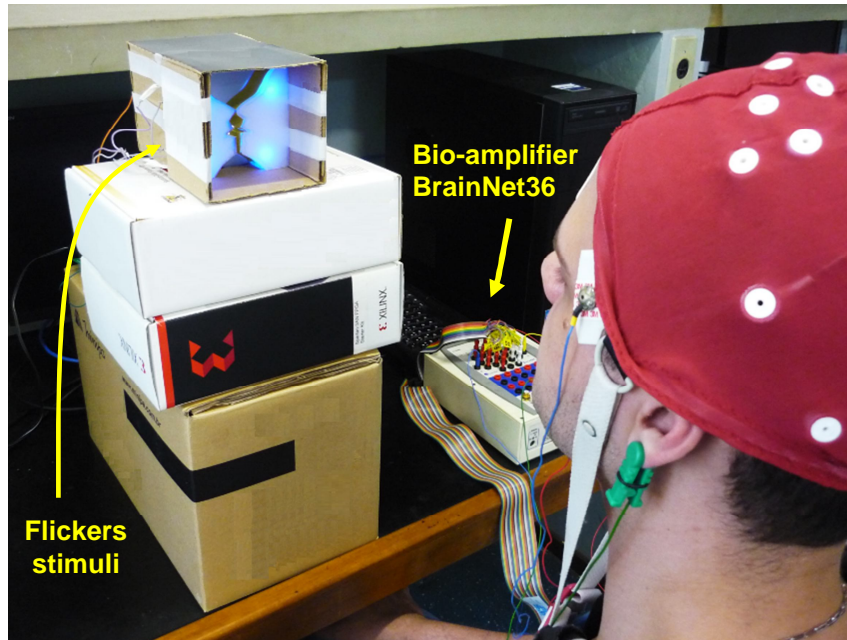
Figure 39: Setup with photo-stimulator and acquisition system.
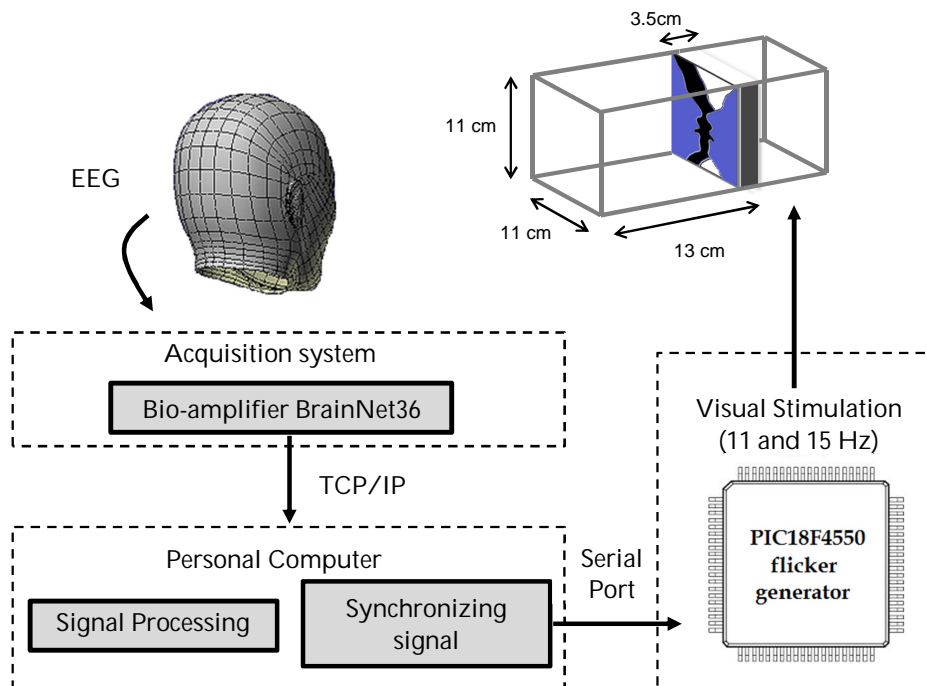
Figure 40: Block diagram of the photo-stimulator.

Hz), ending in 70 s. This visualization was asked to be performed making a minimum visual angle, in order to select the stimulus covertly.

6.5   Offline data analysis

Initially, the data were segmented and windowed in window lengths (WLs) of 1 s and 4 s, each one, with an overlap of 50 %. Then, a spatial filtering was applied using a Common Average Reference (CAR) filter and a band-pass filter between 3 and 60 Hz for the twelve channels. Canonical correlation analysis (CCA) was used for feature extraction to analyze the behavior of the signals independently for each channel for all subjects during the task performed. CCA helps to find the most appropriate electrodes for improving the classification in terms of accuracy. Based on the hypothesis that high values of energy for detection of SSVEPs are located in channels O1, O2 and Oz, a comparison in terms of classification between these three electrodes was done (as feature vectors inset), and the choice of only one channel was performed. Later, it will be shown that the use of a single electrode compared to three electrodes in a set causes a noticeable improvement in the accuracy. Finally, CCA and a modified version of Multivariate Synchronization Index (MSI), both with criterion of maxima for classification, were compared. Both methods were explained in Chapter 3.

6.6   Discussions

6.6.1   Regarding the feature extraction

According to the experiments, the subjects were advised to gaze one target each time (either face or vase). This way, an independent analysis for all channels and for each subject was performed. From these results, it was further hypothesized that the average correlation coefficients (obtained by Equation 3.12) varies inversely during the change of focus from one target to other. This behavior is related to the experimental setup and instructions for each subject were given, where perception helps to increase the correlation between targets. This feature is called as "wished pattern" throughout the text. In our case, when the subject gazes the vase, the correlation coefficients for the frequency of 15 Hz are higher than for 11 Hz (which represents the faces), and vice versa. On the other hand, the number of channels and the selection of channels may play an important role in this novel SSVEP-BCI. From our study, it seems that the gaze and perception capability is not consistent in every subject. Therefore, cautions should be taken about which channel is used for the purpose of quantification.

Once these wished patterns are reached, the evaluated electrodes are categorized as suitable (results are shown in Tables 8 and 9). According to these tables, it is noticeable

that the electrode Oz has the largest number of possibilities of choice for different WLs (both for 1 or 4 s), due to that this feature is present in the major number of subjects (7/10), equivalent to 70 % of votes. Therefore, it is shown that Oz channel might be more suitable to be used in our novel SSVEP-BCI. From our observations, the focus on faces generates higher values regarding correlation. It was found that the magnitudes of the coefficients of the canonical correlation, while the attention was focused in the faces, were slightly higher compared to the vase. This was noticeable in several channels (see in the case of subject 1 – Figure 41 – showing the analysis for WL of 1 s, and Figure 42 for 4 s). One of the possible explanations can be due that the distance to the vase is deep higher in the setup compared to the face. Therefore, the subject's perception was, most of the time, on the face, even while the subjects were advised to look into the vase. Secondly, the other possible reason may be due to our brains receive daily stimulation from human faces, which implies that our brains are highly trained to focus on face.
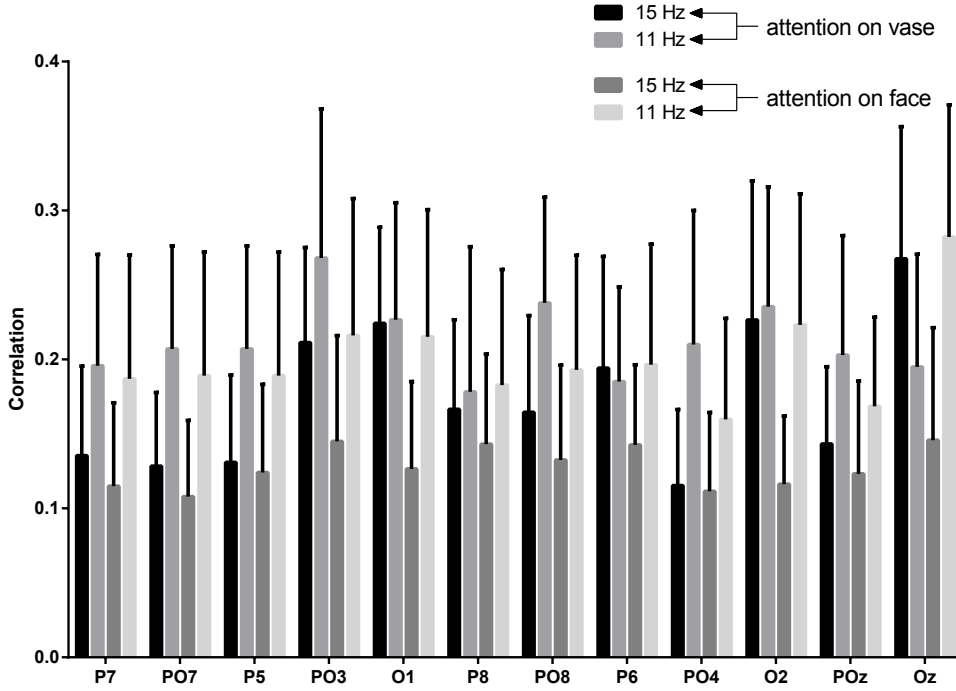
Figure 41: Correlation values in terms of mean (μ) and standard deviation (σ) from 12-channels are shown for WL of 1 s. Here, channel Oz and P6 showed expected results (Results from volunteer 1).

6.6.2   Regarding classification

A way of visualization of the performance of our algorithms is the use of confusion matrices. For our case, signals using the channels O1, O2 and Oz in set, and signals from just Oz were evaluated.

Figure 42: Correlation values in terms of media (μ) and standard deviation (σ) from 12-channels are shown for WL of 4 s. Here, channel O1, P8, P6 and Oz showed expected results (Results from volunteer 1).

Table 8: Channels information showing good results of accuracy using WL of 1 s .

Subjects	P7	PO7	P5	PO3	O1	P8	PO8	P6	PO4	O2	POz	Oz
1								✓				✓
2						✓				✓		
3			✓							✓		
4												✓
5												
6									✓			✓
7										✓		✓
8												✓
9					✓							✓
10												✓

Table 9: Channels information showing good results of accuracy using WL of 4 s.

Subjects	P7	PO7	P5	PO3	O1	P8	PO8	P6	PO4	O2	POz	Oz
1					✓	✓		✓				✓
2						✓				✓		✓
3				✓	✓		✓			✓		
4	✓									✓		✓
5												
6		✓							✓			
7												✓
8												✓
9		✓			✓	✓	✓					✓
10							✓					✓

True Positive (TP) and True Negative (TN) values were used for measuring the accuracy in detecting the SSVEP using Equation 6.1.

$$\text{ACC} = \frac{\text{TP+TN}}{\text{P+N}}, \tag{6.1}$$

where P indicates positive instances, and N indicates negative instances. In addition to the accuracy rate, Command Transfer Interval (CTI) and Information Transfer Rate (ITR) was also computed.

Tables 10-13 show the comparative results of performance (accuracy and ITR) between three channels in a set (called as "before"), and Oz electrode (called as "after") for different WL, both for CCA and MSI, respectively. The gray shaded boxes indicate the cases where we can notice an improvement in the accuracy per subject (between before and after). In this decision criteria, a minimal threshold of 60 % is suggested, which indicates a good choice.

Figures 43 and 44 show a comparison of values of accuracy between these two different methods in terms of average and standard deviation values ($\mu \pm \sigma$) for each subject. Improvements can also be seen between the use of three electrodes and just the channel Oz. In addition, the comparison between different WLs were tested and are also shown in these figures. It is also visible that subjects 3, 5 and 6 did not perform adequately the tasks, which is reflected in the high value of σ and low accuracy.

A way to visualize the comparison between the two methods used (CCA and MSI) is shown in Figure 45. For this, subjects 1, 2, 4, 7, 8, 9 and 10 were selected in our analyses. It seems that MSI surpassed CCA both using three electrodes compared to one, in different WLs. It is even evident that when using larger WLs, the classification increases but the response time is delayed, which hinders real-time applications. Using this method and with only the channel Oz, and WL of 1 s, the average accuracy and SD were 83.67 ± 13.71 %. This result shows that this novel SSVEP-BCI based on perception is feasible and

Table 10: Comparison between accuracy results for WL of 1 s using three electrodes in set (before) and Oz electrode (after) using CCA.

| | Window length [1s] (before) | | | | Window length [1s] (after) | | | |
| | Accuracy | | | | Accuracy | | | |
Subjects	15 Hz (vase)	11 Hz (faces)	Average Accuracy	ITR [bits/min]	15 Hz (vase)	11 Hz (faces)	Average Accuracy	ITR [bits/min]
s1	64.41	93.22	78.81	15.31	77.97	86.44	82.20	19.47
s2	61.67	90.00	75.83	12.14	76.67	90.00	83.33	21.01
s3	33.33	93.33	63.33	3.12	18.33	80.00	49.17	0.02
s4	36.67	76.67	56.67	0.78	41.67	73.33	57.50	0.99
s5	8.33	88.33	48.33	0.06	6.67	83.33	45.00	0.44
s6	42.37	67.80	55.08	0.46	50.85	49.15	50.00	0.01
s7	53.33	60.00	56.67	0.78	66.67	58.33	62.50	2.74
s8	38.98	76.67	57.82	1.07	57.63	68.33	62.98	2.96
s9	55.00	85.00	70.00	7.13	63.33	80.00	71.67	8.41
s10	30.00	91.80	60.90	2.08	60.00	73.77	66.89	5.04

Table 11: Comparison between accuracy results for WL of 4 s using three electrodes in set (before) and Oz electrode (after) using CCA.

| | Window length [4s] (before) | | | | Window length [4s] (after) | | | |
| | Accuracy | | | | Accuracy | | | |
Subjects	15 Hz (vase)	11 Hz (faces)	Average Accuracy	ITR [bits/min]	15 Hz (vase)	11 Hz (faces)	Average Accuracy	ITR [bits/min]
s1	85.71	92.86	89.29	7.63	100.00	92.86	96.43	11.67
s2	85.71	93.33	89.52	7.74	85.71	86.67	86.19	6.31
s3	64.29	93.33	78.81	3.83	35.71	73.33	54.52	0.09
s4	64.29	86.67	75.48	2.95	71.43	80.00	75.71	3.01
s5	0.00	80.00	40.00	0.44	7.14	73.33	40.24	0.42
s6	14.29	85.71	50.00	0.00	28.57	42.86	35.71	0.90
s7	50.00	53.33	51.67	0.01	92.86	53.33	73.10	2.40
s8	42.86	80.00	61.43	0.57	64.29	80.00	72.14	2.20
s9	71.43	100.00	85.71	6.13	92.86	100.00	96.43	11.67
s10	35.71	93.33	64.51	0.93	64.29	100.00	82.14	4.85

Table 12: Comparison between accuracy results for WL of 1 s using three electrodes in set (before) and Oz electrode (after) using MSI.

| | Window length [1s] (before) | | | | Window length [1s] (after) | | | |
| | Accuracy | | | | Accuracy | | | |
Subjects	15 Hz (vase)	11 Hz (faces)	Average Accuracy	ITR [bits/min]	15 Hz (vase)	11 Hz (faces)	Average Accuracy	ITR [bits/min]
s1	67.80	98.31	83.05	20.62	91.53	86.44	88.98	29.98
s2	65.00	95.00	80.00	16.69	96.67	86.67	91.67	35.18
s3	30.00	96.67	63.33	3.12	16.67	80.00	48.33	0.06
s4	33.33	85.00	59.17	1.47	43.33	73.33	58.33	1.22
s5	6.67	95.00	50.83	0.02	13.33	83.33	48.33	0.06
s6	37.29	71.19	54.24	0.32	52.54	49.15	50.85	0.02
s7	50.00	75.00	62.50	2.74	63.33	56.67	60.00	1.75
s8	35.59	88.33	61.96	2.51	52.54	71.67	62.10	2.57
s9	46.67	90.00	68.33	5.97	63.33	80.00	71.67	8.41
s10	33.33	88.52	60.93	2.09	56.67	77.05	66.86	5.03

Table 13: Comparison between accuracy results for WL of 4 s using three electrodes in set (before) and Oz electrode (after) using MSI.

| | Window length [4s] (before) | | | | Window length [4s] (after) | | | |
| | Accuracy | | | | Accuracy | | | |
Subjects	15 Hz (vase)	11 Hz (faces)	Average Accuracy	ITR [bits/min]	15 Hz (vase)	11 Hz (faces)	Average Accuracy	ITR [bits/min]
s1	85.71	100.00	92.86	9.43	100.00	92.86	96.43	11.67
s2	85.71	100.00	92.86	9.43	100.00	93.33	96.67	11.84
s3	57.14	100.00	78.57	3.76	28.57	73.33	50.95	0.01
s4	42.86	100.00	71.43	2.06	71.43	73.33	72.38	2.25
s5	0.00	100.00	50.00	0.00	7.14	53.33	30.24	1.74
s6	7.14	85.71	46.43	0.06	28.57	42.86	35.71	0.90
s7	57.14	80.00	68.57	1.53	85.71	53.33	69.52	1.70
s8	35.71	80.00	57.86	0.27	64.29	80.00	72.14	2.20
s9	78.57	100.00	89.29	7.63	92.86	100.00	96.43	11.67
s10	35.71	100.00	67.86	1.41	64.29	100.00	82.14	4.85
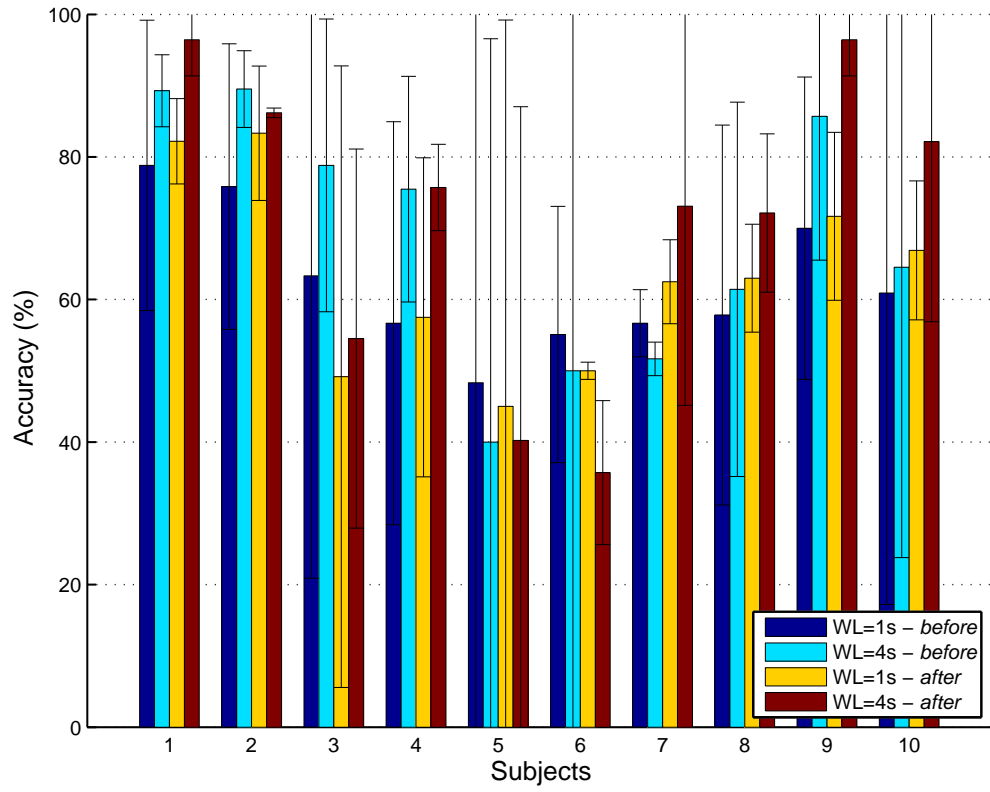
Figure 43: Values of accuracy in the classification in terms of averages and standard deviation values ($\mu \pm \sigma$) using CCA.
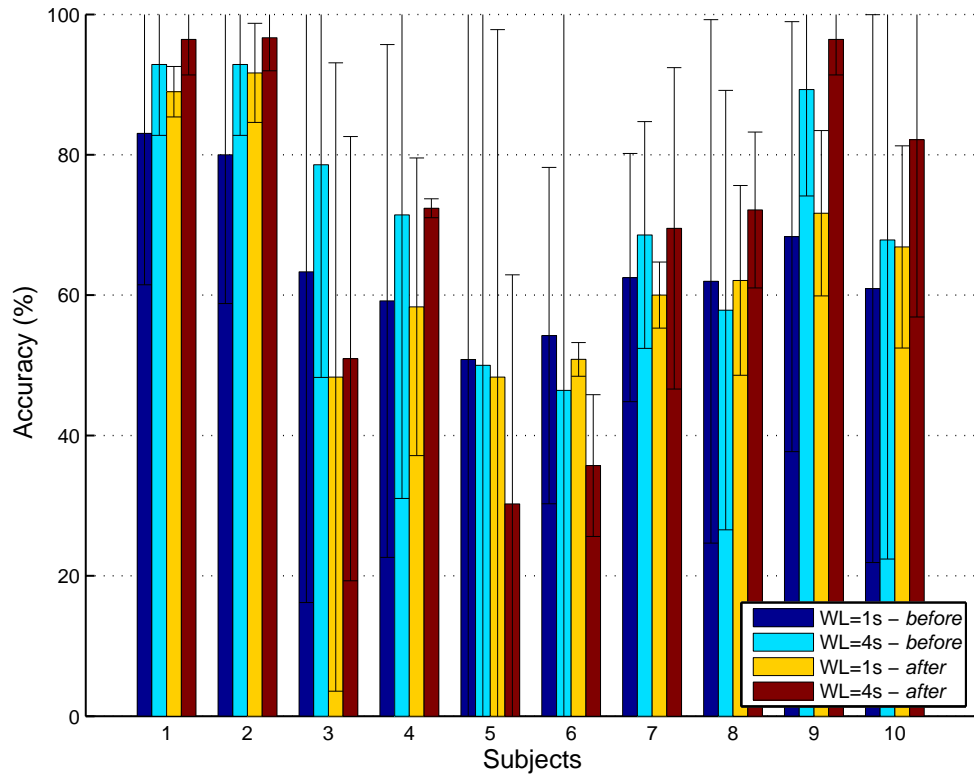
Figure 44: Values of accuracy in the classification in terms of averages and standard deviation values ($\mu \pm \sigma$) using MSI.

has high accuracy, even using only one channel (Oz) from a previous filtering processing of twelve channels, using either of two feature extraction methods. Moreover, this result is quite acceptable considering that the subjects never had used a BCI neither had previous training. These results demonstrate that the perception may play an important role in the attention of the subject and therefore can be used in this novel SSVEP-BCI.
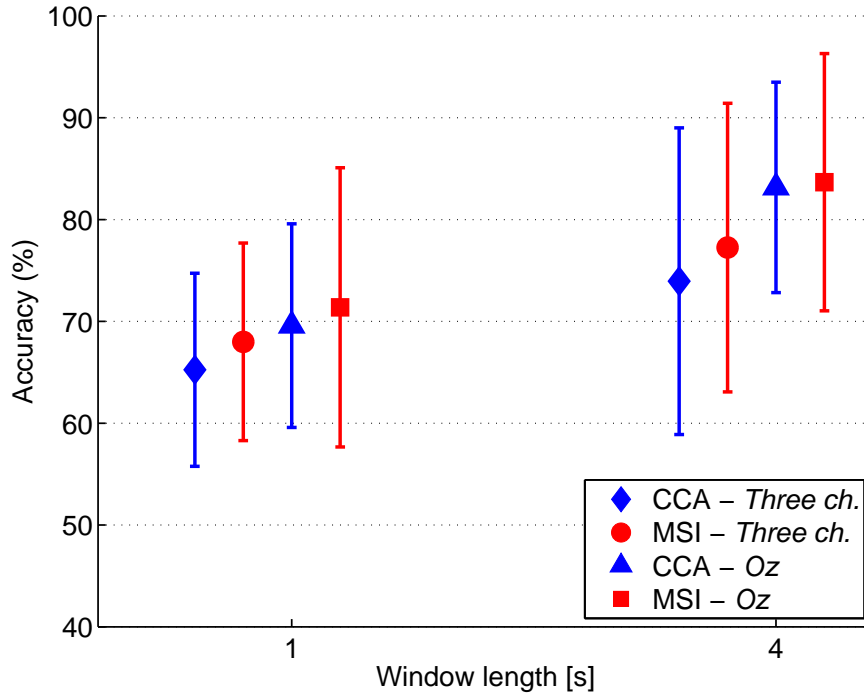
Figure 45: Error bars showing a summary of cases evaluated related to performance of the two methods analyzed.

6.7   Online SSVEP detection and performance

Five participants (5 males, 22-32 years of age; mean age 22.4 years) were instructed to perform the online BCI tasks. The subjects didn't have previous experience with BCI experiments considered in this study. In order to familiarizing the system with the native language of the participants, audio feedback in Portuguese was used (all participants were Brazilian). The words were recorded in wav files and played indicating the suitable instructions and decisions after signal processing. The algorithm was implemented on a PC with 4 GB onboard memory and Intel 32-bit Core 2 duo processor (2.20 GHz, 800 MHz) running Windows 7. BrainNet-36 was the device used for EEG acquisition with a cap of integrated electrodes according to the 10-20 international system. The online data acquisition was obtained by a sniffer based on Java programming language, as the equipment (BrainNet-36) is a clinical device that does not export data in online mode. Additionally, on the computer screen it is possible to follow the process of SSVEP detection and routines of the system during the process of data acquisition. Due to the

good results obtained with the technique of MSI and Oz electrode in offline analysis, we decided to use this setup also for online detection using WLs of 2 s. This decision was adopted in order to improve the results and keep the trade-off between accuracy and speed.

In order to check the proper execution of the experiments performed by the volunteers, a commercial device of eye tracking (Eye Tribe) was used. Data from this device demonstrated that the subjects did not perform eye movements outside the limits established for this experiment. The eye tracker requires an initial calibration that is performed by 9 points shown on the screen, with a distance between subject and eye tracker of 70 cm. The eye tracker has an accuracy ranging from 0.5^0 to 1^0 and a spatial resolution of 0.1^0. Metric parameters related to the distances between the subject and the setup are detailed in Figure 46. Moreover, before beginning the experiments, volunteers performed a previous training between 3 and 10 min. Failed tests were discarded and some subjects got the "frustration state".
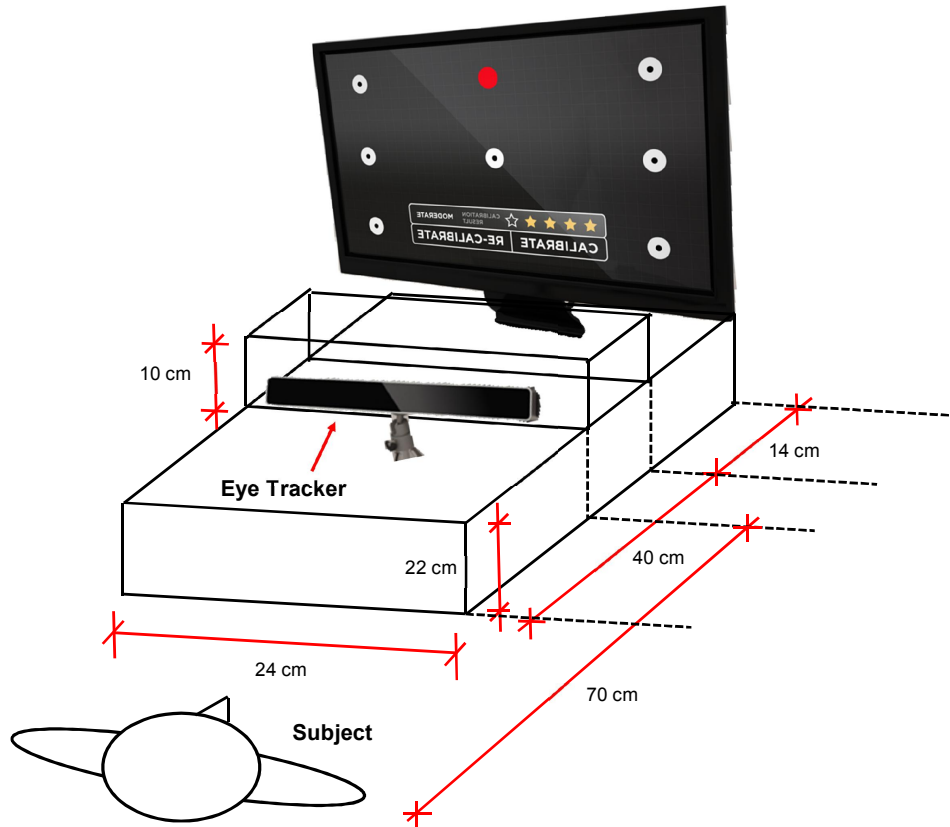
Figure 46: Setup parameters and the designed structure containing calibration devices and visual stimulator for validation of online tasks.

Results of the experiments showed an accuracy of 82.7 % for recognition of faces and 76.0 % for vases (more details in Table 14). Three trials were performed by each subject and each trial was 44 s of duration. According to data obtained by the eye tracker, the tasks were performed in less than 3^0 of angle subtended from the center of users' field of

view. In addition, subjective opinions from volunteers about aspects related to frustration and fatigue were taken into account.

Table 14: Online SSVEP detection in terms of accuracy (%). The values represent the percentages of True Positive (TP), and True Negative (TN). Time duration of each experiment was 44 seconds.

Subjects	Number of trial	WL=2s		Previous time of training [min]	Has he/she reached the frustration?	Has he/she reached the fatigue?
		TP [Face]	TN [Vase]			
		Recognized/Outputs (Accuracy)				
1	1	4/5(80%)	4/5(80%)	10		
	2	5/5(100%)	4/5(80%)	7	Yes	Yes
	3	5/5(100%)	4/5(80%)	4		
2	1	4/5(80%)	3/5(60%)	8		
	2	5/5(100%)	4/5(80%)	5	Not	Yes
	3	4/5(80%)	4/5(80%)	4		
3	1	3/5(60%)	3/5(60%)	8		
	2	3/5(60%)	3/5(60%)	6	Not	Not
	3	5/5(100%)	4/5(80%)	5		
4	1	3/5(60%)	3/5(60%)	7		
	2	3/5(60%)	5/5(100%)	5	Not	Not
	3	5/5(100%)	4/5(80%)	3		
5	1	4/5(80%)	4/5(80%)	8		
	2	4/5(80%)	4/5(80%)	6	Not	Not
	3	5/5(100%)	4/5(80%)	4		
Average		82.7%	76%	6		

6.8   Discussion

In this study, an alternative manner of presenting SSVEP stimuli was evaluated, in which a portable photo-stimulator based on two flickering stimuli representing the model face-vase was also here proposed. This novel concept of SSVEP-BCI is based on perception, where the well-known example of Rubin's face-vase illusion is here used in order to create a bridge of communication for subjects with severe motor disabilities. The contrast between a colored stimulus and other plays an important role because this effect would be related to the visual lateral inhibition process, where photoreceptor cells aid the brain in perceiving contrast within an image. Thus, the visual attention in multistable perception experiments does not require head neuromuscular control or eye movements.

This study evaluated both an offline and an online SSVEP system, suggesting a new concept of analysis and stimulation that might be applicable in daily life. Results of this work provide individual analysis for each subject that can be useful for identifying the behavior of the subject under evaluation. An improvement in terms of accuracy of classification was observed using features from three electrodes (O1, O2 and Oz) compared to using a single electrode (Oz) with both CCA and MSI methods. A comparison between different window lengths showed than WL of 4 s is more accurate compared to 1 s.

Furthermore, MSI was found to be more accurate compared to CCA in cases with same conditions, either using three electrodes or one electrode (Oz) in different WLs. Figure 45 presents a summary of this performance, where seven out of ten subjects reached an average accuracy higher than 60 % for these, with average accuracy of 83.67 %.

The values of ITRs obtained are relative and dependent on setup parameters. The highest value achieved was 35.18 bits/min using MSI, with 1 s of WL (values for subject 2). Our results demonstrate that the electrode Oz is the best channel for characterization of visual perception from a quantitative point of view.

On the other hand, our studies also validated an online SSVEP-BCI using a specific setup built at the laboratory. Muscular activities related to eye movements were also evaluated in this study, using an eye tracker device to observe and evaluate the attention objectively. The online performance seems decreasing the accuracy. The reason could be attributed to the fact that stimuli are located in different depths of field, and the fact that our brains receive daily stimulation of human faces, which implies that our brains are highly trained to focus on faces. As a consequence, the loss of focus on vase could reduce visual attention and thereby lead to the decreased SSVEP amplitude. These results are consistent with our results in offline tasks.

Finally, these findings strongly support the hypothesis of visual selectivity by means of the perception and neural mechanism of spatial attention. This novel SSVEP-BCI based on Figure Ground Perception (FGP) has shown being a new approach compared to traditional SSVEP-BCIs, in which the activation of commands is based on eye movments (gaze), and also a new type of independent SSVEP-BCIs based on bilateral selective attention. Thus, this study contributes directly to the research area of alternative or augmentative communication, oriented to people in locked-in syndrome, in final stages of ALS, or in other extreme case of paralysis situation.

7 Conclusions and Future Works

7.1 Summary of contributions

The major contributions of this thesis are:

1. **Improvements of the Multivariate Synchronization Index (MSI).** From the inconsistency in the formation of the correlation matrix proposed by Zhang et al. (2014a), a reformulation of this technique allowed the proposal of a MSI modified, obtaining the highest rates of success for stimulation by LEDs compared to other techniques of SSVEP detection and technologies of stimulation.

2. **A new method of SSVEPs detection based on tensor models (PARAFAC).** A new way for automatic detection of SSVEPs through correlation analysis between tensor models was developed. This novel technique uses 3-dimensions ($channel \times frequency \times time$), where EEG signals are compared to simulated tensor models ("template"). The classification is obtained from comparison of each of the extracted signatures of the PARAFAC model with the corresponding simulated signatures of a target SSVEP signal. This study was conducted in collaboration with researchers of Ryerson University in Toronto, Canada.

3. **A first study about evaluation of the influence of colored stimuli using LEDs in SSVEPs.** A novel study related to the influence of color in SSVEP was conducted. It is worth to mention that none of the studies in literature did comparison of performance of stimuli colors using LEDs. From results although its high accuracy rates, red color was disregard of our nominations due to its low level of comfort and its trends to evoke epileptic responses. Also, the results confirm that green color is the most suitable option for visual stimuli, where the rule of selection of the best color was applied to each resulting centroid. Finally, the order of choice as a suitable color of stimulation was the following: green, blue and yellow.

4. **Use of Compressive Sensive technique for an SSVEP-BCI.** A Compression technique was applied to EEG signals and SSVEP approach. In this study, different signal compression algorithms (ℓ_p^d-regularized least-squares ($\ell_p^d - RLS$), ℓ_p^{2d}-regularized least-squares ($\ell_p^{2d} - RLS$) and the block-sparse Bayesian learning bound-optimization ($BSBL - BO$)) and different techniques to detect SSVEPs were evaluated. Thus, Compressive Sensing (CS) was considered an emerging and

promising technique for the development of low-power, small-chip, and robust wireless BCI (PANT; KRISHNAN, 2014; ZHANG et al., 2013). This approach is quite novel in the areas of SSVEP-BCI. This study also was conducted in collaboration with researches of Ryerson University.

5. **Development of a new independent SSVEP-BCI using approach of Figure-Ground Perception (FGP).** In this study, offline and online experiments were conducted with a new way of presenting visual stimuli through the model face-vase. In this sense, a portable stimulator based on two flickering stimuli representing the model face-vase was proposed. This novel concept of SSVEP-BCI is based on perception, in which the well-known example of Rubin's face-vase illusion is here used in order to create a bridge of communication for subjects with severe motor disabilities. Thus, this study developed a novel BCI that can offer to people with severe motor disabilities (such as, patients with amyotrophiclateral sclerosis (ALS), multiplesclerosis, and Guillain-Barré syndrome) an alternative of communication through attention modulation without requiring neuromuscular activities or eye movements.

7.2   Future works

The following are suggestions for future works related to the development of Independent SSVEP-BCIs.

1. It is essential the realization of a deeper study about the choice of frequencies of stimulation. A study that involves the participation of a considerable number of volunteers and a greater number of frequencies could help identifying the best frequencies that allow get higher accuracy rates and comfort for the user.

2. The development of technologies of acquisition of low cost is very important. Thus, with the execution and development of a low cost device, it would be possible its mass-production and the development of proprietary technology, versatile and of easy configuration.

3. Experiments with patients that have suffered any type of neurological problem, such as amyotrophiclateral sclerosis (ALS), multiplesclerosis and Guillain-Barré syndrome are necessary to confirm that they can properly command a BCI.

8 Appendix: Stay in Canada, publications and technical visit

During this research, the following awards, publications and technical visit were carried out:

8.1 Stay in Canada

- Obtainment of the first place in the selection process of the Foundation for Research and Innovation of Espirito Santo (FAPES) to conduct scientific technical stage at Ryerson University (Toronto, Canada). Process Number: 66492416/14.

8.2 Technical Visit

- Technical visit at the Machine Learning Lab of Prof. Robert Klaus Müller in the Technische Universität Berlin (Germany).

8.3 Publications

8.3.1 Journal Papers

- TELLO, R. J. M. G.; MULLER, S. M. T.; HASAN, M. A.; FERREIRA, A.; KRISHNAN, S.; BASTOS FILHO, T. F. An Independent-BCI based on SSVEP using Figure-Ground Perception (FGP). In: Biomedical Signal Processing and Control, Elsevier, 2016.

- TELLO, R. J. M. G.; MULLER, S. M. T.; FERREIRA, A.; BASTOS FILHO, T. F. Comparison of the Influence of Stimuli Color on Steady-State Visual Evoked Potentials. Research on Biomedical Engineering, onlineISSN 2446-4740, printISSN 2446-4732. v.31, n.3. 2015.

8.3.2 Chapter of Book

- MULLER, S. M. T.; FERREIRA, A.; CASTILLO, J. F.; TELLO, R. J. M. G.; BASTOS FILHO, T. F.; SARCINELLI FILHO, M. Brain-computer interfaces applied to

a robotic wheelchair and an autonomous car. In: CBEB. (Org.). Tecnologias, Técnicas e Tendências em Engenharia Biomédica. 1ed.Bauru: Canal6 Editora (Brazil), 2014. ISBN 978-85-7917-289-2.

8.3.3   Conference Papers

- TELLO, R. J. M. G.; BASTOS FILHO, T. F. Modulación Atencional en el Control de una Silla de Ruedas Robotizada Basada en SSVEP-BCI Para Personas con Síndrome de Bloqueo. In: VIII Congreso Iberoamericano de Tecnologías de Apoyo a la Discapacidad, 2015, Punta Arenas (Chile). 2015.

- TELLO, R. J. M. G.; VALADAO, C.; MULLER, S. M. T. ; FERREIRA, A.; BISSOLI, A.; CARELLI, R.; BASTOS FILHO, T. F. Performance improvements for navigation of a robotic wheelchair based on SSVEP-BCI. In: XII SBAI - Simpósio Brasileiro de Automação Inteligente 2015, Natal (Brazil). 2015.

- TELLO, R. J. M. G.; MULLER, S. M. T.; FERREIRA, A.; BASTOS FILHO, T. F. A novel system for control of a robotic wheelchair based on SSVEP-BCI for people with Locked-in Syndrome. In: XII SBAI - Simpósio Brasileiro de Automação Inteligente 2015, Natal (Brazil), 2015.

- TELLO, R. J. M. G.; MULLER, S. M. T.; BASTOS FILHO, T. F. Desenvolvimento de uma Cadeira de Rodas Robotizada Baseada em uma SSVEP -BCI Independente. In: International Workshop on Assistive Technology (IWAT), 2015, Vitória (Brazil), 2015.

- TELLO, R. J. M. G.; PANT, J. K.; MULLER, S. M. T.; KRISHNAN, S.; BASTOS FILHO, T. F. An Evaluation of Performance for an Independent SSVEP-BCI Based on Compressive Sensing System. In: XIII IUPESM World Congress on Medical Physics and Biomedical Engineering, 2015, Toronto (Canada). 2015.

- TELLO, R. J. M. G.; POURYAZDIAN, S.; FERREIRA, A.; BEHESHTI, S. ; KRISHNAN, S.; BASTOS FILHO, T. F. A New Approach for SSVEP Detection Using PARAFAC and Canonical Correlation Analysis. In: 37th Annual International Conference of the IEEE Engineering in Medicine and Biology Society (EMBC 15), Milano (Italy), 2015.

- TELLO, R. J. M. G.; BISSOLI, A.; FERRARA, F.; MULLER, S. M. T.; FERREIRA, A.; BASTOS FILHO, T. F. Development of a Human Machine Interface for Control of Robotic Wheelchair and Smart Environment. In: 11th IFAC Symposium on Robot Control (SYROCO), 2015, Salvador (Brazil). IFAC-PapersOnLine, Volume 48, Issue 19, 2015, Pages 136-141, ISSN 2405-8963. 2015.

- TELLO, R. J. M. G.; VALADAO, C.; BASTOS FILHO, T. F. Control de una Silla de Ruedas Robótica de Alto Rendimiento por Medio de Potenciales Evocados Visuales. In: VI Congreso Internacional de Diseño, Redes de Investigación y Tecnología para todos, DRT4ALL 2015, 2015, Madrid (Spain), 2015.

- TELLO, R. J. M. G.; BISSOLI, A.; FERRARA, F.; BASTOS FILHO, T. F. A High Performance Human-Computer Interface to Control a Robotic Wheelchair and an Intelligent Environment. In: VI Congreso Internacional de Diseño, Redes de Investigación y Tecnología para todos, DRT4ALL, Madrid (Spain), 2015.

- TELLO, R. J. M. G.; MULLER, S. M. T.; BASTOS FILHO, T. F.; FERREIRA, A. Comparison of New Techniques Based on EMD for Control of a SSVEP-BCI. In: IEEE International Symposium on Industrial Electronics, Istanbul (Turkey). 2014. p. 1-4.

- TELLO, R. J. M. G.; MULLER, S. M. T.; BASTOS FILHO, T. F.; FERREIRA, A. A Comparison of Techniques and Technologies for SSVEP Classification. In: IEEE-ISSNIP Biosignals and Biorobotics Conference: Biosignals and Robotics for Better and Safer Living (BRC), Salvador (Brazil), 2014.

- TELLO, R. J. M. G.; MULLER, S. M. T.; BASTOS FILHO, T. F.; FERREIRA, A. Comparison Between Wire and Wireless EEG Acquisition Systems Based on SSVEP in an Independent-BCI. In: 36th Annual International Conference of the IEEE Engineering in Medicine and Biology Society (EMBC 14). Chicago (USA). 2014.

- TELLO, R. J. M. G.; MULLER, S. M. T.; BASTOS FILHO, T. F.; FERREIRA, A. Towards the portability of an Independent-BCI based on SSVEP. In: Congresso Brasileiro de Engenharia Biomédica (CBEB), Uberlandia (Brazil). 2014.

- POMER-ESCHER, A.; TELLO, R. J. M. G.; SOUZA, M. D.; BASTOS FILHO, T. F. Análise de estresse e fadiga em bombeiros através de EEG. In: Congresso Brasileiro de Engenharia Biomédica (CBEB), 2014, Uberlandia (Brazil). 2014.

- TELLO, R. J. M. G.; MULLER, S. M. T.; BASTOS FILHO, T. F.; FERREIRA, ANDRE. Evaluation of different stimuli color for an SSVEP-based BCI. In: XXIV Congresso Brasileiro de Engenharia Biomédica (CBEB), Uberlandia (Brazil). 2014.

- TELLO, R. J. M. G.; POMER-ESCHER, A.; BASTOS FILHO, T. F. Análisis del nivel de fatiga basado en EEG en bomberos profesionales. In: VI Jornadas AITADIS de Rehabilitación y Tecnologías de Apoyo a la Discapacidad, Asuncion (Paraguay). 2014.

- POMER-ESCHER, A.; TELLO, R. J. M. G.; BASTOS FILHO, T. F. Analysis of mental fatigue in motor imagery and emotional stimulation based on EEG. In: XXIV Congresso Brasileiro de Engenharia Biomédica (CBEB) 2014, Uberlandia (Brazil), 2014.

Bibliography

ACAR, E. et al. Multiway analysis of epilepsy tensors. *Bioinformatics*, p. i10–i18, 2007. Cited on page 35.

ALLISON, B. et al. A hybrid ERD/SSVEP BCI for continuous simultaneous two dimen-sional cursor control. *Journal of Neuroscience Methods*, v. 209, n. 2, p. 299–307, 2012. Cited 2 times on pages 17 and 18.

ALLISON, B. Z. et al. Towards an independent brain-computer interface using Steady State Visual Evoked Potentials. *Clinical Neurophysiology*, v. 119, Issue 2, n. 399-408, 2008. Cited 3 times on pages xiii, 67, and 68.

AMIRI, S.; FAZEL-REZAI, R.; ASADPOUR, V. A Review of Hybrid Brain-Computer Interface Systems. *Advances in Human-Computer Interaction*, 2013. Cited 2 times on pages 10 and 11.

ANGEL, P. Garrido-del; BOJORGES-VALDEZ, E.; YANEZ-SUAREZ, O. SSVEP-based BCI control of the DASHER writing system. In: *Neural Engineering (NER), 2011 5th International IEEE/EMBS Conference on*. [S.l.: s.n.], 2011. p. 446–448. ISSN 1948-3546. Cited on page 17.

BASTOS, T. et al. Robotic wheelchair com-manded by SSVEP, motor imagery and word generation. *2011 Annual International Conference of the IEEE Engineering in Medicine and Biology Society,EMBC*, p. 4753,4756, 2011. Cited on page 17.

BIAN, Y. et al. Research on Steady State Visual Evoked Potentials based on Wavelet Packet Technology for Brain-Computer Interface . *Procedia Engineering*, v. 15, n. 0, p. 2629 – 2633, 2011. ISSN 1877-7058. <ce:title>CEIS 2011</ce:title>. Cited on page 18.

BIAN, Y. et al. Research on Brain-Computer Interface Technology Based on Steady State Visual Evoked Potentials. In: *Bioinformatics and Biomedical Engineering (iCBBE), 2010 4th International Conference on*. [S.l.: s.n.], 2010. p. 1–4. ISSN 2151-7614. Cited on page 17.

BIEGER, J.; GARCIA-MOLINA, G. Light stimulation properties to influence brain activity: A brain-computer interface application. *Philips Research*, p. 7, 2010. Cited on page 43.

BIEGER, J.; GARCIA-MOLINA, G.; ZHU, D. Effects of Stimulation Properties in Steady-State Visual Evoked Potential Based Brain-Computer Interfaces. *International Conference of the IEEE EMBS*, 2010. Cited 2 times on pages 43 and 44.

BIN, G. et al. An online multi-channel ssvep-based brain-computer interface using a canonical correlation analysis method. *Journal of Neural Engineering*, v. 6, p. p. 46002,, 2009. Cited 2 times on pages 2 and 17.

BORGA, M.; KNUTSSON, H. A canonical correlation approach to blind source separation. *Linkoping University, Linkoping, Sweden, Technical Report LiU-IMT-EX-0062*, 2001. Cited on page 29.

BRITZ, J.; PITTS, M. Perceptual reversals during binocular rivalry: ERP components and their concomitant source differences. *Psychophysiology*, v. 48, n. 11, p. 1490–1499, 2011. Cited on page 69.

BRO, R. *Multi-way Analysis in the Food Industry: Models, Algorithms and Applications.* Tese (Doutorado) — University of Amsterdam (NL) and Royal Veterinary and Agricultural University (DK), 1998. Cited on page 37.

BRO, R.; KIERS, H. A. L. A New Efficient Method for Determining the Number of Components in PARAFAC Models. *Journal of Chemometrics*, John Wiley & Sons, Ltd., v. 17, n. 5, p. 274–286, 2003. ISSN 1099-128X. Cited on page 36.

BUECHNER, V. L. et al. Red-take a closer look. *PLoSONE*, v. 9, n. e108111, 2014. Cited on page 59.

CAO, L. et al. A hybrid brain computer interface system based on the neurophysiological protocol and brain-actuated switch for wheelchair control. *Journal of Neuroscience Methods*, v. 229, p. 33–43, 2014. Cited 4 times on pages xi, 17, 18, and 19.

CAO, T. et al. Flashing color on the performance of SSVEP-based brain-computer interfaces. In: *Engineering in Medicine and Biology Society (EMBC), 2012 Annual International Conference of the IEEE.* [S.l.: s.n.], 2012. p. 1819–1822. ISSN 1557-170X. Cited 2 times on pages 43 and 44.

CARMELI, C. et al. Assessment of EEG synchronization based on state-space analysis. *NeuroImage*, v. 25, n. 339-354, 2005. Cited on page 50.

CECOTTI, H. A Self-Paced and Calibration-Less SSVEP-Based Brain-Computer Interface Speller. *IEEE Transactions on Systems and Rehabilitation Engineering*, v. 18, n. 2, p. 127,133, 2010. Cited on page 17.

CHANG, H.-C. et al. Real-time control of an SSVEP-actuated remote-controlled car. *Proceed-ings of SICE Annual Conference 2010*, p. 1884,1887, 2010. Cited 4 times on pages xi, 17, 18, and 19.

CHELLAPPA, S. L. et al. Non-visual effects of light on melatonin, alertness, and cognitive performance: can blue-enriched light keep us alert? *PLoSONE*, v. 26, n. e16429, 2011. Cited on page 59.

CHEN, C. et al. A noninvasivebrain computer interface using visually-induced near-infrared spectroscopyresponses. *Neurosci. Lett.*, v. 580, p. 22–26, 2014. Cited on page 2.

CHEN, X. et al. Brain-computer interface based on intermodulation frequency. *J. Neural Eng*, 2013. Cited on page 2.

CHEN, Y.; HONGWEI, F. Study and application of lateral inhibition models inimage's contour enhancement. *International Conference on ComputerApplication and System Modeling (ICCASM)*, v. 13, 2010. Cited on page 70.

CHUMERIN, N. et al. Subject-adaptive steady-state visual evoked potential detection for brain-computer interface. In: *Intelligent Data Acquisition and Advanced Computing Systems (IDAACS), 2011 IEEE 6th International Conference on.* [S.l.: s.n.], 2011. v. 1, p. 369–373. Cited on page 17.

CICHOCKI, A. et al. *Nonnegative Matrix and Tensor Factorizations: Applications to Exploratory Multi-way Data Analysis and Blind Source Separation.* [S.l.]: Wiley, 2009. ISBN 0470746661, 9780470746660. Cited 2 times on pages 34 and 35.

DIEZ, P. F. et al. Commanding a robotic wheelchair with a high-frequency steady-state visual evoked potential based brain-computer interface. *Med Eng Phys.*, 2013. Cited 2 times on pages 17 and 18.

DIEZ, P. F. et al. Asynchronous BCI control using high-frequency SSVEP. *Journal of NeuroEngineering and Rehabilitation*, v. 8: 39, 2011. Cited 2 times on pages 17 and 18.

DING, J.; SPERLING, G.; SRINIVASAN, R. Attentional Modulation of SSVEP Power Depends on the Network Tagged by the Flicker Frequency. *Cerebral Cortex*, v. 16, n. 7, p. 1016–1029, 2006. Cited on page 10.

DORNHEGE, G. et al. *Toward Brain-Computer Interfacing.* [S.l.]: Massachusetts Institute of Technology, 2007. Cited on page 13.

DOUGLAS, R.; MARSHALL, J. A review of vertebrate and invertebrate ocular filters. *Adaptive Mechanisms in the Ecology of Vision, Kluwer Academic Publishers*, p. 95–162., 1999. Cited on page 70.

DREW, P. et al. Pupillary response to chromatic flicker. *Exp. Brain Res.*, v. 136 (2), n. 256-262, 2001. Cited 3 times on pages 43, 56, and 59.

EBERSOLE, J. S.; PEDLEY, T. A. Current practice of clinical Electroencephalography. *3rd edition. Philadelphia: Lippincott Williams & Wilkins*, n. 844, 2002. Cited on page 59.

ELLIOT, A. Color and psychological functioning: a review of theoretical and empirical work. *Front. Psychol.*, 2015. Cited 2 times on pages 59 and 60.

ELLIOT, A. J.; FAIRCHILD, M. D.; FRANKLIN, A. Handbook of Color Psychology. *Cambridge University Press*, 2014. Cited on page 59.

FALZON, O.; CAMILLERI, K.; MUSCAT, J. Complex-Valued Spatial Filters for SSVEP-Based BCIs With Phase Coding. *Biomedical Engineering, IEEE Transactions on*, v. 59, n. 9, p. 2486–2495, 2012. ISSN 0018-9294. Cited 2 times on pages 17 and 18.

FAZEL-REZAI, R. *Recent Advances in Brain-Computer Interface Systems.* [S.l.]: InTech, 2011. Cited on page 9.

FELDMAN, M. *Hilbert Transform Applications in Mechanical Vibration.* [S.l.]: Wiley, 2011. Cited on page 26.

FISHER, R. S. et al. Photic and pattern induced seizures: a review for the epilepsy foundation of America working group. *Epilepsia*, v. 46, n. 9, p. 1426–1441, 2005. Cited 2 times on pages 43 and 46.

FRIMAN, O.; VOLOSYAK, I.; GRASER, A. Multiple Channel Detection of Steady-State Visual Evoked Potentials for Brain-Computer Interfaces. *Biomedical Engineering, IEEE Transactions on*, v. 54, n. 4, p. 742–750, 2007. ISSN 0018-9294. Cited 5 times on pages 2, 17, 18, 24, and 27.

GAO, X. et al. A BCI-based environmental controller for the motion-disabled. *Neural Systems and Rehabilitation Engineering, IEEE Transactions*, v. 11, n. 2, p. 137,140, 2003. Cited on page 2.

GARCIA MOLINA, G. High frequency SSVEPs for BCI applications. *In Brain-Computer Interfaces for HCI and Games*, 2008. Cited on page 17.

GOLLEE, H. et al. An SSVEP-Based Brain-Computer Interface for the Control of Functional Electrical Stimulation. *Biomedical Engineering, IEEE Transactions on*, v. 57, n. 8, p. 1847–1855, 2010. ISSN 0018-9294. Cited on page 17.

GRAIMANN, B.; ALLISON, B.; PFURTSCHELLER, G. *Brain-computer interfaces. Revolutionizing Human-Computer Interaction.* [S.l.]: Springer, 2010. Cited 4 times on pages xi, xiii, 4, and 71.

GRAY, M. et al. Cortical neurophysiology of anticipatory anxiety: an investigation utilizing steady state probe topography (SSPT). *Neuroimage*, v. 20, n. 2, p. 975–986, 2003. Cited on page 9.

GREGORY, R. Eye and Brain. The psychology of seeing. *Princeton University Press*, n. 126-127, 1997. Cited 2 times on pages 43 and 59.

GRILL-SPECTOR, K. The neural basis of object perception. *Curr. Opin. Neurobiol.*, v. 13, n. 2, p. 159–166, 2003. Cited on page 69.

HAIRSTON, W. D. et al. Usability of four commercially-oriented EEG systems. *Journal of Neural Engineering*, 2014. Cited on page 61.

HAMMOND, B. The visual effects of intraocular colored filters. *Scientifica*, p. 1–18, 2012. Cited 3 times on pages xiii, 70, and 72.

HAN, C.-H.; HWANG, H.-J.; IM, C.-H. Modified pattern-reversal visual checkerboard stimuli with dual alternating frequencies for multi-class ssvep-based brain-computer interfaces. In: *Brain-Computer Interface (BCI), 2013 International Winter Workshop on.* [S.l.: s.n.], 2013. p. 86–88. Cited on page 17.

HARTLINE, H. K.; WAGNER H. G.AND RATLIFF, F. Inhibition in the eye of limulus. *J. Gen. Physiol.*, v. 39, n. 5, p. 651–673, 1956. Cited on page 70.

HE, B. Neural Engineering. *2nd ed., Springer*, 2013. Cited on page 11.

HERRMANN, C. S. Human EEG responses to 1-100 Hz flicker, resonance phenomena in visual cortex and their potential correlation to cognitive phenomena. *Exp. Brain Res*, v. 137, p. 346–353, 2001. Cited 2 times on pages 46 and 56.

HOOD, S.; JERNIGAN, E. A monolithic silicon nonlinear lateral inhibition model. *IEEE International Conference on Systems, Man, and Cybernetics. Humans,Information and Technology*, v. 1, p. 292–295., 1994. Cited on page 70.

HUANG, M. et al. Application and Contrast in Brain-Computer Interface between Hilbert-Huang Transform and Wavelet Transform. In: *Young Computer Scientists, 2008. ICYCS 2008. The 9th International Conference for.* [S.l.: s.n.], 2008. p. 1706–1710. Cited on page 26.

HUANG, N. E. et al. The empirical mode decomposition and the Hilbert spectrum for nonlinear and non-stationary time series analysis. *Proceedings of the Royal Society of London. Series A: Mathematical, Physical and Engineering Sciences*, v. 454, n. 1971, p. 903–995, 1998. Cited 4 times on pages 2, 24, 25, and 26.

HWANG, H. J. et al. Development of an SSVEP-based BCI spelling system adopting a QWERTY-style LED keyboard. *J. Neurosci. Meth.*, v. 208, p. 59–65, 2012. Cited 4 times on pages xi, 17, 18, and 19.

JANNEK, D. et al. Identification of Signal Components in Multi-Channel EEG Signals via Closed-Form PARAFAC Analysis and Appropriate Preprocessing. In: *4th European Conf. of IFMBE.* [S.l.]: Springer, 2009. p. 1226–1230. ISBN 978-3-540-89207-6. Cited on page 35.

JIA, C. et al. Frequency and Phase Mixed Coding in SSVEP-Based Brain–Computer Interface. *Biomedical Engineering, IEEE Transactions on*, v. 58, n. 1, p. 200–206, 2011. ISSN 0018-9294. Cited on page 17.

KELLY, S. et al. A comparison of covert and overt attention as a control option in a steady-state visual evoked potential-based brain computer interface. *26th Annual International Conference of the IEEE. Engineering in Medicine and Biology Society 2004 (IEMBS '04)*, v. 2, p. 4725–4728, 2004. Cited 2 times on pages xiii and 68.

KELLY, S. et al. Comparison of covert and overt attention as a control option in a steady-state visual evoked potential-based brain computer interface. *Engineering in Medicine and Biology Society, 2004. IEMBS' 04. 26th Annual International Conference of the IEEE*, v. 2, n. 4725-4728, 2004. Cited on page 67.

KELLY, S. P. et al. Independent Brain Computer Interface Control using Visual Spatial Attention-Dependent Modulations of Parieto-occipital Alpha. *Neural Engineering. Conference Proceedings. 2nd International IEEE EMBS Conference*, n. 667-670, 2005. Cited on page 59.

KELLY, S. P. et al. Visual spatial attention tracking using high-density SSVEP data for independent brain-computer communication. *Neural Systems and Rehabilitation Engineering, IEEE Transactions*, v. 13, no 2., n. 172,178, 2005. Cited 4 times on pages xiii, 2, 67, and 68.

KIM, Y. J. et al. Attention induces synchronization-based response gain in steady-state visual evoked potentials. *Nature Neuroscience*, v. 10, n. 117-125, 2007. Cited on page 58.

KIMURA, Y. et al. SSVEP-Based Brain-Computer Interfaces Using FSK-Modulated Visual Stimuli. *IEEE Transactions on Biomedical Engineering*, v. 60, n. 10, p. 2831,2838, 2013. Cited on page 17.

KROLAK-SALMON, P. et al. Human lateral geniculate nucleus and visual cortex respond to screen flicker. *Ann Neurol.*, v. 53: 73-80, 2003. Cited on page 45.

KWAK, N.-S.; MULLER, K.-R.; LEE, S.-W. Toward exoskeleton control based on steady state visual evoked potentials. *International Winter Workshop on Brain-Computer Interface (BCI), 2014*, p. 1,2, 2014. Cited on page 17.

LEE, P.-L. et al. A Brain-Wave-Actuated Small Robot Car Using Ensemble Empirical Mode Decomposition-Based Approach. *Systems, Man and Cybernetics, Part A: Systems and Humans, IEEE Transactions on*, v. 42, n. 5, p. 1053–1064, 2012. ISSN 1083-4427. Cited on page 17.

LEE, P. L. et al. An SSVEP-actuated brain computer interface using phase-tagged flickering sequences: A cursor system. *Ann. Biomed. Eng.*, v. 38, p. 2383–2397, 2010. Cited 2 times on pages 17 and 18.

LESENFANTS, D. et al. An independent SSVEP-based brain computer interface in locked-in syndrome. *Journal of Neural Engineering*, v. 3, n. 035002, 2014. Cited 3 times on pages xiii, 67, and 68.

LI, J.; ZHANG, L.; ZHAO, Q. Pattern Classification of Visual Evoked Potentials Based on Parallel Factor Analysis. In: *Advances in Cognitive Neurodynamics ICCN 2007*. [S.l.]: Springer, 2008. p. 571–575. ISBN 978-1-4020-8386-0. Cited on page 35.

LI, Y. et al. Analysis of phase coding SSVEP based on canonical correlation analysis (CCA). In: *Neural Engineering (NER), 2011 5th International IEEE/EMBS Conference on*. [S.l.: s.n.], 2011. p. 368–371. ISSN 1948-3546. Cited on page 17.

LIM, J.-H. et al. Development of a hybrid mental spelling system combining SSVEP-based brain-computer interface and webcam-based eye tracking. *Biomedical Signal Processing and Control*, v. 21, p. 99 – 104, 2015. ISSN 1746-8094. Cited 2 times on pages 17 and 18.

LIN, Z. et al. Frequency Recognition Based on Canonical Correlation Analysis for SSVEP-Based BCIs. *Biomedical Engineering, IEEE Transactions on*, v. 54, n. 6, p. 1172–1176, 2007. ISSN 0018-9294. Cited 5 times on pages 2, 3, 17, 24, and 27.

LINDSAY, D. T. et al. Color channels, not color appearance of color categories, guide visual search for desaturated color targets. *Psychol.Sci.*, v. 21, n. 1208-1214, 2010. Cited on page 59.

LOPEZ-GORDO, M. A.; PELAYO, F.; PRIETO, A. A high performance SSVEP-BCI without gazing. *Proc. Int. Joint Conf. on Neural Networks*, p. 1–5, 2010. Cited on page 17.

LUTH, T. et al. Low level control in a semi-autonomous rehabilitation robotic system via a Brain-Computer Interface. *IEEE 10th International Conference on Rehabilitation Robotics, ICORR 2007.*, p. 721,728,, 2007. Cited 2 times on pages 17 and 18.

MANYAKOV, N. V. et al. Decoding SSVEP Responses based on Parafac Decomposition. In: *Biosignals*. [S.l.]: SciTePress, 2012. p. 443–447. ISBN 978-989-8425-89-8. Cited on page 35.

MATERKA, A.; BYCZUK, M.; PORYZALA, P. A virtual keypad based on alternate half-field stimulated visual evoked potentials. *In Proceedings of the International Symposium on Information Technology Convergence*, p. 296–300, 2007. Cited 2 times on pages 17 and 18.

MCFARLAND, D. J. et al. Spatial filter selection for EEG-based communication. *Electroencephalography and clinical Neurophysiology, Elsevier*, p. 103(3):386–394, 1997. Cited on page 48.

MEHTA, R.; ZHU, R. Blue or red? Exploring the effect of color on cognitive task performances. *Science 323*, n. 1226-1229, 2009. Cited on page 60.

MIWAKEICHI, F. et al. Decomposing EEG data into space-time-frequency components using Parallel Factor Analysis. *NeuroImage*, v. 22, n. 3, p. 1035 – 1045, 2004. ISSN 1053-8119. Cited 4 times on pages xii, 35, 36, and 37.

MOLINA, G. G.; ZHU, D.; ABTAHI, S. Phase detection in a visual-evoked-potential based brain computer interface. *Proc. 18th European Signal Proc. Conf.*, p. 949–953, 2010. Cited 2 times on pages 17 and 18.

MOLLER, A. C.; ELLIOT, A. J.; MAIER, M. A. Basic hue-meaning associations. *Emotion*, v. 9, n. 898-902, 2009. Cited on page 60.

MORGAN, S. T.; C., H. J.; HILLYARD, S. A. Selective attention to stimulus location modulates the steady-state visual evoked potential. *Proc. Natl. Acad. Sci. Neurobiology*, v. 93:, n. 477-4774, 1996. Cited 4 times on pages xiii, 59, 67, and 68.

MORUP, M. et al. Parallel Factor Analysis as an exploratory tool for wavelet transformed event-related EEG. *NeuroImage*, p. 938–947, 2006. ISSN 1053-8119. Cited on page 35.

MÜLLER-PUTZ, G. R. et al. Comparison of DFT and lock-in amplifier features and search for optimal electrode positions in SSVEP-based BCI. *Journal of Neuroscience Methods*, v. 168, p. 174–181, 2008. Cited 2 times on pages 17 and 18.

MÜLLER, S.; BASTOS-FILHO, T.; SARCINELLI-FILHO, M. Incremental SSVEP analysis for BCI implementation. In: *Engineering in Medicine and Biology Society (EMBC), 2010 Annual International Conference of the IEEE.* [S.l.: s.n.], 2010. p. 3333–3336. ISSN 1557-170X. Cited 3 times on pages 17, 24, and 25.

MÜLLER, S.; BASTOS-FILHO, T.; SARCINELLI-FILHO, M. Using a SSVEP-BCI to command a robotic wheelchair. In: *Industrial Electronics (ISIE), 2011 IEEE International Symposium on.* [S.l.: s.n.], 2011. p. 957–962. ISSN Pending. Cited on page 17.

MÜLLER, S. et al. SSVEP-BCI implementation for 37-40 Hz frequency range. In: *2011 Annual International Conference of the IEEE Engineering in Medicine and Biology Society,EMBC.* [S.l.: s.n.], 2011. p. 6352–6355. ISSN 1557-170X. Cited 2 times on pages 17 and 18.

MÜLLER, S. M. T. et al. Brain-computer interface based on visual evoked potentials to command autonomous robotic wheelchair. *J. Med. Biol. Eng.*, v. 30:, p. 407–416, 2010. Cited on page 17.

MÜLLER, S. M. T. et al. Spectral techniques for incremental SSVEP analysis applied to a BCI implementation. *V Latin American Congress on Biomedical Engineering CLAIB 2011 May 16-21, 2011, Habana, Cuba*, p. 1090–1093, 2011. Cited on page 17.

NECKER, L. Observations on some remarkable optical phenomena seen in Switzerland; and on an optical phenomenon which occurs on viewing a figure of a crystal or geometrical solid. *Lond. Edinb. Phil. Mag. J. Sci.*, v. 1, n. 5, p. (1832) 329–337, 1832. Cited on page 69.

ORTNER, R. et al. An SSVEP BCI to Control a Hand Orthosis for Persons With Tetraplegia. *Neural Systems and Rehabilitation Engineering, IEEE Transactions on*, v. 19, n. 1, p. 1–5, 2011. ISSN 1534-4320. Cited on page 17.

PAN, J. et al. Discrimination Between Control and Idle States in Asynchronous SSVEP-Based Brain Switches: A Pseudo-Key-Based Approach. *IEEE Transactions on Neural Systems and Rehabilitation Engineering*, n. 21, p. 435–443, 2013. Cited on page 17.

PANT, J. K.; KRISHNAN, S. Reconstruction of ECG signals for compressive sensing by promoting sparsity on the gradient. *IEEE Int. Conf. on Acoustics, Speech and Signal Processing (ICASSP)*, 2013. Cited 2 times on pages 61 and 63.

PANT, J. K.; KRISHNAN, S. Compressive sensing of electrocardiogram signals by promoting sparsity on the second-order difference and by using dictionary learning. *IEEE Trans. Biomed. Circuits Syst.*, v. 61, n. 3, p. 198–202, 2014. Cited 6 times on pages 6, 61, 63, 64, 65, and 88.

PARINI, S. et al. A Robust and Self-Paced BCI System Based on a Four Class SSVEP Paradigm: Algorithms and Protocols for a High-Transfer-Rate Direct Brain Communication. *Computational Intelligence and Neuroscience*, 2009. Cited 2 times on pages 17 and 18.

PASTOR, M. A. et al. Human cerebral activation during steady-state visual-evoked responses. *The Journal of Neuroscience*, v. 23, no. 37,, n. 11621-11627, 2003. Cited 3 times on pages 10, 45, and 46.

PERLSTEIN, W. et al. Steady state visual evoked potentials reveal frontally-mediated working memory activity in humans. *Neurosci. Lett.*, v. 342, n. 3, p. 191–195., 2003. Cited on page 9.

PETERSON, M.; SALVAGIO, E. Attention and competition in figure-ground perception. *N. Srinivasan (Ed.), Progress in Brain Research. Elsevier*, v. 176, p. 1–13, 2009. Cited on page 70.

PFURTSCHELLER, G. et al. Self-Paced Operation of an SSVEP-Based Orthosis With and Without an Imagery-Based. *Neural Systems and Rehabilitation Engineering, IEEE Transactions on*, v. 18, n. 4, p. 409–414, 2010. ISSN 1534-4320. Cited on page 17.

PITTS, M. A.; NERGER, J. L.; DAVIS, T. J. Electrophysiological correlates of perceptual reversals for three different types of multi-stable images. *J. Vis.*, v. 7, p. 1–14, 2007. Cited 2 times on pages 69 and 70.

POMERLEAU, V. J. et al. Colour-specific differences in attentional deployment for equiluminant pop-out colours: evidence from lateralized potentials. *Int. J. Psychophysiol*, v. 91, n. 194-205, 2014. Cited on page 59.

POURYAZDIAN, S.; ERFANIAN, A. Detection of steady-state visual evoked potentials for brain-computer interfaces using PCA and high-order statistics. *Proc. World Congress on Medical Physics and Biomedical Engineering, Munich, Germany.*, v. 25, p. 480–483, 2009. Cited on page 17.

PUNSAWAD, Y.; WONGSAWAT, Y. Minimal-assisted SSVEP-based brain-computer interface device. In: *Signal Information Processing Association Annual Summit and Conference (APSIPA ASC), 2012 Asia-Pacific.* [S.l.: s.n.], 2012. p. 1–4. Cited 4 times on pages xi, 17, 18, and 19.

PUNSAWAD, Y.; WONGSAWAT, Y. Hybrid SSVEP-motion visual stimulus based BCI system for intelligent wheelchair. *2013 35th Annual International Conference of the IEEE Engineering in Medicine and Biology Society (EMBC)*, p. 7416,7419, 2013. Cited on page 17.

QIU, F.; HEYDT, R. Von der. Neural representation of transparent overlay. *Nat.Neuroscience*, v. 10, p. 283–284., 2007. Cited on page 69.

RECHY-RAMIREZ, E. J.; HU, H. Bio-signal based control in assistive robots: A survey. *Digital Communications and Networks*, n. 0, 2015. ISSN 2352-8648. Cited on page 1.

REGAN, D. An effect of stimulus colour on average steadystate potentials evoked in man. *Nature*, v. 210, n. 5040, p. 1056–1057, 1966. Cited 4 times on pages 43, 44, 56, and 59.

REGAN, D. Some characteristics of average steady-state and transient responses evoked by modulated light. *Electroencephalography and Clinical Neurophysiology*, v. 20, p. 238–248, 1966. Cited on page 9.

REGAN, D. Electrical responses evoked from the human brain. *Scientific American*, v. 241, n. 6, p. 134–146, 1979. Cited on page 10.

REGAN, D. Human Brain Electrophysiology: Evoked Potentials and Evoked Magnetic Fields in Science and Medicine. *Elsevier, New York*, 1989. Cited 2 times on pages 9 and 10.

RUBBOLI, G. et al. EEG diagnostic procedures and special investigations in the assessment of photosensitivity. *Epilepsia 45*, v. 1, n. 35-39, 2004. Cited on page 59.

RUSSO, F. D. et al. Spatiotemporal analysis of the cortical sources of the steady-state visual evoked potential. *Human Brain Mapping*, v. 28, n. 323-334, 2007. Cited on page 45.

SA, A. et al. Spectral F-Test power eval-uation in the EEG during intermittent photic stimulaton. *Arq. Neuropsiquiatr*, v. 64, n. (2a), p. 228–232, 2006. Cited 3 times on pages 2, 24, and 25.

SA, A. M. F. M. de et al. Assessing Time-and Phase-Locked Changes in the EEG during Sensory Stimulation by Means of Spectral Techniques. *IFMBE Proceedings 25-IV. Springer*, p. 2136–2139, 2009. Cited on page 25.

SAMMER, G. et al. Acquisition of typical EEG waveforms during fMRI: SSVEP, LRP, and frontal theta. *NeuroImage*, v. 24, n. 1012-1024, 2005. Cited on page 45.

SHANNON, C. E.; WEAVER, W. The Mathematical Theory of Communication. *Urbana, IL: Univ. Illinois Press*, 1964. Cited on page 11.

SHYU, K.-K. et al. Adaptive SSVEP-Based BCI System With Frequency and Pulse Duty-Cycle Stimuli Tuning Design. *IEEE Transactions on Neural Systems and Rehabilitation Engineering*, v. 21, no.5, pp.697,703, Sept. 2013., n. 5, p. 697,703, 2013. Cited 2 times on pages 17 and 18.

SHYU, K.-K. et al. Total Design of an FPGA-Based Brain Computer Interface Control Hospital Bed Nursing System. *Industrial Electronics, IEEE Transactions on*, v. 60, n. 7, p. 2731–2739, 2013. ISSN 0278-0046. Cited 2 times on pages 17 and 18.

SINGLA, R.; A., H. B. BCI Based Wheelchair Control Using Steady State Visual Evoked Potentials and Support Vector Machines. *International Journal of Soft Computing and Engineering (IJSCE)*, v. 3, 2013. Cited on page 17.

SOOMRO, M. et al. Automatic eye-blink artifact removal method based on EMD-CCA. In: *Complex Medical Engineering (CME), 2013 ICME International Conference on*. [S.l.: s.n.], 2013. p. 186–190. Cited on page 26.

SRINIVASAN, R.; BIBI, F. A.; NUNEZ, P. L. Steady-State Visual Evoked Potentials: Distributed Local Sources and Wave-Like Dynamics Are Sensitive to Flicker Frequency. *Brain Topography*, v. 18, n. 3, p. 167–187, 2006. Cited on page 10.

STERZER, P.; KLEINSCHMIDT, A.; REES, G. The neural bases of multistable perception. *Trends Cogn. Sci.*, v. 13, p. 310–318, 2009. Cited on page 69.

TANAKA, T.; ZHANG, C.; HIGASHI, H. SSVEP frequency detection methods considering background EEG. In: *Joint 6th International Conference on Soft Computing and Intelligent Systems (SCIS) and 13th International Symposium on Advanced Intelligent Systems (ISIS), 2012*. [S.l.: s.n.], 2012. p. 1138–1143. Cited on page 27.

TELLO, R. et al. A new approach for SSVEP detection using PARAFAC and canonical correlation analysis. *37th Annual International Conference of the IEEE in Engineering inMedicine and Biology Society (EMBC)*, p. 6174–6177, 2015. Cited on page 2.

TELLO, R. et al. Performance improvements for navigation of a robotic wheelchairbased on SSVEP-BCI. *XII SBAI - Simposio Brasileiro de Automacao Inteligente*, 2015. Cited on page 30.

TELLO, R. J. M. G. et al. Development of a human machine interface for control of robotic wheelchairand smart environment. *11th IFAC Symposium on Robot Control (SYROCO)*, n. 144-149, 2015. Cited 2 times on pages 30 and 45.

TELLO, R. J. M. G. et al. Comparison of new techniques based on EMD for control of a SSVEP-BCI. *IEEE 23rd International Symposium on Industrial Electronics (ISIE)*, p. 992,997, 2014. Cited 4 times on pages 30, 45, 46, and 73.

TELLO, R. J. M. G. et al. A comparison of techniques and technologies for SSVEP classification. In: *Biosignals and Biorobotics Conference (2014): Biosignals and Robotics for Better and Safer Living (BRC), 5th ISSNIP-IEEE*. [S.l.: s.n.], 2014. p. 1–6. Cited 5 times on pages 2, 30, 45, 46, and 73.

TELLO, R. J. M. G. et al. Comparison between wire and wireless EEG acquisition systems based on SSVEP in an independent-BCI. *36th annual international conference of the IEEE Engineering in Medicine and Biology Society (EMBC 14), Chicago, USA. 2014*, 2014. Cited 2 times on pages 30 and 46.

TELLO, R. J. M. G. et al. Comparison of the influence of stimuli color on Steady-State Visual Evoked Potentials. *Research on Biomedical Engineering*, v. 31, n. 3, p. 218–231, 2015. Cited 2 times on pages 30 and 70.

TELLO, R. J. M. G. et al. An Evaluation of Performance for an Independent SSVEP-BCI Based on Compressive Sensing System. *13th Proc. IUPESM World Congress on Medical Physics and Biomedical Engineering, Toronto, Canada*, 2015. Cited 2 times on pages 30 and 61.

TIBSHIRANI, R. Regression shrinkage and selection via the lasso. *Jornal of the Royal Statistical Society*, p. 267–288, 1996. Cited on page 29.

VALBUENA, D. et al. Brain-Computer Interface for high-level control of rehabilitation robotic systems. In: *Rehabilitation Robotics, 2007. ICORR 2007. IEEE 10th International Conference on.* [S.l.: s.n.], 2007. p. 619–625. Cited on page 17.

VIALATTE, F. B. et al. Analyzing Steady State Visual Evoked Potentials Using Blind Source Separation. *Proceedings of the Second APSIPA Annual Summit and Conference. Singapore*, p. 578–582, 2010. Cited on page 24.

VIALATTE, F. B. et al. Steady-state visually evoked potentials: Focus on essential paradigms and future perspectives. *Progress in Neurobiology*, v. 90, p. 418–438, 2010. Cited 6 times on pages xi, 2, 9, 10, 11, and 43.

VOLOSYAK, I. SSVEP-based Bremen-BCI interface -Boosting information transfer rates. *Journal of Neural Engineering*, v. 8, p. 1–11, 2011. Cited on page 17.

VOLOSYAK, I. et al. A novel calibration method for SSVEP based brain-computer interfaces. *Proc. 18th European Signal Proc. Conf.*, p. 939–943, 2010. Cited 2 times on pages 17 and 18.

VOS, M. D. et al. Canonical Decomposition of Ictal Scalp EEG and Accurate Source Localisation: Principles and Simulation Study. *Computational Intelligence and Neuroscience*, p. 10, 2007. Cited on page 35.

WAGEMANS, J. et al. A century of Gestalt psychology in visual perception: I. Perceptual grouping and figure-ground organization. *Psychol. Bull.*, v. 138, n. 6, p. 1172–1217, 2012. Cited on page 69.

WANG, H.; LI, T.; HUANG, Z. Remote control of an electrical car with SSVEP-Based BCI. In: *Information Theory and Information Security (ICITIS), 2010 IEEE International Conference on.* [S.l.: s.n.], 2010. p. 837–840. Cited 2 times on pages 17 and 18.

WANG, N. et al. Discrimination between idle and work states in BCI based on SSVEP. In: *Advanced Computer Control (ICACC), 2010 2nd International Conference on.* [S.l.: s.n.], 2010. v. 4, p. 355–358. Cited 2 times on pages 17 and 18.

WANG, R.; GAO, X.; GAO, S. Frequency Selection for SSVEP-based Binocular Rivalry. In: *2nd International IEEE EMBS Conference on Neural Engineering, 2005. Conference Proceeding.* [S.l.: s.n.], 2005. p. 600–603. Cited on page 25.

WANG, Y. et al. A practical VEP-based brain-computer interface. *Neural Systems and Rehabilitation Engineering, IEEE Transactions on*, v. 14, n. 2, p. 234–240, 2006. ISSN 1534-4320. Cited 4 times on pages 2, 24, 48, and 56.

WANG, Y.; WANG, Y. T.; JUNG, T. P. Visual stimulus design for high-rate SSVEP BCI. *Electron. Lett*, v. 46, p. 1057–1058, 2010. Cited on page 2.

WEI, Q.; XIAO, M.; LU, Z. A Comparative Study of Canonical Correlation Analysis and Power Spectral Density Analysis for SSVEP Detection. In: *Intelligent Human-Machine Systems and Cybernetics (IHMSC), 2011 International Conference on.* [S.l.: s.n.], 2011. v. 2, p. 7–10. Cited on page 27.

WOLPAW, J. et al. Brain-computer interface technology: a review of the first international meeting. *Rehabilitation Engineering, IEEE Transactions on*, v. 8, n. 2, p. 164–173, 2000. ISSN 1063-6528. Cited on page 2.

WONG, C. M. et al. An improved phase-tagged stimuli generation method in steady-state visual evoked potential based brain-computer interface. In: *Biomedical Engineering and Informatics (BMEI), 2010 3rd International Conference on.* [S.l.: s.n.], 2010. v. 2, p. 745–749. Cited on page 17.

WONG, C. M. et al. A solution to harmonic frequency problem: Frequency and phase coding-basedbrain-computer interface. In: *Neural Networks (IJCNN), The 2011 International Joint Conference on.* [S.l.: s.n.], 2011. p. 2119–2126. ISSN 2161-4393. Cited on page 17.

WU, C. H.; CHANG, H. C.; LEE, P. L. Instantaneous gaze-target detection by empirical mode decomposition: Application to brain computer interface. *Proc. World Congress on Medical Physics and Biomedical Engineering*, v. 25:, p. 215–218, 2009. Cited 2 times on pages 17 and 18.

WU, C.-H. et al. Frequency recognition in an SSVEP-based brain computer interface using empirical mode decomposition and refined generalized zero-crossing. *Journal of Neuroscience Methods*, v. 196, n. 1, p. 170–181, 2011. ISSN 0165-0270. Cited 7 times on pages xi, 11, 17, 18, 19, 26, and 31.

WU, Z. et al. Stimulator selection in SSVEP-based BCI. *Medical Engineering & Physics*, v. 30, n. 8, p. 1079–1088, 2008. Cited 4 times on pages 10, 11, 18, and 44.

XU, Z. et al. Steady-State Visually Evoked Potential (SSVEP)-Based Brain-Computer Interface (BCI): A Low-Delayed Asynchronous Wheelchair Control System. *Springer*, v. 7663, p. 305–314, 2012. Cited on page 17.

YEH, C.-L. et al. Improvement of classification accuracy in a phase-tagged steady-state visual evoked potential-based brain computer interface using multiclass support vector machine. *BioMedical Engineering OnLine*, 2013. Cited 4 times on pages xi, 17, 18, and 19.

YIN, E. et al. A Dynamically Optimized SSVEP Brain-Computer Interface (BCI) Speller. *IEEE Transactions on Biomedical Engineering*, v. 62, n. 6, p. 1447–1456, 2015. ISSN 0018-9294. Cited 2 times on pages 17 and 18.

ZHANG, C. et al. A simple platform of brain-controlled mobile robot and its implementation by SSVEP. In: *Neural Networks (IJCNN), The 2012 International Joint Conference on.* [S.l.: s.n.], 2012. p. 1–7. ISSN 2161-4393. Cited on page 17.

ZHANG, D. et al. An independent brain computer interface based on covert shifts of non-spatial visual attention. *Engineering in Medicine and Biology Society, 2009. EMBC 2009. Annual International Conference of the IEEE*, n. 539-542, 2009. Cited 3 times on pages xiii, 67, and 68.

ZHANG, D. et al. An independent brain-computer interface using covert non-spatial visual selective attention. *J. Neural Eng.*, 2010. Cited 3 times on pages 3, 11, and 67.

ZHANG, Y. et al. LASSO based stimulus frequency recognition model for SSVEP BCIs. *Biomed. Signal Process. Control*, v. 7, p. 104–111, 2012. Cited 4 times on pages 11, 17, 24, and 29.

ZHANG, Y. et al. Source Estimation of Contrast-related Perception Based on Frequency-Tagged Binocular Rivalry. *Engineering in Medicine and Biology Society EMBS '06. 28th Annual International Conference of the IEEE*, n. 1177-1180, 2006. Cited on page 45.

ZHANG, Y. et al. Multivariate synchronization index for frequency recognition of SSVEP-based brain computer interface. *Journal of Neuroscience Methods*, v. 221, n. 0, p. 32 – 40, 2014. ISSN 0165-0270. Cited 11 times on pages 2, 3, 17, 24, 27, 29, 30, 49, 50, 56, and 87.

ZHANG, Y. et al. SSVEP recognition using common feature analysis in brain-computer interface. *Journal of Neuroscience Methods*, 2014. Cited on page 17.

ZHANG, Y. et al. Multiway canonical correlation analysis for frequency components recognition in SSVEP-based BCIs. *Proc. 18th Int. Conf. on Neural Information Processing*, p. 287–295, 2011. Cited on page 17.

ZHANG, Z. et al. Compressed sensing for energy-efficient wireless telemonitoring of noninvasive fetal ECG via block sparse Bayesian learning. *IEEE Trans. Biomed. Eng*, v. 60, n. 2, p. 300–309, 2013. Cited 3 times on pages 6, 61, and 88.

ZHANG, Z.; LI, X.; DENG, Z. A CWT-based SSVEP classification method for brain-computer interface system. In: *Intelligent Control and Information Processing (ICICIP), 2010 International Conference on.* [S.l.: s.n.], 2010. p. 43–48. Cited on page 17.

ZHANG, Z.; RAO, B. D. Extension of SBL algorithm for the recovery of block sparse signals with intra-block correlation. *IEEE Trans. Signal Process*, v. 61, n. 8, 2013. Cited 2 times on pages 63 and 64.

ZHU, D. et al. A survey of stimulation methods used in SSVEP-based BCIs. *Computational Intelligence and Neuroscience,Hindawi Publishing Corporation*, 2010. Cited on page 11.

ZHU, D. et al. Online BCI implementation of high-frequency phase modulated visual stimuli. *Universal Access in Human-Computer Interaction. Users Diversity.*, v. 6766, p. 645–654, 2011. Cited on page 17.

ZHU, D. et al. Phase synchrony analysis for SSVEP-based BCIs. In: *2nd International Conference on Computer Engineering and Technology (ICCET), 2010.* [S.l.: s.n.], 2010. v. 2, p. V2–329–V2–333. Cited 2 times on pages 17 and 18.